DEVELOPMENT AND EVALUATION OF CURCUMIN DELIVERY SYSTEMS FOR ORAL ADMINISTRATION TO IMPROVED BRAIN HEALTH

SUCHIWA PAN-ON

A Thesis Submitted to the Graduate School of Naresuan University
in Partial Fulfillment of the Requirements
for the Doctor of Philosophy in Pharmaceutical Sciences
2022

DEVELOPMENT AND EVALUATION OF CURCUMIN DELIVERY SYSTEMS FOR ORAL ADMINISTRATION TO IMPROVED BRAIN HEALTH

SUCHIWA PAN-ON

A Thesis Submitted to the Graduate School of Naresuan University
in Partial Fulfillment of the Requirements
for the Doctor of Philosophy in Pharmaceutical Sciences
2022

Thesis entitled "Development and evaluation of curcumin delivery systems for oral administration to improved brain health"

By Suchiwa Pan-on

has been approved by the Graduate School as partial fulfillment of the requirements for the Doctor of Philosophy in Pharmaceutical Sciences of Naresuan University

Oral Defense Committee

..... Chair
(Associate Professor Piyameth Dilokthornsakul, Ph.D.)

..... Advisor
(Associate Professor Waree Tiyaboonchai, Ph.D.)

..... Co Advisor
(Associate Professor Sutisa Thanoi, Ph.D.)

..... Internal Examiner
(Associate Professor Nanteetip Limpeanchob, Ph.D.)

..... Internal Examiner
(Assistant Professor Ph.D. Worawut Kriangkrai)

Approved

.....
(Associate Professor Krongkarn Chootip, Ph.D.)
Dean of the Graduate School

Title	DEVELOPMENT AND EVALUATION OF CURCUMIN DELIVERY SYSTEMS FOR ORAL ADMINISTRATION TO IMPROVED BRAIN HEALTH
Author	Suchiwa Pan-on
Advisor	Associate Professor Waree Tiyaboonchai, Ph.D.
Co-Advisor	Associate Professor Sutisa Thanoi, Ph.D.
Academic Paper	Ph.D. Dissertation in Pharmaceutical Sciences, Naresuan University, 2022
Keywords	curcumin, solid dispersion, self-emulsification drug delivery system, caco-2 cell, Dex-induced depression rat

ABSTRACT

Curcumin is a multitherapeutic agent with great therapeutic potential in central nervous system (CNS) diseases. However, its hydrophobicity and low bioavailability hinder its application. To circumvent these drawbacks, we developed polymer-based and lipid-based curcumin nano-formulations.

This study aimed to compare the physicochemical properties, *in vitro* release studies, permeation studies in Caco-2 cells and antidepressant activity of polymer-based and lipid-based of curcumin nano-formulations (CNF). The curcumin solid dispersions, as a polymer-based, were developed using melting solvent method. Two formulations of curcumin solid dispersion were prepared with polyvinylpyrrolidone (PVP) as a carrier without (CSD) and with surfactant as a co-carrier (CSD-S). While curcumin loaded solid self- emulsifying drug delivery systems (C-SSEDDS), as a lipid-based, were developed using Neusilin®UFL2 as a solid carrier. All developed CNF significantly showed improvement in curcumin water solubility, > 100-folds as compared to the free curcumin. Spherical droplets of < 200 nm were obtained when CNF were diluted with water. Within 5 min, 100% of the curcumin could be released from CSD and CSD-S, whereas only 60–70% of the curcumin from C-SSEDDS could be released. Moreover, permeation studies in Caco-2 cell monolayer revealed that all formulations provided significantly greater cellular accumulation and absorption

compared with the free curcumin. In addition, the physical and chemical stability of CNF was stable for at least 6-month storage at 4 ºC and room temperature.

Then, the antidepressant activities of CNF were investigated using a dexamethasone (Dex)-induced depression rat model. Results showed that Dex administration conduct to a range of depression-related behavioral traits, including anhedonia, despair, weight loss and anxiety-like behavior. All CNF given orally for 3 weeks showed an antidepressant-like effect on depressive rat model, as confirmed by the significantly higher rat body weight and sucrose consumption. Both of CSD and C-SSEDDS significantly reduced the immobility duration ($p<0.05$). Additionally, Dex-induced damage to the hippocampus and liver cells can be repaired with CNF. Consequently, CNF development has the potential to serve as a drug delivery system for curcumin, thus improving brain health as a supplement.

ACKNOWLEDGEMENTS

I wish to express my deepest sincere appreciation to my advisor, Associate Professor Dr. Waree Tiyaboonchai, for her constructive guidance, patience, inspiring words, understanding and her insights in pharmaceutical sciences. Through six long years travelling with me in the PhD journey, her kindness and expertise flourished me remarkably, both in the academic knowledge and the way of life. She helped me develop mentally and physically so I could be a better adult.

I am thankful to my co-advisor, Associate Professor Dr. Sutisa Nudmamud-Thanoi for his encouragement and advice. I am thankful to Associate Professor Dr. Nanteetip Limpeanchob, Naresuan University for their utmost kindness, and for being members of my internal committees. I also would like to give special thanks to all of my thesis committee members, to whom I am deeply grateful for their helpful comments.

I am also thankful to all staff in all the related academic staff and technicians at the Naresuan University, for their help throughout my study here at Naresuan University. Also, I would like to express my gratitude to all others for all supports to make me a complete this thesis but are not named in this acknowledgement.

For the financial support to this study, I would like to acknowledge the Center of Excellence for Innovation in Chemistry (PERCH-CIC) and Faculty of Pharmaceutical Sciences, Naresuan University, and the Agricultural Research Development Agency (ARDA).

I am grateful to all of my friends for teaching me the value of being kind, encouraging, and happy moments.

Lastly, I would like to give specially thank to my parents for all their sacrifice in providing me the best possible education. I also want to thank myself for never giving up on anything I try to do to better myself.

Suchiwa Pan-on

TABLE OF CONTENTS

Page

LIST OF TABLES

Page

LIST OF FIGURES

Page

CHAPTER I

INTRODUCTION

The first chapter contains four parts including statement of purpose, the objectives, expected output and the expected outcome. The details of each part are described below.

Statement of purpose

The incidence of neurodegenerative disease is continually growing. Moreover, increasing worldwide human lifespan has led to a significant rise in the prevalence of stroke, Alzheimer's disease (AD), Parkinson's disease (PD) and depressant activity (1). Thus, treatments for central nervous system (CNS) diseases are among the top therapeutics for drug research and development (2).

Curcumin is the active principle in this extract of rhizomes of Curcuma longa *Linn*. It has been reported as possessing to be a potent antioxidant, anti-inflammatory and monoamine oxidase (MAO) inhibitor, which decreases the oxidative stress and neurodegeneration (3, 4). The present study shows that curcumin in the doses of 100 mg/kg in mice has antidepressant-like action, similar to that of fluoxetine and imipramine when administered by the oral route. Thus, its antidepressant like activity could be due to an increase in serotonin, norepinephrine and dopamine levels in the brain. (4). Moreover, the potentially valuable curcumin antioxidant that protects β-Amyloid (βA). β-Amyloid (βA)-induced oxidative stress to neuronal cells was found to be one of the major causes of Alzheimer’s pathology (5). In addition, Curcumin pretreatment protects brain mitochondria against peroxynitrite *in vitro* by direct detoxification and prevention of 3-nitrotyrosine formation and *in vivo* by elevation of total cellular glutathione levels. These results suggest a potential therapeutic role for curcumin against nitrosative stress in neurological disorders (6).

Though curcumin has good therapeutic efficacy, its clinical application has been limited due to its low solubility and stability in aqueous solution (7-9). Researchers have shown that the curcumin degradation in water solution is linked to

hydrolysis that occurs rapidly above neutral pH (10). Moreover, one of the major limits related to curcumin studies involves very low serum levels, due to poor intestinal absorption, rapid metabolism, and rapid systemic elimination following oral use (7-9). In the present study were unable to demonstrate clinical or biochemical evidence of the efficacy of Curcumin Alzheimer's disease in this 24-week placebo-controlled trial although preliminary data suggest limited bioavailability of this compound (11). To overcome these limitations, the nanocarrier based delivery systems has been proposed to increase bioavailability of curcumin, as an attractive model poor bioavailability drug.

It has been reported that the interaction of curcumin with lipid-based or polymer-based nanoparticle improve its bioavailability. Solid dispersion (SD) has been proposed as a polymer-based system to increase curcumin bioavailability. SD is a solid dosage form whereby the active substance is dispersed in an inert carrier (12). Previous study reported that the Zn(II)–curcumin SD at 12-48 mg/kg body weight protect against cold resistant stress (CRS) induces ulcer lesions similar to that of lansoprazole (antiulcer drug) at 8 mg/kg in mice. Moreover, this study observed that Zn(II)–curcumin SD significantly decreased the depressant effect (13). However, it has been reported that the chemical stability of curcumin was shown to be affected by zinc oxide (14).

Another approach to improve curcumin oral bioavailability and pass through the BBB is self-emulsification drug delivery system (SEDDS), lipid-based system. This system is defined as a pre-concentrate containing a mixture of oil, surfactant, co-surfactant, co-solvent and drugs. SEDDS can be classified as self-microemulsifying drug delivery system (SMEDDS) and self-nanoemulsifying drug delivery system (SNEDDS). SMEDDS forms transparent microemulsions with a droplet size lower than 50 nm whereas SNEDDS are more recent with a droplet size less than 150 nm (15). Previous study reported that SMEDDS were successfully prepared with borneol as an oral brain-targeting enhancer. The pharmacokinetics results observed that borneol with doses of more than 50 mg/kg could increase both intestinal absorption and brain penetration of puerarin. These results suggested borneol in combination with SMEDDS could improve both the oral absorption and the brain penetration of puerarin in mice, which was promising for the development of an oral formulation of puerarin used in cerebrovascular diseases (16).

Recently, carrier-based approaches have been implemented which can bypass the majority of the challenges and is able to achieve desired delivery in the most efficient form. The principal advantages of nanocarriers include their increased solubilization potential, superior encapsulation, altered absorption pathways, prevention of metabolic degradation within gastrointestinal tract, chemical versatility of materials eligible for nanomedicines, flexibility in surface functionalization, drug and disease specific tailor made design capability, targeting potential and ability to incorporate wide variety of drug substances (17). SD and SEDDS showed high potential to delivery drug across the brain. Even though, there are many reports on the efficacy of these delivery system to brain, but there is no comparison among the efficacy of each system.

Accordingly, this study aimed to compare the physicochemical properties of polymer-based and lipid-based of curcumin nano-formulations (CNF). Additionally, the Caco-2 cell was cocultured to establish the transportation of curcumin across the gastrointestinal tract (GI tract) will be investigated. Finally, the antidepressant activities of CNF were investigated using a dexamethasone (Dex)-induced depression rat model. Curcumin is used as a model drug as there are many reports on its neuroprotective effects.

Objectives of the study

1. To systematically review current evidence of nanocarrier-based drug delivery system for an oral delivery of curcumin focusing on in vivo models and clinical studies.

2. To develop and characterize the processing parameters effecting the physicochemical properties of curcumin solid dispersion (CSD) and curcumin loaded solid self-emulsification drug delivery system (C-SSEDDS).

3. To evaluate the dissolution profile of CSD and C-SSEDDS.

4. To investigate the permeability and potential of CSD and C-SSEDDS delivering curcumin across Caco-2 cell model.

5. To compare the efficacy of lipid-based, C-SSEDDS and polymer-based, curcumin solid dispersion without (CSD) and with surfactant (CSD-S) in a dexamethasone (Dex)-induced depression model.

CHAPTER II

REVIEW OF RELATED LITERATURE AND RESEARCH

This chapter provides literature reviews related to this study. The reviews consist of five parts as follow; curcumin, gastrointestinal tract, solid dispersions, self-emulsification drug delivery system and nanocarrier drug delivery system. Each issue is described individually below.

Curcumin

Curcumin is widely used as a dietary spice, coloring agent in food, and herbal medicine and textile industry in Asian countries. Curcumin is a naturally yellow pigment obtained from dried rhizomes of Curcuma longa, Figure 1, belongs to the family Zingiberaceae. The rhizome of turmeric plant contains several phytochemicals including turmerin, essential oils and curcuminoids. Curcuminoids are the active ingredients present in turmeric and are responsible for its diverse pharmacological actions (18).

Figure 1 The rhizome of Curcuma longa

Source: http://www.samunpri.com/%E0%B8%82%E0%B8%A1%E0%B8%B4%E0%B9%89%E0%B8%99%E0%B8%8A%E0%B8%B1%E0%B8%99/

Physicochemical property

Curcuminoids consist of three phenolic compounds including curcumin (~94%), demethoxycurcumin (~6%) and bisdemethoxycurcumin (~0.3%), Figure 2 (18, 19). Curcumin is a major compound in curcuminoids. Curcumin, the polyphenolic yellow pigment which occurs naturally in turmeric has been shown a wide range of pharmacological activities (19). However, curcumin is practically insoluble in water (20). In fact, curcumin is practically insoluble in both acidic and neutral pH solution but soluble in alkali, ethanol, ketone, acetic acid and chloroform. Moreover, it has a high melting point in a range of 176-177°C (19). Its chemical unstable by hydrolysis, oxidation and photodegradation (20, 21).

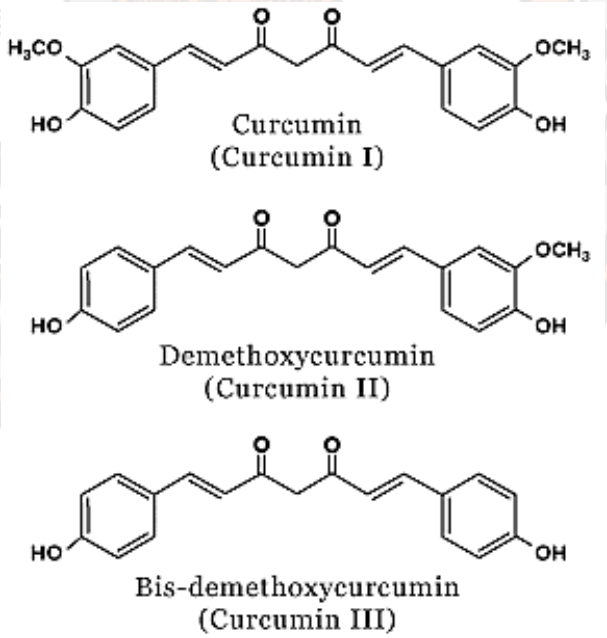

Figure 2 The chemical structures of curcumin, demethoxycurcumin and bisdemethoxycurcumin (22)

Curcumin undergoes pH-dependent first order degradation and the degradation is faster in neutral and basic pH. The half-life of curcumin in buffer at pH 3, 6.8 and 7.2 are 118.63, 39.75 and 9.40 min, respectively (Table 1). Trans-6-(40-

Hydroxy-30-methoxyphenyl)-2, 4-dioxo-5-hexenal is a major degradation product whereas vanillin, ferulic acid, feruloylmethane are minor degradation products, Figure 3. Most curcumin (>90%) is rapidly degraded within 30 min in 0.1 M phosphate buffer (pH 7.2, 37°C). In comparison, curcumin is more stable in cell culture media containing 10% fetal calf serum and human blood, less than 20% of curcumin is degraded after 1 h and approximately 50% decomposed after 8 h (23). Recently, curcumin has been reported to be stabilized by plasma proteins. The effects of plasma proteins (HSA, fibrinogen, IgG, and transferrin) on the hydrolysis of curcumin at pH 7.4 are investigated. The strong interactions with HSA and fibrinogen inhibit hydrolysis of curcumin and in turn lead to effective suppression of degradation (24). Moreover, tetrahydrocurcumin (THC), the major metabolites of curcumin, is more stable than curcumin in 0.1 M phosphate buffer (pH 7.2, 37°C) (25). Curcumin undergoes much faster degradation when exposed to sunlight. The colorless products identified during photodegradation of curcumin are vanillin, ferullic acid, and other small phenols (26).

Table 1 Buffer systems, observed rate constant and $t_{1/2}$ for the degradation of curcumin at 37°C (23)

pH	Buffer system	Buffer concentration (M)	k_{0bs} min^{-1} x 10^3	$t_{1/2}$ (min)
3.0	Citrate-phosphate	0.1	5.842	118.63
5.0	Citrate-phosphate	0.1	3.481	199.08
6.0	Phosphate	0.1	3.541	195.69
6.5	Phosphate	0.1	4.529	153.02
6.8	Phosphate	0.1	39.755	39.75
7.2	Phosphate	0.1	73.715	9.40
7.2	Phosphate	0.5	72.645	9.54
7.2	Phosphate	0.025	73.218	9.47
8.0	Phosphate	0.1	656.65	1.05

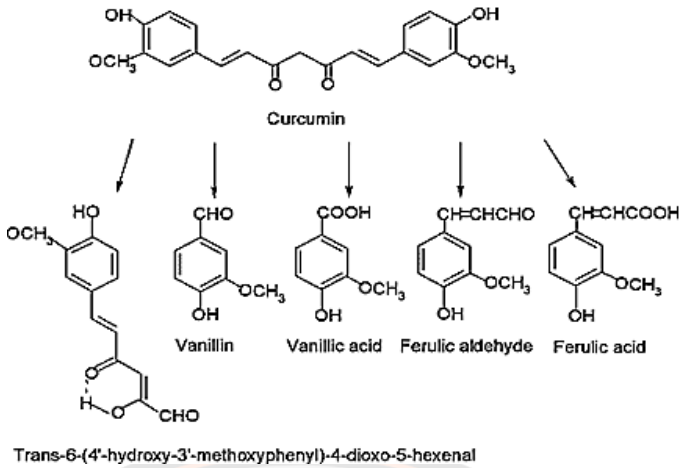

Figure 3 Structure of the degradation products of curcumin (23)

Therapeutic properties

Curcumin has been used for various therapeutics and culinary since ages in Indian subcontinents and well referenced in Ayurveda, an Indian system of medicine (27). Curcumin (diferuloylmethane) has been proved to be a potent antioxidant, anti-inflammatory, anticancer and MAO inhibitor, which decreases the oxidative stress and neurodegeneration (3, 4). Although curcumin wide – ranging therapeutic effects may be attributable to several multiple pharmacological activities, this study has focused on neuroprotective property.

Tentative evidence have observed that the consumption of turmeric/curcumin in curry by the Asian subjects is probably the reason for the better cognitive function when compared to the subjects who had never or rarely consumed curry (28).

In addition, there was no change in the number of nigral neurons with advancing age in the Asian Indian population. This findings of preserved nigral dopaminergic neurons suggest no age-related loss of nigral function in Asian Indians, unlike the Americans. This may explain the lower incidence of Parkinson's disease in Asian Indians (29).

Furthermore, the effect of 100 mg/kg curcumin in acute and chronic study of forced swimming test (FST) and tail suspension test (TST) in mice were too similar to that of fluoxetine and imipramine (antidepressant drug). From the results suggested that

antidepressant activity from curcumin could be due to an increase in serotonin, norepinephrine and dopamine levels in the brain (4).

Pharmacokinetics of curcumin

The pharmacokinetics of curcumin have been extensively studied in animals and humans (Table 2-3). In rats, curcumin administered as an aqueous suspension (2 g/kg) provided a maximum plasma concentration of 1 µg/ml within 1 hour, and dropped rapidly to undetectable levels within 5 hours (30). In another study, an oral dose of 2 g/kg to rats resulted in a plasma concentration of 1.35 ± 0.23 µg/ml whereas the same dose in humans resulted in undetectable (31). Even in clinical studies, Healthy volunteers who ingested 2 g pure curcumin powder after fasting showed less than 10 ng/ml curcumin in their plasma 1 h post-dose (30). In various clinical studies, only a few patients responded to curcumin despite high doses used (Table 3). The fact that curcumin also undergoes extensive metabolism in the liver and intestine means that high concentrations of curcumin cannot be achieved and maintained in plasma and tissue after oral ingestion. Pan et al. identified that 99% of curcumin is presented in the plasma as glucuronide conjugates and the plasma curcumin concentration in rats decline rapidly within 1 and 6 hours after intraperitoneal and oral administration, respectively (25). These results are in agreement with Ireson *et al*. who examined curcumin metabolism in rats that showed the majors metabolites of oral administration are curcumin glucuronide and curcumin sulfate and the metabolic reduction occurs very rapidly, in a matter of minutes (31). Moreover, Wahlstrom and Blennow reported that when 1 g/kg curcumin was given orally to rats, 75% of it was excreted in the feces, and negligible amounts were found in the urine. A clinical study of 15 patients receiving oral curcumin in doses between 36 and 180 mg daily for up to 4 months found neither curcumin nor its metabolites in urine, but the drug was recovered from feces (32).

Table 2 Examples of some preclinical studies reported with curcumin (33)

Animal	Route	Dose	Findings
Rats	Oral	1 g/kg	• Poorly absorbed • 75% excreted in feces
Rats	Oral	2% Diet	• 12 nmol/L in plasma
Mice	Intraperitoneal	100 mg/kg	• 2.25 μg/mL in 15 minutes • Disappeared within 3 hours
Rats	Intravenous	40 mg/kg	• Disappeared within 1 hour

Table 3 Examples of some clinical studies reported with curcumin (33)

Route	Dose	Findings
Oral (*n* = 34)	1–4 g/d for 6 months	• No reduction in peripheral biomarkers of inflammation. • No improvement in cognitive performance in Alzheimer's patients.
Oral (*n* = 21)	8 g/d until disease progression	• 1 patient showed stable disease (<18 months) and one showed tumor regression with an increase in serum cytokines 22–41 ng/ml peak plasma levels.
Oral (*n* = 25)	8 g/d for 3 months	• ∼1.77 μmol/l plasma concentration peaked at 1–2 hours and declined within 12 hours.
Oral (*n* = 12)	450–3,600 mg/d for 1 week prior to surgery	• Curcumin was poorly available, insufficient hepatic levels for inhibition of hepatic metastasis from colorectal cancer.

Safety of turmeric extract

According to the Food and Agriculture Organization of the United Nations, turmeric has been well received by Western countries as a coloring agent, food preservative and flavoring spice. To date, animals or humans studies have established no toxicity connected with the intake of curcumin at a high dose. A single daily oral dose ranging from 500 mg to 8 g/day for 3 months as a supplemental intake of curcumin

in human showed no toxicity (34). Moreover, the clinical study appeared that oral administration of curcumin was well tolerated at doses of 12 g/day which indicates that curcumin is safe. Only minor side effects such as diarrhea a have been reported in human trails with oral administration of curcumin (35). In addition, the research found that curcumin has no toxicity when administered at doses of 1-8 g/day and 10 g/day on human clinical trials (19).

Gastrointestinal tract (GI Tract)

Intravenous, intramuscular, intranasal, intradermal/transdermal and oral administration are the main routes of drug delivery. Each administration method faces specific barriers against the delivery of the drugs. Oral administration is the most widely accepted and preferred route for pharmaceuticals, due to its high convenience and better patient compliance (36). In comparison with other routes, the absorption mechanism of oral drugs is more complex. Oral drugs need to be soluble in gastric fluid and then they can be absorbed in the stomach, the small intestine or the colon, Table 4.

Gastrointestinal tract (GI)

The GI tract can be divided into upper and lower parts. The upper GI tract includes the oral cavity, pharynx, esophagus, stomach and duodenum which is the initial part of the small intestine. The lower GI tract includes the rest of the small intestine (jejunum and ileum), as well as the large intestine (colon and rectum) (37).

Table 4 Characteristics of different segments of the human gastrointestinal tract (GI) (37)

Segment	pH	Length (cm)	Mean Diameter (cm)	Mucus Average Thickness (μm)	Mucus Turnover (hour)
Stomach	0.8–5	20	NA	245 ± 200	
Duodenum	~7	17–56	4	15.5	
Jejunum	≥ 7	280–1000	2–2.5	15.5	24–48
Ilium	≥ 7	280–1000	3	15.5	
Colon	7–8	80–313	4–4.8	135 ± 25	

Mechanism of oral absorption

Absorption of active mainly occurs at the duodenum and jejunum segments of small intestine due to high amount of villi and microvilli which provide a large surface area (37). The microvilli have glycoproteins protruding in the luminal fluid and consist of goblet cells which releases mucus, a gel like structure containing approximately 95% water and mucin which blankets the surface. This is significant barrier to drug absorption for lipophilic drug. Transport of drug occurs through the apical side of the enterocyte membrane and then across a mucosal barrier (polarized enterocytes) crossing the basolateral membrane and entering the systemic circulation via the capillary network. These enterocytes are closely linked leading to producing the tight junctions (38). Molecules of drug can cross the luminal membrane through either mechanisms that involve passive diffusion or active transport, Figure 4.

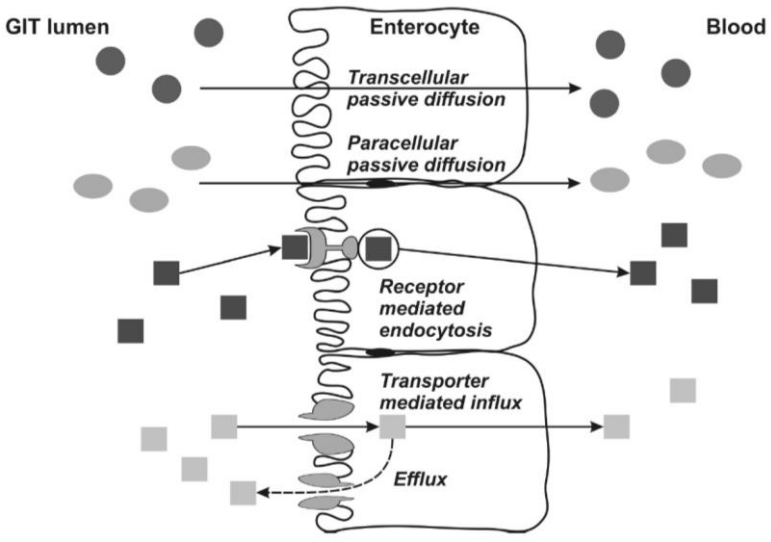

Figure 4 Pathways of drug absorption from the gastrointestinal tract (39).

1. Passive diffusion

Passive diffusion of a drug is driven by concentration gradient when the drug moves from higher to lower concentration. This route is comprised of two routes include paracellular and transcellular route.

Paracellular is the route which drug diffuses through the aqueous pores at the tight junctions between the intestinal enterocytes (38). Generally, drugs that are absorbed with this pathway are small molecules (molecular weight, MW < 250 g/mole) and hydrophilic in nature (Log P < 0). Because the junctional complex has a net negative charge, positively charged molecules pass through more readily, whereas negatively charged molecules are repelled (40).

Transcellular absorption occur through enterocytes, by passive diffusion, carrier mediated transport and endocytosis. Transcellular (lipophilic) route is requires drug diffusion across the lipid cell membrane of the enterocyte (38). This pathway is the major route of absorption for most of drug molecules (37). Normally, passive transcellular permeability rate is mainly determined by the transport rate across the apical cell membrane, which is controlled by the physicochemical properties of the absorbed compound. The compounds that are absorbed via the transcellular route are unionized which lipophilicity of Log P > 0 and MW > 300 g/mole (41). Transporter and receptor mediated absorption is controlled by membrane anchored transporters or receptors, which are able to transport the compound in the direction of absorption (influx) or excretion (efflux). Whereas, endocytosis is a process by which a particle enters into a cell without passing through the cell membrane (42).

2. Active transport

The carrier-mediated transport processes involve both facilitated and active mechanisms engineered by transport proteins responsible for uptake or efflux of drugs in the intestine. Commonly, efflux transporters expressed in the intestine membranes include P-glycoprotein (P-gp), multidrug resistance proteins (MRP 1–6), and breast cancer resistance protein (BCRP). These are members of the ATP-binding cassette (ABC) transport proteins which utilize ATP as energy source to transport substrates against a concentration gradient from the intestinal cells back to the intestinal lumen or to the blood (43).

Furthermore, the pharmacokinetic is another factor that significantly affects oral bioavailability and efficacy of many drugs. The pharmacokinetic factors as followed;

Absorption

A simple measure of absorption is the ratio of the concentration of a compound in blood following intravenous and non-intravenous (e.g., oral) administration. Because the entire blood supply of the upper gastrointestinal tract passes through the liver before reaching the systemic circulation, it may be metabolized during the first passage of drug absorption (44).

$$\text{Absorption} = D_{oral}/D_i*100$$

Where D_{oral} is the distribution of a compound after oral administration and D_i is its distribution after intravenous administration (44).

Distribution

Once in the bloodstream, the drug then distributes across the body. It is not possible to determine this directly; there is a relationship between drug concentration in blood and its volume of distribution (V_d) (44):

$$V_d = D_{body}/D_{blood}$$

Where D_{body} is the amount of drug in the body at any time and D_{blood} is the corresponding amount of drug in blood at the same time (44).

Metabolism

The purpose of drug metabolism is to make drugs more water soluble so they can be more easily excreted from the body. There are three general types of biotransformation reactions involved in the metabolism of drugs and other foreign compounds: 1) oxidation- reduction, 2) hydrolysis, and 3) conjugation. Most of these drug-metabolizing enzymes are found in the liver, but they are also found in other tissues. Oxidative metabolism by cytochrome p450 enzymes is the primary method of drug metabolism and are mainly located in the endoplasmic reticulum and mitochondria of cells, particularly in the liver and small intestine (44).

Excretion

The kidney serves as the major organ responsible for the removal of most drugs, especially those that are water soluble. Another key organ of excretion is the liver. Because the passage from the blood into liver is normally not restricted, they often reach the hepatic extracellular fluid from the plasma (44).

The key measure of drug elimination is clearance, which may be defined as the theoretical volume of fluid from which a drug is completely removed in a given period of time. It can be considered at both the level of a given organ or the body as a whole. The total body clearance (Cl_T) of a drug is defined by the following equation (44):

$$Cl_T = D_0/AUC$$

Where AUC is the area under the blood concentration time curve. As well as affecting the absorption and metabolism of a drug, lipophilicity also influences its distribution (44).

Half-life ($t_{1/2}$)

The $t_{1/2}$ of a drug in plasma is one of the major factors to establish the optimal dosage regimen. Administration of drugs with a short $t_{1/2}$ requires frequent dosing and often results in poor patient compliance. Because the $t_{1/2}$ of a drug is determined by both of distribution volume and its elimination clearance, the prolongation of $t_{1/2}$ can be achieved by increasing the volume of distribution or decreasing the clearance, or both (44).

Caco-2 cell line

The Caco-2 cell line is the most common and extensively characterized cell-based model for the absorption assessment of drugs through the membrane enterocytes. The Food and Drug Administration (FDA) recognized the model system as useful in classifying a compound's absorption characteristics in the Biopharmaceutics Classification System. It is used in many pharmaceutical companies to screen drug candidates for their absorption. More recently, they have been used to determine the efflux mechanisms of drugs and natural products (45).

Caco-2 cells spontaneously differentiate into monolayers with the most of the morphological, structural and functional characteristics of the intestinal mucosa. Full differentiation requires about 20 days of culture. After this culture period, the polarized cells have formed tight junctions at their lateral interfaces and they express various enzymes, including glutathione S-transferees and some CYP isoenzyme. Additionally, several active uptake carriers (e.g., for peptides, amino acids, glucose, bile acids) and efflux carriers (e.g., MRPs and P-gp) are expressed in differentiated Caco-2 cells. The complete polarized Caco-2 cells resemble human small intestinal mucosa cells expressing brush borders, tight junctions and, efflux and uptake transporters at both apical and basolateral compartments, Figure 5 (45, 46).

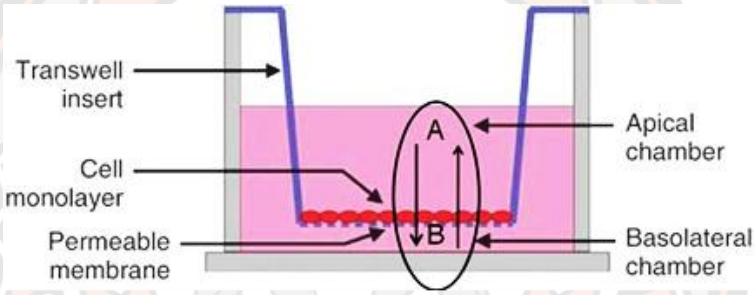

Figure 5 Schematic representation of the Caco-2 cell monolayer grown onto a polycarbonate membrane (46)

Although Caco-2 cells express many enzymes and transporters present in the small intestine, the high TEER and poor paracellular permeability properties. Many active transport proteins, enzymes, and efflux transporters are expressed in the Caco-2 cells. For instance, while CYP3A4 and CYP3A5 are the main CYP isoenzymes in human enterocytes, their expression level is extremely low in Caco-2 cells. With respect to efflux carriers, human jejunal enterocytes display higher expression of BCRP than MRP2. In the Caco-2 cell system, however, the opposite is true (45).

Evaluation of epithelial integrity and maturity of the monolayers can be performed by measuring transepithelial electrical resistance (TEER). TEER measurement is done by using a volt-ohm meter that is equipped with electrodes placed in the upper and lower chambers of the insert. TEER values depend on the surface area of the transwell inserts, the numbers of cells seeded, filter support, culture condition,

and passage number and are reported to range between 150 to 1600 $\Omega \cdot cm^2$. An alternative method for assessing monolayer integrity is the measurement of permeability of hydrophilic and hydrophobic marker molecules, such as (^{3}H)-mannitol, (^{14}C)-mannitol, poly(ethylene glycol), fluorescent compounds (fluorescein, Lucifer yellow, inulin or fluorescein-isothiocyanate (FITC)-labeled dextran with various molecular weights), and propranolol, which are passively transported across the monolayers by the paracellular and transcellular routes. The intact monolayer should exclude the passage of marker molecules (47).

In addition, these cell lines can be used for screening and studying interactions of drugs with transporters through blood brain barrier (BBB) (48, 49). To evaluate whether the simple P_{app} value is able to predict how well the drug is transferred across the blood brain barrier (BBB). The differences in P_{app} values of model drugs between brain microvessels endothelial cells (BBMEC) and Caco-2 cell were studied. The correlation between BBMEC and Caco-2 was $r = 0.93$ ($P < 0.001$). Moreover, the correlation between *in vivo* and *in vitro* model was found in BBMEC model ($r = 0.99$, $P < 0.001$) and the Caco-2 ($r = 0.91$, $P < 0.01$), respectively (50). This also emphasizes the importance of *in vivo* methods in assessing the ability of drugs to cross the blood–brain barrier: although *in vitro* methods are advantageous during early drug discovery, *in vivo* methods clearly provide more extensive and diverse information of the new drug candidate (51).

Solid dispersion (SD)

A drug with low solubility is rate limiting steps leads to low bioavailability of a drug. Several methods have been attempted to enhance the aqueous solubility of drugs such as crystal modification, particle size reduction, self-emulsification and solid dispersion (52).

Solid dispersion (SD) is one of the most techniques to improve water solubility of the drug. SD can enhance the dissolution of poorly soluble drug while the preparation process is simpler and applicable than some other techniques (53).

SD refers to the group of the solid state consisting of one or more active ingredients in an inert carrier or matrix by melt, solvent or melting solvent method. The drug or drugs dispersion in diluent or diluents by traditional mechanical mixing is not included in this category (54).

Classification of SD

The classification of SD based on their molecular arrangement can be divided in to 6 types as shown in Table 5 (55). Moreover, the designation from several studies is based on the preparation method. However, different preparation methods can result in the same subtypes that SD should preferably be designated according to their molecular arrangement (56).

Table 5 Molecular arrangement in SD (55)

	Type of SD	matrix*	drug**	remarks	no. phases
I	eutectics	C	C	the first type of SD prepared	2
II	amorphous precipitations in crystalline matrix	C	A	rarely encountered	2
III	solid solutions				
	continuous solid solutions	C	M	miscible at all compositions, never prepared	1
	discontinuous solid solutions	C	M	partially miscible, 2 phases even though drug is molecularly dispersed	2
	substitutional solid solutions	C	M	molecular diameter of drug (solute) differs less than15% from matrix (solvent) diameter. In that case the drug and matrix are substitution. Can be continuous or discontinuous. When discontinuous: 2 phases even though drug is molecularly dispersed	1 or 2
	interstitial solid solutions	C	M	drug (solute) molecular diameter < 59% of matrix (solvent) diameter. Usually limited miscibility, discontinuous. Example: Drug in helical interstitial spaces of PEG.	2

	Type of SD	matrix*	drug**	remarks	no. phases
IV	glass suspension	A	C	particle size of dispersed phase dependent on cooling/evaporation rate. Obtained after crystallization of drug in amorphous matrix	2
V	glass suspension	A	A	particle size of dispersed phase dependent on cooling/evaporation rate many solid dispersions are of this type	2
VI	glass solution	A	M	requires miscibility/solid solubility, complex formation or upon fast cooling/evaporation during preparation, many (recent) examples especially with PVP	1

*A; matrix in the amorphous state, C; matrix in the crystalline state

** A; drug dispersed as amorphous clusters in the matrix, C; drug dispersed as crystalline particles in the matrix, M; drug molecularly dispersed throughout the matrix

The molecular arrangements control the properties of SD. Therefore, it is necessary to usage expression that point the molecular arrangement in the SD, Figure 6 (56).

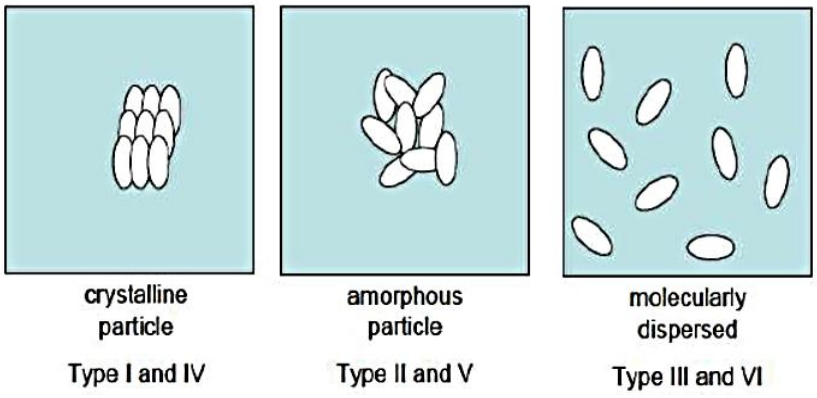

Figure 6 Molecular arrangement in SD *(56)*

In addition, the SD have also been developed based on the physical state of the carrier which in crystalline or amorphous. The SD are divided into crystalline and amorphous SD, respectively. The classification of SD according to their realization, advancement and composition can also be classified into four generations, Figure 7, as follows first, second, third and fourth generation (53).

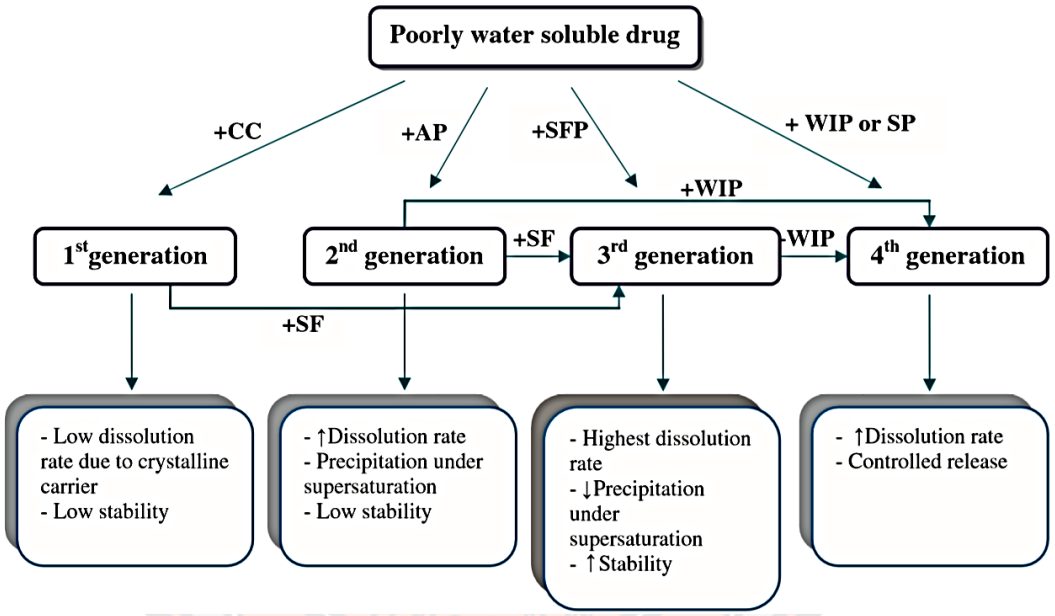

Figure 7 Composition and properties of four generations of solid dispersions. CC: crystalline carrier, AP: amorphous polymer, SFP: surfactant polymer, WIP: water insoluble polymer, SP: swellable polymer, SF: surfactant, (↑): increase, (↓): decrease (53)

First generation of SD

The first generation of SD was prepared using a crystalline drug and a crystalline carriers such as urea, sorbitol and mannitol. The crystalline SD has dispersed a crystalline drug within a crystalline carrier for forming a eutectic or monotectic mixture. In the eutectic mixture, the melting point of the mixture is lower than the melting point of the drug and carrier while the stability of the drug and carrier

in the monotectic mixture not changed. However, the SD containing a mixture of the micro fine dispersion and another component will be separated phase because the mixture of the drug and carrier not exacted as the eutectic composition. The SD in crystalline form may also exist in amorphous particles or separate molecules (crystalline solid solutions). The main reasons for improving drug solubility and dissolution rate are particle size reduction, wettability improvement and polymorphic change. However, the main disadvantages of crystalline SD are low dissolution rate and drug release when compared with amorphous SD (53).

Second generation of SD

The second generation of SD containing amorphous carriers instead of crystalline carrier (56). The classification of amorphous SD includes amorphous solid solutions (glass solutions) and amorphous solid suspensions depend on the physical state of the drug. The drug and amorphous carrier are completely miscible to form a molecularly homogenous mixture for the amorphous solid solution while amorphous solid suspension consists of two separate phases with the limitation of carrier soluble or an extremely high melting point. The amorphous SD exists more than one state, for instance, an amorphous SD can both dissolve and suspend in a carrier or exist in amorphous and crystalline state at the same time (53). In addition, in these systems are reduce the size of drug particle to nearly a molecular level with solubilizing or co–dissolve the drug by water soluble carrier. Moreover, the carrier enhance wettability and dispersibility of the drug by the carrier, and to produce amorphous forming of drug and carriers (56).

Amorphous carriers are divided into fully synthetic polymers and natural product based polymers (53, 55). The fully synthetic polymers include polyvinylpyrrolidone (PVP) (57), polyethylene glycol (PEG) (58), Eudragit RS (59), polyvinylpyrrolidone -co- vinylacetate (PVPVA) (60) and polymethacrylates (55). The natural product based polymer consists of cellulose derivatives such as ethyl cellulose (EC) (61), hydroxypropylcellulose (HPC) (61), hydroxypropylmethyl cellulose (HPMC) (62), hydroxypropylmethylcellulose phthalate (HPMCP) (61) and starch derivatives (55). Among them, PEG and PVP are the most frequently investigated polymeric carriers (63). The aqueous solubility of these polymers often decreases and then the viscosity increases due to their chain lengths or molecular weight increase. The

high viscosity of polymer can prevent the recrystallization of the drug in the preparation method, storage and dissolution process (53).

Third generation of SD

The amorphous SD can increase the rate of drug release. However, drug can precipitate and then decrease the drug concentration in *in vitro* and *in vivo* study, thus negatively affecting the drug bioavailability. In the preparation process (cooling or solvent removal) and during storage, the drug may also recrystallize from amorphous state. In the third generation of SD, the carriers or additives with surface active agents or self-emulsifiers properties are introduced due to showed significant improvement in overcoming the above problems such as precipitation and recrystallization (53). Thus, in this process are prepared by using a surfactant carrier or mixtures both of amorphous polymer and surfactant (56). Surfactants or emulsifiers in SD are introduced because of their increase the physical and chemical stability of drug. In fact, the amphiphilic structure of surfactant can improve miscibility, a degree of bioavailability of a poorly soluble drug, stabilize the SD and avoid the recrystallization of drug. In addition, the wettability of drugs could be increased from surfactants or emulsifier and prevent the precipitation of drug due to supersaturation by absorbing to the outer layer of drug particles or forming micelles to encapsulate drug (53). Several surfactants used as carriers such as soluplus® (64), Tween 80 (65), sodium lauryl sulfate (SLS) (65), Poloxamer 188 (66).

Fourth generation of SD

The fourth description of SD is a controlled release solid dispersion (CRSD) containing poorly water-soluble drug with a short biological half-life. CRSD often requires solubility improvement and extended-release in a controlled manner. In CRSD, the poorly water soluble drug in carriers could improve the drug solubility due to the molecular dispersion while water insoluble polymer or swellable polymers can be used to retard release of drug in the dissolution medium (53). Therefore, the carrier with water soluble or miscible carrier appears in a fast release of the drug and a poorly soluble or insoluble carrier induces to a slow release of the drug from the matrix (54). In addition, the polymer with insoluble or slowly dissolve in water can sustain release of poorly water-soluble drug. The conventional polymers used for retarding the release of poorly water-soluble drugs in CRSD include ethyl cellulose (EC), HPC, Eudragit®

RS, RL, poly (ethylene oxide) (PEO) and carboxyvinylpolymer (Carbopol®). CRSD system, it's used the sustainable polymers or mixing of these polymers in SD system or can use other materials having the solubilizing capacity and sustaining the action. The mechanism of CRSD which the drug can be released include diffusion and erosion (53).

Materials used as carrier in SD

There are many factors that affect to solubility and dissolution of SD include nature of the carrier, ratio of drug to the carrier, preparation method, molecular weight of the carrier and synergistic effect of carriers (67). The carrier selection has the influence on the solubility and dissolving in water for improving the dissolution rate of a drug (55). Various carriers used for preparing the solid dispersion are tabulated in Table 6.

Table 6 Materials used as carrier for SD (68)

No	Category	Carriers
1	Sugars	Sucrose, sorbitol, maltose, xylitol, mannitol, lactose
2	Acids	Citric acid, succinic acid
3	Polymeric materials	Polyvinyl pyrrolidone (PVP), polyethylene glycol (PEG), hydroxypropyl methyl cellulose (HPMC)
4	Insoluble or enteric polymer	Hydroxy propyl methyl cellulose phthalate (HPMCP), eudragit L100, eudragit E100, eudragit RL, eudragit RS
5	Surfactants	Polyoxyethylene stearate, poloxamer 188, deoxycholic acid, tweens, spans
6	Miscellaneous	Pentaerythritol, pentaerythrityl tetraacetate, urea, urethane, hydroxy alkyl xanthins

Preparation methods of SD

Several preparation methods for SD have been reported in literature. These methods are given below.

Melting method

For this method, drug and carrier are melted together above the melting point of both components (69). The mass of homogenous molten is rapidly solidified by placing it in a freezer, using an ice bath, immersing in liquid nitrogen or placing inside

a desiccator at room temperature (70). After solidification, the mixture was crushed, pulverized and sieved. Under some conditions, the solution molecule is arrested in the solvent matrix by the rapid solidification process (56). Simple and easier to upscale are the advantages of this method. However, it's not suitable for drug and excipients that degraded with high temperature (69).

Solvent method

SD in this method is dissolve the physical mixture of drug and carrier in a common solvent, followed by solidified rapidly and evaporation the solvent (54). The main advantage of this method solve the problems from melt (53). However, this method has several disadvantages include residual solvent remaining after evaporation process that causes toxicity due to difficult in complete removing the liquid solvent. In addition, a suitable solvent for dissolving drug and carrier are difficult because carriers are hydrophilic while drugs are hydrophobic (53).

Melting solvent method (melt evaporation)

Melting solvent method is a combination both of the melt method and the solvent method. The drugs are dissolved in a suitable solvent and then incorporating the solution directly into the melt of carrier followed by solidification and solvent removal the solvent. It is a useful method when formulating the drug that has a high melting point, and the mixing time is lower than melt method leads to protect the drug from thermal degradation. In addition, the molten carrier is more easily dispersed and dissolved in the solvent in comparison with solvent method (53).

Melt extrusion method

This technology is similar to melt method except for the applying of an extruder. A mixture of active and carrier are simultaneously melted and homogenized by hot stage extrusion using a co-rotating twin-screw extruder which shaped as tablets, granules, pellets, stick or powder (56). The main effect is melting rate relating to the physical and rheological properties of a polymer. When an amorphous polymer is a low viscosity leads to high melting rate. The advantage of this method is the low residence time of high temperature in the extruder which decreases the risk of drug degradation, and also easy scale up (53). However, the high local temperature with high shear forces in extruder could be a problem for heat sensitive material (56).

Lyophilization technique/freeze drying

This technique is employed to remove the common solvent from the mixture of active and carrier including two steps: freezing and lyophilization. The process consisting of a drug-carrier solution immersed in liquid nitrogen until it is completely frozen, and the frozen solution is then lyophilized. Decreases the risk of phase separation is the advantage and the disadvantage is low freezing temperature from most organic solvents with not stay frozen during sublimation (53).

Melt agglomeration process

In this method, SD used a binder acts as a carrier. SD is prepared by a heating binder, drug and excipient with a temperature higher than a melting point of binder (melt-in procedure) or by spraying a dispersion of the drug in a molten binder on a heated excipient (spray-on procedure) by using a high shear mixer. However, disadvantages of this method is larger of the drug particles resulting to distribution and coalescence of the fine particles (56).

The use of surfactant

The surfactant in this system is very important in solubilization. The SD containing surfactant can modify their hydrophobicity. Moreover, a charge of surface and other properties is governed interfacial processes such as flocculation/dispersion, floatation, wetting, solubilization, detergency and increased oil recovery and corrosion inhibition. Many types of research have been reported that the surfactant for solvation or plasticization leads to decrease short melt time. Moreover, glass transition temperature and the combined glass transition temperature of SD is a unique property of surfactants (56).

Electrospinning/electrostatic spinning method

Electrospinning is equipment which prepared SD by placed a drug-polymer solution into a spinneret connected with a micro syringe pump. Then a high voltage super supply (5-30 kV) is applied to the needle tip to induce a charge on a surface solution (53, 69). After the drug polymer solution is applied by high voltage, it cause a cone shaped deformation of the drop of polymer and then the electrostatic force on the deformed polymer drop can break the surface tension barrier with a jet stream leading to from the drug polymer solution (69). This technique has a high potential for preparing a nanofibers and control drug release of biomedicine (56).

Supercritical fluid technique

This technique uses supercritical carbon dioxide (CO2) with the temperature and pressure higher than a critical point as a solvent or anti-solvent. This technique is prepared by dissolving the drug and carrier in a supercritical fluid and then sprayed through a nozzle into an expansion vessel with low pressure. The rapid nucleation of the drug and carrier is induced by rapid expansion leads to form SD with a desirable size distribution in a short time. However, if the solution is quickly sprayed by the supercritical carbon dioxide leads to SD precipitation (53).

Mechanism behind improve solubility

There are many reasons of SD techniques for improving solubility of the poorly soluble drug.

Reduced the size of particles

Preparation of SD can reduce the particle size to nearly a molecular level leading to increasing a surface area resulting in an improved solubility and bioavailability (55, 56).

Increased wettability of the particles

It was observed that even carriers without any surface activity improved drug wettability. Moreover, carriers can influence the drug dissolution profile by direct dissolution or co-solvent effects (56).

Particles with high porosity

The SD particles have been found to have a higher degree of porosity and increase porosity also depends on the carrier properties (55, 56). SD particles increased porosity accelerate to the drug release profile (55).

Drugs in amorphous state

The preparation of SD is changed a polymorphic form of the drug from crystalline to amorphous state leads to enhance the dissolution rate because less energy is required to break up the crystal lattice during the dissolution process and then the drug solubility improved (53).

Reported on solid dispersion improving drug cross the brain

It has been reported that gastrodin co-administrated with borneol using solid dispersion was rapidly absorbed from the GI tract as compared to administration of gastrodin alone. This is because gastrodin is readily soluble in water and can be quickly

absorbed in the intestinal tract (71). Additionally, according to Abd-Elrasheed et al., Zelapon-loaded solid dispersion improved zelapon delivery to the systemic circulation through drug absorption, avoiding first-pass metabolism and improving drug bioavailability and brain targeting (72). In addition, naringenin-loaded solid dispersion in Sprague-Dawley rats had a 2.16-fold higher relative oral bioavailability than the free drug (73).

Characterization a physicochemical properties of SD

The dissolution enhancement of poorly water soluble drug from SD can be proven by the standard dissolution method, while the physicochemical properties of drugs should be evaluated such as the physical state, the interaction between drug and carrier and stability of SD. These properties can measure by using instruments and analytical techniques. The crystalline state of drugs and the degree of crystalline are characterized (53). The drug in crystalline form is characterized following Table 7.

Table 7 Various characterization methods to assess SD (74)

Characterization	Methods	Significance
Drug-carrier miscibility	- Hot stage microscopy (HSM) - Differential scanning calorimeter (DSC) - Transmission electron microscopy (TEM) - X-ray Diffraction (XRD) - Nuclear magnetic resonance (NMR)	To find out the complex formation between drug and carrier. To check the degree of amorphization.
Drug-carrier interactions	- Fourier transform infrared spectroscopy (FTIR) - Raman spectroscopy Solid state NMR studies	To find out the solid state interaction between drug and carrier and formation of inclusion complex.
Surface properties	- Dynamic vapor sorption - Inverse gas chromatography - Atomic force microscopy Raman microscopy	To study the morphology and degree of crystallinity.
Stability	- Humidity studies Isothermal calorimeter	To find out the degree of recrystallization.

Characterization	Methods	Significance
	- DSC (Tg, temperature recrystallization) - Dynamic vapor sorption Saturated solubility studies	
Amorphous content	- Polarized light optical microscopy - Hot stage microscopy - Humidity stage microscopy - DSC (MTDSC) - Powder XRD	To find out the amorphous transition.
Dissolution rate	- Dissolution studies - Intrinsic dissolution - Dynamic solubility studies	To find out the rate and extent of drug release.

Advantages of SD

When compared SD techniques with other techniques to enhance bioviability of poorly water soluble drug such as salt formation, particle size reduction by using milling or micronization, SD show many important advantages to become one of the most promising strategies. The SD can decrease the size of drug particle into a molecular level while other techniques have a limitation of particle size limit ~2-5 μm which easily agglomerate when combined in the formulation, dissolution process or during storage (53).

The interaction between drug and carrier in SD is an advantage for rapid absorption due to a release of the drug in supersaturation state and prevents the agglomeration of the drug particles. In addition, the particle size of drug from SD are still in submicron (<1 μm) after precipitated in the dissolution medium due to supersaturation, and the dissolution rate is still higher than other techniques (53).

The SD techniques can be used in solid oral dosage forms because more acceptable for patients. Moreover, this process is more simple and applicable than some techniques such as salt formation or nanoparticle/nanoemulsion (53).

Disadvantages of SD

The main problem of SD is changed amorphous to crystalline state during processing (mechanical stress) or storage (temperature and humidity stress) (55). Moisture of polymer is an effect on the storage stability of amorphous SD because it may increase the drug mobility and then promote drug recrystallization as well as decreased the performance of *in vivo* permeation (55, 56). Drug crystallization including two steps: nucleation and then crystal growth that resulting in diffusion or rearrangement of drug molecules, Figure 8 (53).

Physical stability of amorphous SD

The SD containing crystalline particles leads to form nuclei that can be a starting point to further crystallization while the SD containing amorphous drug particles also crystallization but a nucleation step is required prior to that. The drug in homogeneous SD is molecularly dispersion, and crystallization requires another step. The migration of drug molecules can occur through the matrix before nucleation and then physical degradation by both diffusion and crystallization of drug molecules in the matrix, Figure 8 (75).

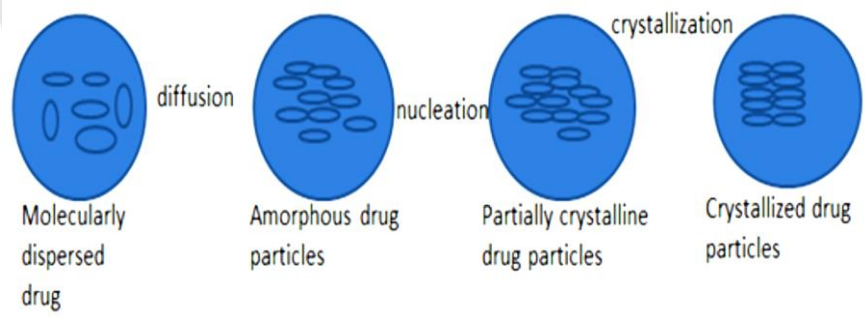

Figure 8 Physical changes in solid dispersions resulting in crystallization *(75)*

The amorphous SD can be stabilized primarily by reducing their molecular mobility (which turn prevents crystallization), while the simplest approach is store below its T_g with retarding the molecular mobility of the amorphous state making it sufficiently stable to provide a practical shelf life (76). However, the stability of SD properties also depends on the interaction of molecular level between the drug and the carrier. A model of the physical stability of amorphous drug polymer SD consisting 2

general including thermodynamic and physicochemical. The thermodynamic approach is based on free energy, entropy and enthalpy while the physicochemical approach focusing on chemical structure and intermolecular interactions, especially hydrogen bonding, as well as molecular mobility. The stability of physical SD following factors should be considered to achieve optimal physical stability (77).

Polymers as stabilizers

The polymer is a repetitive structure of monomer units which each monomer linked to another monomer and formed an extended structural framework. Based on their origin, the classification of the polymer includes natural polymers, e.g., such as cellulose derivatives or gum and synthetic polymers, e.g., such as poly (vinylpyrrolidone) or poly (ethylene glycol). Moreover, the classification of the polymer can divide into amorphous, semi-crystalline or crystalline with polymer strength and stiffness increases as well as increases in the degree of crystallinity as a result of greater intermolecular interactions. The polymers can form extensive inter and intra chain cross links and then ultimately form a network like complex structural properties. After incorporated the drug into these networks hinders the molecular mobility of the latter with any heterogeneous molecule, polymer chains act as crystallization inhibitor resulting that preserve the viability of amorphous form intact (76).

Increasing T_g of drug by using anti-plasticization

The ratio of melting temperature (T_m) to glass transition temperature (T_g) is an indicator of its glass forming ability with also linked to the SD stability. As higher the ratio of T_m to T_g may be probability of crystallization due to high T_m will have high lattice energy and will have higher risk of crystallization. Whereas, the drugs that have low T_g will have higher mobility at room temperature and then changes to crystalline state (69). Incorporating of an amorphous drug that has a low T_g with a high T_g polymer at the molecular level leads to develop the new system with T_g moderate from these two components. The T_g of drug after mixing with polymers increases due to the amorphous drug undergoes antiplasticizer, whereas the T_g of the polymer decreases and it undergoes plasticization with decreases the drug molecular mobility and stabilizing the amorphous state (76).

Chemical interaction between drug and polymer

The drug excipient interaction is one of the ways towards stabilization of amorphous SD with ionic interaction or due to intermolecular hydrogen bonds leads to stabilization and prevents recrystallization of SD during storage (69, 76). The chemical interaction of SD between drug and polymers is characterized by FTIR, Raman and NMR spectroscopy (69). It has been reported that interactions between PVP and indomethacin (IMC) were mainly hydrogen bonding interactions with a proton acceptor (through either the oxygen or nitrogen atoms of the pyrrole ring) from PVP and the OH group of the carboxyl acid function from IMC using IR spectra to confirmed the presence of hydrogen bonding interaction between IMC and PVP in amorphous solid dispersion (76). In addition, the interaction intensity was found to be increasing when increases the polymer and then dissolution rate increased (69).

Self-emulsification drug delivery systems (SEDDS)

Self-emulsification drug delivery systems (SEDDS) are defined as a pre-concentrate containing a mixture of oil and surfactant, sometimes it contains co-surfactant or co-solvent, and active compound which emulsify spontaneously to produce the fine oil-in-water emulsions, when this emulsion introduced into aqueous phase under gentle agitation. Upon oral administration, these systems form fine emulsions (or microemulsions) in the gastrointestinal tract (GIT) with mild agitation provide by gastric mobility (15).

Type of SEDDS

SEDDS include both self-microemulsifying drug delivery systems (SMEDDS) and self-nanoemulsifying drug delivery systems (SNEDDS). SMEDDS indicate the formulations producing transparent microemulsions with droplets size of less than 50 nm whereas SNEDDS form emulsions with the globule size range between 100 to 300 nm (78). The term ‘droplet’ is determined to micelles, mixed micelles which exist in the emulsions. Generally, the microemulsions is a thermodynamically stable colloidal dispersion consisting of small spheroid particles (composed of oil, surfactant, and possibly co-surfactant and/or co-solvent) dispersed within an aqueous medium and thus in equilibrium (15). In contrast, the nanoemulsion is non-equilibrium colloidal dispersion system that over time spontaneously will exhibit coalescence of the

dispersed droplets. Actually, the droplet structure in both nanoemulsion and microemulsions are very similar: surfactant molecules with non-polar tails protrude into the lipophilic core formed by the oil, while the polar head groups protrude into the surrounding aqueous phase, Figure 9 (79).

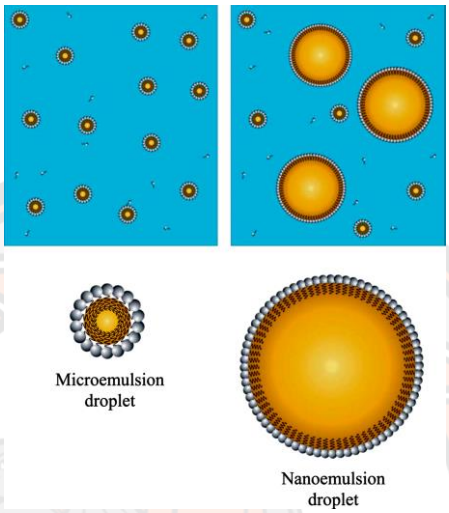

Figure 9 Schematic of microemulsions droplet and nanoemulsions droplet formed from oil, water and surfactant (79)

Excipients screening for SEDDS

The self-microemulsification process is specific to the nature of the oil/surfactant pair, the concentration of surfactant and oil/surfactant ratio, the concentration and nature of co-surfactant and surfactant/co-surfactant ratio at which self microemulsification occurs (80). Supporting these facts, only a specific combination of pharmaceutical excipient combinations could form fine self-emulsifying systems. The following points should be considered in the SEDDS excipients selection:

- Solubility of drug in different excipients (80)

- The final selection of oil, surfactant and co-surfactant/co-solvent based on solubility studies and the ternary phase diagrams preparation (80)

Oil phase

Oil is the most important excipient which can solubilize the lipophilic drug or facilitate self-emulsification in a specific dose and it can increase the fraction of lipophilic drug transported via the intestinal lymphatic system, thereby increasing absorption from the GI tract depending on the molecular nature of the triglyceride (15). Both of long and medium chain triglyceride (LCT and MCT) oils with different degrees of saturation have been used for the design of self-emulsifying formulations. Furthermore, edible oils which could represent the logical and preferred lipid excipient choice for the development of SMEDDS are not frequently selected due to their poor ability to dissolve large amounts of lipophilic drugs. Modified or hydrolyzed vegetable oils have been widely used since these excipients form good emulsification systems with a large number of surfactants approved for oral administration and exhibit better drug solubility properties. They offer formulated and physiological advantages and their degradation products resemble the natural end products of intestinal digestion (78).

Surfactants

Surfactants with amphiphilic properties help the solubilization of lipophilic drugs so preventing their precipitation in the gastrointestinal lumen. The most widely recommended ones being the non-ionic surfactants with a relatively high hydrophilic−lipophilic balance (HLB) due to their less toxicity and because typically possess low critical micelle concentration (78). These surfactants are added to SEDDS formulation because their ability to decrease the surface tension and form monolayer between the oil and aqueous phase. So, the SEDDS become more stable and stay in GIT for longer time in soluble form, which is useful for the absorption of the drug (15).

Co-surfactants

Co-surfactant mainly helps improve the drug load capacity, resulting in the reduction of the surfactant concentration when it is added to the formulation. The addition of co-surfactant reduces chances of variability and local irritancy caused by the surfactants by increasing the interfacial fluidity. Commonly used co-surfactants such as ethanol and propylene glycol (15).

Co-solvent

High concentrations (generally more than 30% w/w) of surfactants is requires to the production of an optimum SEDDS. The co-surfactant such as, ethanol, propylene glycol (PG), and polyethylene glycol (PEG) are suitable for oral delivery, and they enable the dissolution of large quantities of either the hydrophilic surfactant or the drug in the lipid base. However, alcohols and other volatile co-solvents have the disadvantage of evaporating into the shells of the soft gelatin, or hard, sealed gelatin capsules in conventional SEDDS leading to drug precipitation (78).

Dosage Forms of SEDDS

SEDDS can exist in either liquid or solid states. To some extent, S-SEDDS are combinations of SEDDS and solid dosage forms, so many properties of S-SEDDS (e.g. excipients selection, specificity, and characterization) are the sum of the corresponding properties of both SEDDS and solid dosage forms. S-SEDDS focus on the incorporation of liquid/semisolid ingredients into powders/nanoparticles by different solidification techniques (e.g. adsorptions to solid carriers, spray drying, melt extrusion, nanoparticle technology, and so on) (81).

Mechanism of SEDDS

The mechanism by which self-emulsification takes place is not yet well understood. Nevertheless, it has been suggested that self-emulsification occurs when the entropy change favoring dispersion is greater than the energy required to increase the surface area of the dispersion. The free energy of a conventional emulsion formulation is a direct function of the energy required to create a new surface between the oil and water phases. The two phases of the emulsion tend to separate with time to reduce the interfacial area and thus the free energy of the systems. The conventional emulsifying agents stabilize emulsions resulting from aqueous dilution by forming a monolayer around the emulsion droplets, reducing the interfacial energy and forming a barrier to coalescence. On the other hand, emulsification occurs spontaneously with SEDDS because of the free energy required to form the emulsion is either low and positive or negative. The interface between the oil and aqueous continuous phases is formed upon addition of a binary mixture (oil/non-ionic surfactant) to water. The solubilization of water within the oil phase is a result of aqueous penetration through the interface which limited by the reached closed to the interphase. Thus, following

gentle agitation of the self-emulsifying system, water will rapidly penetrate into the aqueous cores leading to interface disruption and droplet formation (78).

Reported on self-emulsifying drug delivery system improving drug cross the brain

After oral administration to rabbits, the self-microemulsifying formulation containing curcumin together with resveratrol increased the total plasma concentrations of curcumin and resveratrol by 10-fold and 6-fold, respectively, compared to the unformulated combination (82). It has been suggested that drug-loaded self-emulsifying tablets could possibly permeate via the passive diffusion, take up into cells, and undergo the process of lipoprotein synthesis and secretion for lymphatic transport (83).

Characterization of SEDDS

Table 8 Various characterization methods to assess SEDDS (78)

Characterization	Significance
Ternary phase diagrams	To comparison of different surfactants and their synergistic effect with co-surfactant To determine the optimum concentration ranges of different excipients To identify the self-emulsification regions
Turbidity measurement	To identify the efficient self-emulsification
Droplet size	To measure the particles or droplets
Zeta potential	To identify the charge of the droplets
Morphology	To identify the size and shape of the droplets
Dissolution rate	To find out the rate and extent of drug release.

Advantages of SEDDS

Self-emulsifying drug delivery systems are new approach for enhancing the oral bioavailability of lipophilic drugs. They offer a number of advantages over the conventional micro/nanoemulsions systems owing to their interesting properties. Potential advantages of SEDDS include:

- Enhances oral bioavailability (84)
- Available in both liquid and solid dosage form (81)
- Poorly water soluble drugs can be used (84)

- The drug is protected by oil droplets (84)
- Gives prolonged release due to use of appropriate polymer (81)
- Reduction in the drug dose (84)

Limitations of SEDDS

High content of surfactant in the SEDDS formulation may irritate GI tract and result in toxicity. This problem can be solved by designing and optimizing SEDDS with decreased amount of surfactants (84). In addition, presence of high amount of surfactant or co-solvent may cause the degradation and instability of the drugs (81).

Absorption mechanisms by which NCS improve the oral bioavailability of drug

The rate-limiting process of absorption for drugs is the dissolution step. The rate and extent of such drugs' gastrointestinal tract absorption are greatly influenced by their formulation. Many various techniques for increasing curcumin bioavailability have been studied in the recent past, including the design and manufacturing of NCS for effective drug administration. Figure. 10. depicts various absorption mechanisms by which NCS improve the oral bioavailability of drugs.

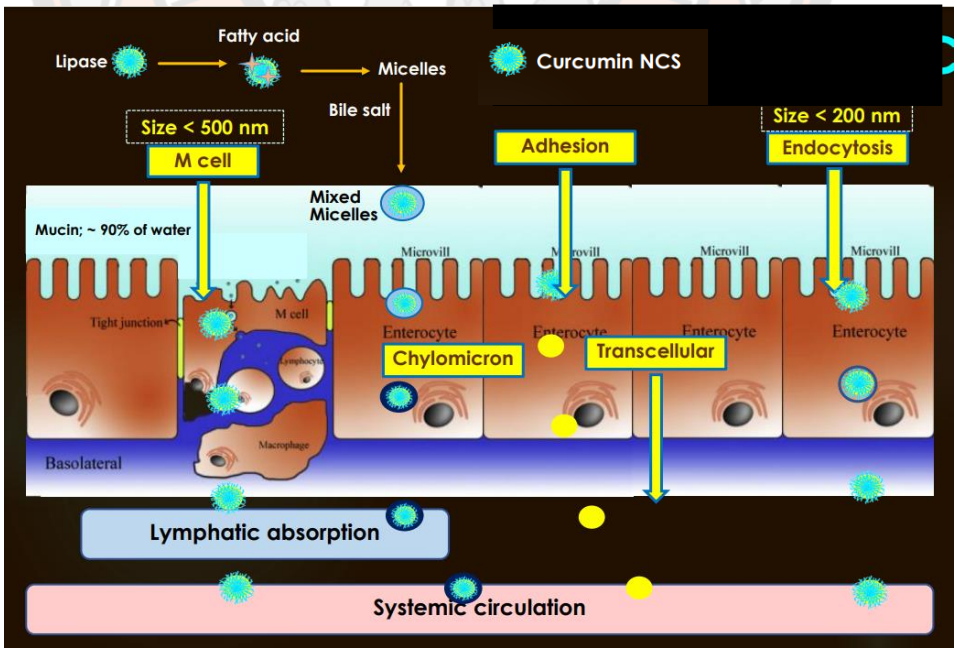

Figure 10 Absorption mechanisms implemented by NCS for improving the bioavailability of drugs

The nano-size of NCS is responsible for increasing water solubility of drug. In general, the intrinsic water solubility is related to the particle size; as a particle becomes smaller, the surface area to volume ratio increases. After oral administration, adhesion of nanoparticles to the GI tract is a common performance of most nanoparticles owing to their nano-size (85). Mucoadhesive can increase the contact time of the system with the mucosal surface of the intestine (mucoadhesive polymers swell and fill the cervices of the mucous membrane), enhance the drug concentration gradient due to the prolonged contact and, as a consequence, improve drug oral bioavailability (85, 86).

Endocytosis pathway is one of the main entry routes of nanoparticles into the cell. The size and surface properties of nanoparticles influence the route of internalization. NCS with particle size < 200 nm are preferentially uptake by enterocytes via endocytosis. The surface modification with amino grafted on micelles may cause different endocytic pathway in Caco-2 cells, because the micelles with different surface modification may bind or adsorb different cell-surface membrane proteins (85-87).

In addition, NCS, especially lipid-based NCS, can bypass the liver first pass metabolism by selectively shifting uptake via the lymphatic pathway (85). The presence of lipid in the NCS formulation enhances the secretion of lipase/co-lipase and bile salt in the duodenum which hydrolyses the triglycerides into monoglycerides and fatty acids forming micelles. The formed micelles will then be absorbed by enterocytes, where it gets converted to the chylomicrons. The formed chylomicrons are then subjected to lymphatic transport system and ultimately enter the systemic circulation by lymphatic drainage at thoracic duct (87). In addition, it has been reported that NCS particles less than 500 nm can cross the M cells in the Peyer'spatches of the intestine and easily taken up by the lymphatic system thus overcome the presystemic hepatic metabolism and enhance the bioavailability of the drug (86).

CHAPTER III

TRENDS IN ADVANCED ORAL DRUG DELIVERY SYSTEM FOR CURCUMIN: A SYSTEMATIC REVIEW

Abstract

Although curcumin is globally recognized for its health benefits, its clinical application has been restricted by its poor aqueous solubility and stability. To overcome these limitations, nanocarrier-based drug delivery systems (NDS) are one of the most effective approaches being extensively explored over the last few decades to improve curcumin's physicochemical and pharmacological effects. Various NDS could provide productive platforms for addressing the formulation challenge of curcumin, but evidence of such systems has not been summarized. This study aimed to systematically review current evidence of lipid and polymer-based NDS for an oral delivery of curcumin focusing on *in vivo* models and clinical studies. Among the 48 included studies, 3 studies were randomized controlled clinical trials, while 45 studies were animal models. To date, only five curcumin NDS have been studied in healthy volunteers: γ-cyclodextrin, phytosome, liposome, microemulsion and solid dispersion, while most curcumin NDS have been studied in animal models. Most included studies found that NDS could increase oral bioavailability of curcumin as compared to free curcumin. In conclusion, this systematic review showed evidence of the positive effect of NDS for enhancement of oral bioavailability of curcumin.

Keywords; curcumin, stability, solubility, bioavailability, nanocarriers, oral

Executive summary

Curcumin is globally recognized for its health benefits, but its clinical application has been limited by its poor aqueous solubility and stability, which causes poor absorption in the gastrointestinal tract (GI tract) via oral administration. Nanocarrier-based drug delivery systems (NDS) are considered as a productive platform to solve the formulation challenge of curcumin, but evidence of such systems has not been summarized. This study aimed to systematically review current evidence of lipid and polymer-based NDS for an oral delivery of curcumin focusing on *in vivo* models and clinical studies. Overall, most studies found that all studied NDS could increase the absorption of curcumin as compared to free curcumin. Curcumin was rapidly absorbed and exhibited a long residence time after oral administration of curcumin NDS. In summary, this systematic review showed positive impacts of NDS for enhancement of oral absorption of curcumin.

List of abbreviations and their descriptions

AUC	=	area under the curve
C_{max}	=	maximum concentration of the drug achieved in the plasma
CMCS	=	carboxymethyl chitosan
ERL	=	Eudragit RL
ERS	=	Eudragit RS
Gal-BSA	=	galactosylated albumin
GI tract	=	gastrointestinal tract
HPC	=	hydroxypropyl cellulose
NDS	=	nanocarrier-based drug delivery systems
NLC	=	nanostructure lipid carrier
PLGA	=	polylactic glycolic acid
PVA	=	polyvinyl alcohol
PVP	=	polyvinyl pyrrolidone
SLN	=	solid lipid nanoparticle
SMEDDS	=	self-microemulsifying drug delivery system
SNEDDS	=	self-nanoemulsifying drug delivery system
T_{max}	=	time of maximum drug concentration observed
TMC	=	N-trimethyl chitosan chloride
TPGS	=	TPGS; D-α-tocopheryl polyethylene glycol 1000 succinate
TPGS2000	=	D-α-tocopheryl polyethylene glycol 2000 succinate
HPMC	=	hydroxypropyl methylcellulose
HPMC-AS	=	hydroxypropyl methylcellulose acetate succinate
MPP	=	Methoxy poly (ethylene glycol)-poly(lactide) (mPEG-PLA)

1. Introduction

Curcumin, isolated from the rhizome of *Curcumin longa* Linn, has received worldwide attention for its multiple health benefits (3, 88). Supported by a number of proved pharmacological activities including anti-oxidation, anti-inflammation and monoamine oxidase (MAO) inhibitor, curcumin can help in the management of oxidative and inflammatory conditions, metabolic syndrome, arthritis, anxiety, cancer, and neurodegeneration (3, 4). However, its clinical application has been limited due to its poor aqueous solubility, rapid metabolism, as well as subjected for hydrolysis and oxidation in gastro-intestinal medium, subsequently leading to low oral bioavailability (7-9).

To overcome these obstacles, nanocarrier-based drug delivery systems (NDS) are one of the most effective approaches being explored during the last few decades, with promising evidence for clinical uses. NDS refers to the manipulation in the development of materials and other structures with particle size less than 1000 nm (89). Generally, as a nano-size particle, NDS improves dissolution rate of poorly soluble molecules and adheres well to the intestinal mucus membrane providing prolonged residence time and enhances drug permeation (43, 90-92). It also improves drug stability from the harsh environment in the gastrointestinal tract (GI tract) by encapsulating drugs in its nanocarriers (93). In addition, first pass metabolism could be bypassed by transport via M-cell (94). The developed NDS for an oral curcumin could be divided to 2 types, lipid and polymer-based NDS. Although many papers have been focused on development and *in vitro* characterization of the carriers, but to prove the effectiveness of NDS, *in vivo* studies need to be done to determine their oral bioavailability, defined as the rate and extent of a bioactive compound absorption which can reach into the bloodstream (95). The bioavailability experiment could be performed in animals or humans. After treating subjects, the drug amount entering the systemic circulation is determined at varying time point and plotted to get the area under the curve (AUC), maximum drug concentration (C_{max}) and peak time (T_{max}). These kinetic parameters could be used to characterize the properties of different NDS on bioavailability (92).

To track current progress in research on the application of NDS approaches in enhancing the oral bioavailability of curcumin, it is necessary to conduct a thorough investigation and analysis of related studies compiled with in vivo study both in human and animal models. Therefore, the objective of this study is to systematically review and summarize the findings from independent studies to determine the potential effects of NDS on the improvement of curcumin bioavailability.

2. Methods

2.1 Search strategy

To identify studies determining the clinical and *in vivo* of curcumin nanocarrier drug delivery systems, we searched PubMed, Scopus and ISI Web of science from inceptions to January 28, 2021 without language restriction. The search strategies are presented in appendix 1. The bibliographies of retrieved articles that met the selection criteria were also screened as shown in Fig. 1.

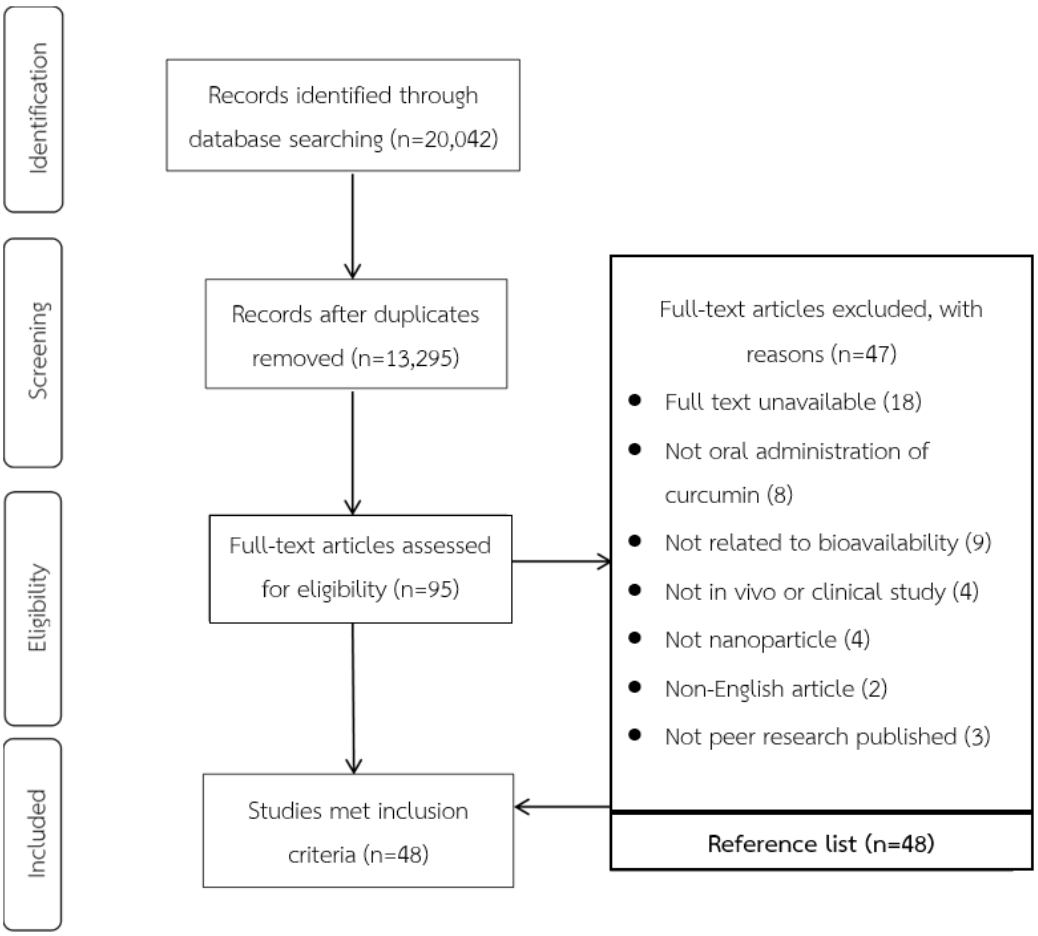

Figure 11 A PRISMA flow diagram describing study selection process.

2.2 Study selection

The *in vivo*, and clinical studies evaluating efficacy and bioavailability of curcumin nanocarrier drug delivery systems were eligible in our systematic review. The inclusion criteria were as follows: (1) studies determining the effect of curcumin nanocarrier system on bioavailability including absorption, pharmacokinetics, mucoadhesive, caco-2 cell, or stability (2) conducted in *in vivo* model or clinical studies. We reviewed all the titles and abstracts to determine whether the studies assessed the inclusion criteria following PRSIMA guideline. All studies were primarily reviewed by SP and verified by WT and PD. Any disagreements were solved by a consensus.

2.3 Data extraction and analysis

The extracted data included: types of study, type of curcumin delivery system (CDS), particle size of CDS. Dose of curcumin, area under the curve (AUC), maximum concentration (C_{max}), and time to maximum concentration (T_{max}). All studies were primarily extracted by SP and verified by PD and WT. Any disagreements were solved by a consensus. Data was qualitatively summarized and reported based on types of curcumin NDS.

3. Results

3.1 Study characteristics

Initial search yielded 20,042 articles. Of those, 6,552 duplicates were removed. The remaining articles were screened through titles and abstracts, of which 13,295 articles were excluded because of the irrelevant of curcumin, curcumin combined with another active ingredient and *in vitro* studies. This resulted in 48 articles being included in our review (Figure 1). Among the included studies, 3 studies (6.25%) were randomized controlled clinical trials, while 45 studies (93.75%) were animal models. We summarized characteristics of NDS and bioavailability of the included studies based on types of NDS as lipid-based and polymer-based and are presented in Table 1 and Table 2, respectively

3.2 Lipid-based nanocarrier systems

A total of 31 studies on lipid-based nanocarrier drug delivery systems including phytosome (n=4), liposome (n=4), microemulsion (n=3), nanoemulsion (n=5), self-microemulsifying drug delivery system (SMEDDS) (n=6), self-nanoemulsifying drug delivery system (SNEDDS) (n=3), solid lipid nanoparticle (SLN) (n=4) and nanostructure lipid carrier (NLC) (n=1). Some studies compared ≥ 2 NDS. Table 1 shows the type of NDS in human and animal models, as well as AUC, C_{max}, t_{max}, and relative bioavailability, as reported by a systematic review study. The composition of each NDS formulations is depicted in Table 3.

3.2.1 Phytosome

Purpura et al., (96) and Jäger et al., (97) developed curcumin phytosome consisting of curcumin: soy lecithin: microcrystalline cellulose and determined the effect of curcumin phytosome formulation in 12 healthy volunteers in a

randomized, double-blinded manner. Subjects consumed optically identical 6 hard gel capsules of free curcumin and curcumin phytosome, 1,800 mg and 376 mg of curcuminoids, respectively. Blood sample from each volunteer was then drawn at 1, 2, 3, 4, 5, 6, 8- and 12-hours intervals following oral administration. These time points were selected as past studies have shown that the majority of digestion and absorption are practically complete within this timeframe. The blood plasma samples were evaluated by tandem mass spectrometry detection (HPLC/MS/MS). When compared to free curcumin, these studies showed a relative bioavailability of 9 and 12.7 folds, respectively (96, 97). In the same way, Flory et al., studied the effect of curcumin phytosome in 12 healthy volunteers in a randomized, double-blinded manner. For the clinical trial, free curcumin and curcumin phytosome were normalized to 6 capsules (curcumin 207 mg) and orally administered. Blood samples were collected immediately before and 1, 2, 4, 6, 8, and 24 h after capsule intake. The blood plasma samples were evaluated by HPLC method. Flory et al., reported that curcumin loaded phytosome had an 8-fold higher relative bioavailability than free curcumin in 12 healthy volunteers (98). Marczylo et al., prepared curcumin phytosome with soy lecithin and determined its oral bioavailability in animal model. The relative bioavailability for curcumin phytosome was 5.6 fold higher than that for free curcumin (99).

Table 9 Pharmacokinetic parameters of curcumin loaded lipid based NDS

Authors	NDS	Subject	Dose of curcumin (mg)	C_{max} ±SD (ng/ml)	AUC±SD (ng/ml/h)	T_{max} ±SD (h)	Relative Bioavailability (folds)
Purpura et al. (96)	Phytosome	Human	curcuminoids 367 mg	4.7±1.8	35.1±4.5	1	9
Jäger et al. (97)	Phytosome	Human	curcuminoids 367 mg	2.8±0.3	28.7±2.6	1.7±1.0	12.7
Flory et al. (98)	Phytosome	Human	207 mg	6.1±3.7	54.5±25.0	< 1	7.8
Marczylo et al. (99)	Phytosome	Sprague Dawley rats	340 mg/kg	12.3±2.6	445	0.25	5.6
Flory et al. (98)	Liposome	Human	207 mg	0.7±0.4	5.43±3.2	< 1	0.8
Chen et al. (100)	Uncoated liposome	Wistar rats	40 mg/kg	32.1±9.4	263.8±43.0	2.0±0.3	1.2
	TMC-coated liposome	Wistar rats	40 mg/kg	46.1±5.3	416.6±48.2	2.0±0.6	1.7
Tian et al. (101)	Uncoated liposome	Sprague Dawley rats	10 mg/ kg	48.2 ± 6.7	528.9 ± 31.2	4	6
	TMC-Liposome	Sprague Dawley rats	10 mg/ kg	78.3 ± 10.1	1,218.2±127.4	3	12
	CMCS/TMC-Liposome	Sprague Dawley rats	10 mg/ kg	167.8±18.3	3,021.2±231.5	6	38
Takahashi et al. (102)	Liposome	Sprague Dawley rats	100 mg/kg	319.2±70.4	441.7	0.5	5
Flory et al. (21)	Microemulsion	Human	207 mg	152.0±147.2	399.0±263.8	< 1	56.8
Peng et al. (103)	Microemulsion	Sprague Dawley rats	100 mg/kg	2740±500	6510±850	1	2.7−3.6
Hu et al. (104)	Microemulsion	Sprague Dawley rats	200 mg/kg	3570±1180	11508.2 ±2500.8	2.3±1.3	22.6
Esperon-Rojas et al. (105)	Nanoemulsion-n3	Wistar rats	20 mg/kg	63.2±2.3	629.2	4	n/a
	Nanoemulsion-CLA	Wistar rats	20 mg/kg	88.7±2.3	760.5	8	n/a
Lu et al. (106)	Nanoemulsion	Sprague Dawley rats	50 mg/kg	70.0	797.5	1	46
		Sprague Dawley rats	100 mg/kg	140.0	4113.3	2	5.2

Authors	NDS	Subject	Dose of curcumin (mg)	C_{max} ±SD (ng/ml)	AUC±SD (ng/ml/h)	T_{max} ±SD (h)	Relative Bioavailability (folds)
Ochoa-Flores et al. (107)	Nanoemulsion-PC	BALB/c mice	50 mg/kg	116.5±24.9	389.7±58.8	0.5	188
	Nanoemulsion-PCE	BALB/c mice	50 mg/kg	316.8±24.1	720.3±86.6	0.5	347
Onoue et al. (108)	Nanoemulsion	Sprague Dawley rats	20 mg/kg	451±166	333.3±106.7	0.15±0.04	7.9
Chavez-Zamudio et al. (109)	Nanoemulsion	BALB/c mice	50 mg/kg	610,000±65,000	2,387,500	2	n/a
Yan et al. (110)	Solid SMEDDS	Sprague Dawley rats	25 mg/kg	34.0±9.8	37.1±17.7	0.54±0.10	4.6
		Sprague Dawley rats	100 mg/kg	155.6±18.3	282.6±61.2	0.58±0.13	7.6
Wu et al. (111)	SMEDDS	Mice	200 mg/kg	196.6	277.1	0.5	12.7
Setthacheewakul et al. (112)	SMEDDS	Wistar rats	50 mg/kg	4.4±0.1	537.9±13.8	1	14
	pellet SMEDDS	Wistar rats	50 mg/kg	4.2±0.3	408.1± 4.2	1	11
Dhumal et al. (113)	SMEDDS	Wistar rats	50 mg/kg	4921±420	17,300±1,530	1	26.5
Petchsomrit et al. (114)	SMEDDS	New Zealand white rabbits	12.5 mg/kg	1930±160	3983.4±270.7	1	7
	Sponge SMEDDS	New Zealand white rabbits	12.5 mg/kg	1,770±130	2,615.7±97.8	1	5
Jaisamut et al. (115)	SMEDDS	New Zealand white rabbits	50 mg/kg	5130±310	57,683.3±5,786.2	1	43.7
	Solid SMEDDS	New Zealand white rabbits	50 mg/kg	5,840±190	70,187.5±3,373.8	1	53.1
Zhongfa et al. (116)	SNEDDS	CD2F1 mice	1000 mg/kg	4641.8	7974.6	0.33	10.5

Authors	NDS	Subject	Dose of curcumin (mg)	C_{max} ±SD (ng/ml)	AUC±SD (ng/ml/h)	T_{max} ±SD (h)	Relative Bioavailability (folds)
Nazari-Vanani et al. (117)	SNEDDS	Sprague Dawley rats	100 mg/kg	790,000±360,000	2,020,000.2±70,000.2	0.33	1.9
Ji et al. (118)	SLNs	Rats	50 mg/kg	75,100±440	124,510±14,530	5.71±0.75	9.4
Gupta et al. (119)	SLNs	Wistar rats	100 mg/kg	55.75	124.2	1	69.8
Ramalingam et al. (120)	SLNs	Balb/c mice	50 mg/kg	1,040±280	2,930±260	1	6.9
Kakkar et al. (94)	SLNs	Wistar rats	50 mg/kg	14,290±150	41,990±6,180	0.5±0.02	39.1
		Wistar rats	25 mg/kg	8,000±1,870	17,156±3,240	0.25±0.04	16
		Wistar rats	12.5 mg/kg	7,870±3,020	15,789±2,290	0.25±0.05	14.7
		Wistar rats	1 mg/kg	1,000±10	3,343±1,170	0.5±0.01	3.1
Fang et al. (121)	NLC	Sprague Dawley rats	80 mg/kg	~ 570	820.4± 25.1	n/a	2

- n/a; Not available
- AUC; Area under the curve
- C_{max}; Maximum concentration of the drug achieved in the plasma
- T_{max}; Time of maximum drug concentration observed
- TMC; N-trimethyl chitosan chloride
- CMCS; Carboxymethyl chitosan
- SMEDDS; Self-microemulsifying drug delivery systems
- SNEDDS; Self-nanoemulsifying drug delivery systems
- SLNs; Solid lipid nanoparticles
- NLC; Nanostructured lipid carrier

Table 10 Pharmacokinetic parameters of curcumin loaded polymer based NDS

Authors	NDS	Subject	Dose of curcumin (mg)	C_{max}±SD (ng/ml)	AUC±SD (ng/ml/h)	T_{max}±SD (h)	Relative Bioavailability (folds)
Purpura et al. (96)	γ-cyclodextrin	Human	curcuminoids 367 mg	73.2±17.5	327.7±58.1	1	16.6
Flory et al. (98)	γ-cyclodextrin	Human	207 mg	42.0±37.1	209±175	< 1	29.8
Jäger et al. (97)	Solid dispersion	Human	curcuminoids 367 mg	27.3±6.4	307.6±44.6	1.4±0.5	45.9
Munjal et al. (93)	Solid dispersion	Sprague Dawley rats	250 mg/kg	78.1±13.7	119.8±35.9	0.5±0.1	4.5
Gao et al. (122)	Solid dispersion	Sprague Dawley rats	40 mg/kg	100.0 ± 68.1	45.7 ± 274	0.15 ± 0.09	19.4
Liao et al. (46)	Solid dispersion	Sprague Dawley rats	60 mg/kg	109.2±41.7	111.8±16.4	0.38±0.14	58.6
Onoue et al. (108)	Nanocrystal solid dispersion	Sprague Dawley rats	20 mg/kg	194±58	603.3±180.0	0.92±0.00	16
	Amorphous solid dispersion	Sprague Dawley rats	20 mg/kg	147±53	451.7±111.7	1.0±0.2	12
Chuah et al. (123)	Solid dispersion	Sprague Dawley rats	20 mg/kg	184±1	344.8±13.9	1.38±0.08	12.8
Wan et al. (124)	Solid dispersion	Wistar rats	50 mg/kg	187.0±34.6	1094.8±195.0	1.95±0.17	7
Fan et al. (125)	Solid dispersion	Sprague Dawley rats	100 mg/kg	330.4±186.7	1481.8±812.9	2.7±1.3	3
Hu et al. (126)	Solid dispersion	Sprague Dawley rats	400 mg/kg	2,620±740	9,010±1,520	0.75±0.71	2.6

Authors	NDS	Subject	Dose of curcumin (mg)	C_{max}±SD (ng/ml)	AUC±SD (ng/ml/h)	T_{max}±SD (h)	Relative Bioavailability (folds)
Zhang et al. (127)	Solid dispersion Cur/Na_2GA 1:1	Sprague Dawley rats	150 mg/kg	9,040±350	64,500±3,120	0.08	7.3
	Solid dispersion Cur/Na_2GA 1:2	Sprague Dawley rats	150 mg/kg	17,680±220	104,380±6,210	0.08	12.7
	Solid dispersion Cur/Na_2GA 1:3	Sprague Dawley rats	150 mg/kg	29,870±2,710	181,600±87,600	0.25	19.6
Zhang et al. (128)	Solid dispersion	Sprague Dawley rats	150 mg/kg	6,120±1,330	27,950±12,110	0.50±0.02	7.8
Harigae et al. (129)	PLGA nanoparticle	Sprague Dawley rats	100 mg/kg	1,286.8±245.7	n/a	1.5	5-26
Marin et al. (130)	Chitosan nanocapsule	Swiss mice	25 mg/kg	28.28±3.02	6,750±1,130	n/a	9
Khalil et al. (131)	PLGA nanoparticle	Wistar rats	50 mg/kg	11.8±0.5	134.3±3.4	2	15.8
	PLGA-PEG nanoparticle	Wistar rats	50 mg/kg	29.8±4.6	447.8±64.0	3	55.9
Tsai et al. (132)	PLGA- low MW nanoparticle	Sprague Dawley rats	50 mg/kg	42±5	125.33±10.5	0.5	1.2
	PLGA- high MW nanoparticle	Sprague Dawley rats	50 mg/kg	57±5	208.3±13.7	0.25	2
Sun et al. (91)	Poloxamer nanoparticle	Wistar rats	50 mg/kg	45.5±25.6	419.6±102.7	n/a	8.5
Huang et al. (133)	Gal-BSA nanoparticles	Sprague Dawley rats	40 mg/kg	48.7±7.4	1,047.6±41.2	0.5	1.4
Duan et al. (134)	TPGS nanoparticle	Wistar rats	75 mg/kg	197.9±61.7	1,020±930	0.67±0.39	9.3

Authors	NDS	Subject	Dose of curcumin (mg)	C_{max}±SD (ng/ml)	AUC±SD (ng/ml/h)	T_{max}±SD (h)	Relative Bioavailability (folds)
Wang et al. (135)	TPGS2000 nanoparticle	Sprague Dawley rats	50 mg/kg	342.3±122.4	870,000±294,310	0.22±0.09	2.9
Khatik et al. (136)	Chitosan nanoparticle	Wistar rats	10 mg/kg	1,102.4±25.3	9,817.1±87.0	4.1±0.1	2.1
	Eudragit coated chitosan nanoparticle	Wistar rats	10 mg/kg	904.7±38.5	16,906.6±103.9	8.33±1.30	3.6
Xie et al. (137)	Polymeric nanoparticle	Sprague Dawley rats	100 mg/kg	6,750±1,540	34,433.3±5,533.3	2	5.6
Raja et al. (138)	Chitosan nanoparticle	Sprague Dawley rats	100 mg/kg	99,720±30,470	295,470±82,440	2	4.5
Wang et al. (64)	Valine coated TPGS nanoparticle	Sprague Dawley rats	50 mg/kg	n/a	583.7±49.9	0.25	10.5
	Phenylalanine coated TPGS nanoparticle,	Sprague Dawley rats	50 mg/kg	n/a	597.5±42.3	0.25	3.4
	TPGS nanoparticle	Sprague Dawley rats	50 mg/kg	n/a	348±21	0.25	2.2

- n/a; Not available
- AUC; Area under the curve
- C_{max}; Maximum concentration of the drug achieved in the plasma
- T_{max}; Time of maximum drug concentration observed
- MW; Molecular weight

- PLGA; Polylactic glycolic acid
- Gal-BSA; Galactosylated albumin
- Cur/Na_2GA; Curcumin/Disodium glycyrrhizin
- TPGS; D-α-tocopheryl polyethylene glycol 1000 succinate
- TPGS2000; D-α-tocopheryl polyethylene glycol 2000 succinate
- ERL; Eudragit RL
- ERS; Eudragit RS

Table 11 Composition ingredients of each lipid-based NDS

Authors	NDS	Curcumin form	Particle size (nm)	Carrier/Co-carrier	Coating agent/ Cryo-protectant/ Adsorbent
Purpura et al. (96)	Phytosome	Curcuminoids	n/a	Soy lecithin/ Microcrystalline cellulose	-
Jäger et al. (97)	Phytosome	Curcuminoids	n/a	Soy lecithin/ Microcrystalline cellulose	-
Flory et al. (98)	Phytosome	Curcumin	n/a	n/a	n/a
Marczylo et al. (99)	Phytosome	Curcuminoids	n/a	Soy lecithin	-
Flory et al. (98)	Liposome	Curcumin	n/a	n/a	n/a
Chen et al. (100)	Uncoated liposome	Curcumin	221.4	Soy lecithin/Chitosan	
	TMC-coated liposome	Curcumin	657.7	Soy lecithin/Chitosan	TPGS
Tian et al. (101)	Uncoated liposome	Curcumin	119.2 ±10.6	L-α- Phosphatidylcholine	-
	TMC-Liposome	Curcumin	140.3±11.1	L-α- Phosphatidylcholine/TMC	
	CMCS/TMC-Liposome	Curcumin	161.6±12.3	L-α- Phosphatidylcholine/TMC	Carboxymethyl chitosan
Takahashi et al. (102)	Liposome	Curcumin	263±86	Soy lecithin	-
Flory et al. (21)	Microemulsion	Curcumin	n/a	n/a	n/a
Peng et al. (103)	Liposome	Curcumin	60.8±3.7	Sophorolipid	-
Hu et al. (104)	Microemulsion	Curcumin	29.8±2.2	Capryol 90/Cremophor RH 40/Transcutol P	
Esperon-Rojas et al. (105)	Nanoemulsion- n-3 fatty acids	Curcumin	151.1±2.2	MCT, Glycerol, emulsifier	n-3 fatty acids
	Nanoemulsion conjugated linoleic acid	Curcumin	190.6±1.3	MCT, Glycerol, emulsifier	Conjugated linoleic acid
Lu et al. (106)	Nanoemulsion	Curcuminoids	110	Lecithin, Tween 80	-
Ochoa-Flores et al. (107)	PC nanoemulsion	Curcumin	84.4±2.2	Phosphatidylcholine/MCO/Glycerol	-
	PCE nanoemulsion	Curcumin	29.6±2.3	Phosphatidylcholine enriched/MCO/Glycerol	-
Onoue et al. (108)	Nanoemulsion	Curcumin	196	PEG400/Propylene glycol /Tween 80	-

Authors	NDS	Curcumin form	Particle size (nm)	Carrier/Co-carrier	Coating agent/ Cryo-protectant/ Adsorbent
Chavez-Zamudio et al. (109)	Nanoemulsion	Curcumin	154.3±3.1	MCO/Glycerol/Lysophosphatydilcholine	-
Yan et al. (110)	Solid SMEDDS	Curcumin	147.3±5.8	Lauroglycol Fcc/Labrasol/Transcutol HP	Aerosil 200
Wu et al. (111)	SMEDDS	Curcumin	27.8±3.2	Isopropyl myristate, Cremophor RH40	-
Setthacheewakul et al. (112)	SMEDDS	Curcumin	27.5±0.3	Capryol 90, Labrafag, PG, Cremophor, Labrasol	-
	SMEDDS pellets	Curcumin	32.4±0.4	Capryol 90, Labrafag PG, Cremophor, Labrasol	Microcrystalline cellulose
Dhumal et al. (113)	SMEDDS	Curcumin	22.7±0.5	Heterolipid E1E/Solutol HS15/ Transcutol HP	-
Petchsomrit et al. (114)	SMEDDS	Curcumin	34.80±0.1	Capryol 90/Labrafac PG/Cremophor EL/Labrasol	-
	Sponge SMEDDS	Curcumin	43.36±4.54-123.22±8.19	Capryol 90/Labrafac PG/Cremophor EL/Labrasol	Hydroxyl propyl methyl cellulose
Jaisamut et al. (115)	SMEDDS	Curcumin	28.1±0.3	Lauroglycol Fcc/Labrasol/Transcutol HP	-
	Solid SMEDDS	Curcumin	21.6±0.1	Lauroglycol Fcc/Labrasol/Transcutol HP	Aerosil 200
Zhongfa et al. (116)	SNEDDS	Curcumin	68.7±26.1	PEG 600/Cremophor EL/Tween 80	-
Nazari-Vanani et al. (117)	SNEDDS	Curcumin	6.9	Ethyl oleate/PEG 600/Tween 80	-
Ji et al. (118)	SLNs	Curcumin	135.3±1.5	Soy lecithin/Glyceryl mono stearate/TPGS/Brij78	-
Gupta et al. (119)	SLNs	Curcumin	n/a	Phospholipon 90G/ Tween 80	-
Ramalingam et al. (120)	SLNs	Curcumin	739.3±53.1	Glycerol stearate/PG esters of fatty acids/Palmitic acid/Tween 80	-
Kakkar et al. (94)	SLNs	Curcumin	134.6±15.4	Compritol 888 ATO/Soy lecithin/Tween 80	-

Authors	NDS	Curcumin form	Particle size (nm)	Carrier/Co-carrier	Coating agent/ Cryo-protectant/ Adsorbent
Fang et al. (121)	NLC	Curcumin	129±15.5	Glyceryl monostearate/Lexol/Poloxamer 188/Soy lecithin	Sucrose

- MCT; Medium chain triacylglycerides
- TPGS; D-a-tocopherol poly-ethylene glycol 1000 succinate
- PEG; Polyethylene glycol
- PG; Propylene glycol
- MCO; Medium chain oil

3.2.2 Liposome

Flory et al., developed curcumin loaded liposome and evaluated in 12 healthy adult volunteers, in a randomized, double-blinded manner. The study design was similarly with the study of the Flory et al., section 3.2.1. Curcumin loaded liposome produced non-significant clinical parameters in comparison to free curcumin (98).

Nevertheless, Takahashi et al., reported that rat treated with liposome showed 5-fold greater oral curcumin bioavailability than those treated with free curcumin (102). In addition, the polymer coated liposome showed greater bioavailability enhancement. Chen et al., reported that in animal model the curcumin liposome coated with N-trimethyl chitosan chloride (TMC) demonstrated the greater absorption (~ 1.7 folds) than curcumin uncoated liposomes (~ 1.2 folds) (100). Conversely, Tian et al., compared the relative bioavailability of curcumin liposome prepared with lecithin, TMC coated liposome and carboxymethyl chitosan (CMCS)/TMC coated liposome. CMCS/TMC coated liposome had the highest relative bioavailability (38 folds) compared to TMC liposome (12 folds) and uncoated liposome (6 folds), respectively (101).

3.2.3 Microemulsion and nanoemulsion

Flory et al., developed curcumin loaded microemulsion and determined the effect of curcumin in 12 healthy adult volunteers, in a randomized, double-blinded manner. The study design was similarly with the study of the Flory et al., section 3.2.1. Micellar curcumin was absorbed faster and led to significantly higher mean C_{max} compared to free curcumin (98). Two studies reported the effect of curcumin loaded microemulsion in animal models. Peng et al., prepared sophorolipid-coated curcumin nanoparticles and found the relative bioavailability in the range between 2.7-3.6 folds when compared to free curcumin (103). Surprisingly, Hu et al. found that the relative bioavailability of curcumin loaded microemulsions employing Capryol 90 and Cremophor RH 40 as a surfactant was 22.6 folds greater than free curcumin (104).

Five studies reported the curcumin loaded nanoemulsion in animal models could increase curcumin oral bioavailability. Esperon-Rojas et al., studied the curcumin loaded nanoemulsion with linoleic acid (CLA) and n-3 fatty acids (n-3FA). Experimental data showed greater AUC than their emulsion counterpart, with T_{max} at 4 and 8 h, respectively (105). In controversy, Onoue et al., showed that with a similar

single oral dose (20 mg/kg) of curcumin nanoemulsion in rat, a rapid elevation of curcumin blood levels within 10 min was observed (108). According to Ochoa-Flores et al., phospholipid nanoemulsions showed T_{max} within 30 min (107). However, Chavez-Zamudio et al., found that the T_{max} of curcumin from phospholipid nanoemulsion was 2 h (109). Lu et al., compared the dose of curcumin, 50 and 100 mg/kg, from curcuminoid nanoemulsion with lecithin and Tween 80. The time to reach maximum concentration of curcumin with a high dose (100 mg/kg) was 2 h, whereas a low dose (50 mg/kg) showed a rapid elevation of curcumin blood levels from curcumin within 1 h (106).

3.2.4 Self-emulsification drug delivery system (SEDDS)

Depending upon the particles size, these systems could be further classified as self-microemulsifying drug delivery systems (SMEDDS) or self-nanoemulsifying drug delivery systems (SNEDDS).

Six studies reported the effect of curcumin loaded SMEDDS in animal models. According to Wu et al., the relative bioavailability of liquid curcumin SMEDDS increased to 12.7-fold higher than free curcumin (111). However, Dhumal et al., found a 26-fold increase in relative bioavailability of liquid curcumin SMEDDS as compared to free curcumin (113). However, Yan et al., showed the greater relative bioavailability of curcumin solid SMEDDS using Aerosil 200 as a binder with the dose ranging from 25 mg/kg to 100 mg/kg were increased by 4.6 and 7.6, respectively, as compared to free curcumin (110). Setthacheewakul et al., compared liquid curcumin SMEDDS to curcumin-SMEDDS pellets with croscarmellose sodium as a solid binder. The relative bioavailability of curcumin in the liquid curcumin SMEDDS and curcumin SMEDDS pellets were 14 and 11 fold higher, respectively, than the same dose of free curcumin (112). Noteworthy, Jaisamut et al., found that curcumin solid SMEDDS with Eudragit® EPO as a binder had a 53.1-fold greater relative bioavailability than liquid curcumin SMEDDS without binder (43.7-fold) (115). Controversy, Petchsomrit et al., reported that liquid curcumin SMEDDS had a 7-fold greater relative bioavailability than hydroxypropylmethyl cellulose (HPMC)-based sponges containing liquid curcumin SMEDDS (5-fold) (114).

Two studies investigated the effect of SNEDDS on curcumin oral bioavailability in animal models. Nazari-Vanani et al., showed that the relative bioavailability of curcumin SNEDDS was increased by 1.9-fold, compared to free curcumin (117). Noteworthy, Zhongfa et al., found that curcumin SNEDDS had a 10.5-fold greater relative bioavailability than free curcumin (116). In addition, all studies proved that the SEDDS could successfully increase curcumin oral bioavailability with a T_{max} of less than 1 h, indicating rapid absorption of curcumin.

3.2.5 Solid lipid nanoparticle (SLN) and nanostructure lipid carrier (NLC)

Four studies reported the effect of curcumin-loaded SLN in animal models. Ji et al., showed relative bioavailability of curcumin SLN, formulated with P-glycoprotein (P-gp) modulator, TPGS and Brij78, was 9.4 folds greater than free curcumin (118). Gupta et al., developed curcumin loaded SLN using Compritol® 888 ATO as a solid lipid. It showed 69.8 times higher oral bioavailability with respect to free curcumin (119). Ramalingam et al., investigated the potential of chitosan coated SLN. AUC of curcumin coated SLN was increased, with the relative bioavailability of 6.9 as compared to free curcumin (120). Kakkar et al., investigated the effect of different doses (50, 25, 12.5 and 1mg/kg dose) of curcumin. The results showed that curcumin loaded SLN equivalent to 50 mg/kg of curcumin could substantially increase AUC and C_{max} compared to those of 1 mg/kg of curcumin (94).

Only one study reported the effect of curcumin loaded NLC in animal model. Fang et al., presented curcumin loaded NLC prepared with poloxamer 188 as a surfactant. Following intragastric administration, it showed 2 times higher relative bioavailability than the free curcumin. In addition, tissue concentrations of curcumin also increased, especially in the brain, suggesting that NLC could improve the ability of curcumin to cross the blood–brain barrier (121).

3.3 Polymer-based nanocarrier systems

A total of 21 studies focused on the polymer based nanocarrier systems including cyclodextrin (n=2), solid dispersion (n=12) and polymeric nanoparticles (n=12). Some studies compared ≥ 2 NDS. Table 2 shows the type of NDS in human and animal models, as well as AUC, C_{max}, T_{max}, and relative bioavailability,

as reported by a systematic review study. The composition of each NDS formulation is depicted in Table 4.

Table 12 Composition ingredients of each polymer-based NDS.

Authors	NDS	Curcumin form	Particle size (nm)	Carrier/Co-carrier	Coating agent/ Cryo-protectant/ Adsorbent
Purpura et al. (96)	γ-cyclodextrin	Curcuminoids	n/a	γ-cyclodextrin	-
Flory et al. (98)	γ-cyclodextrin	Curcumin	n/a	γ-cyclodextrin	-
Jäger et al. (97)	Solid dispersion	Curcuminoids	n/a	PVP/Cellulose	-
Munjal et al. (93)	Solid dispersion	Curcumin	n/a	PVP K30	-
Gao et al. (122)	Solid dispersion	Curcumin	n/a	PVP K30	-
Liao et al. (46)	Solid dispersion	Curcumin	141.9±5.1	PVP K30	-
Onoue et al. (108)	Nanocrystal solid dispersion	Curcumin	250	HPC SL	-
	Amorphous solid dispersion	Curcumin	n/a	HPMC-AS	-
Chuah et al. (123)	Solid dispersion	Curcumin C3 complex powder	n/a	HPMC/Lecithin/Isomalt	-
Wan et al. (124)	Solid dispersion	Curcumin	n/a	Cellulose acetate/Mannitol	-
Fan et al. (125)	Solid dispersion	Curcumin	n/a	Eudragit RS/RL	-
Hu et al. (126)	Solid dispersion	Curcumin	n/a	Poloxamer 188/ PEG 4000/Cremophor RH40	Sodium carboxymethyl starch
Zhang et al. (127)	Solid dispersion Cur/Na_2GA 1:1	Curcumin	79.3	Na_2GA	-
	Solid dispersion Cur/Na_2GA 1:2	Curcumin	80.6	Na_2GA	-
	Solid dispersion	Curcumin	84.8	Na_2GA	-

Authors	NDS	Curcumin form	Particle size (nm)	Carrier/Co-carrier	Coating agent/ Cryo-protectant/ Adsorbent
	Cur/Na_2GA 1:3				
Zhang et al. (128)	Solid dispersion	Curcumin	349	Polysaccharide arabinogalactan	-
Harigae et al. (129)	PLGA nanoparticle	Curcumin	186.9±2.8	PLGA/PVA	Sucrose
Marin et al. (130)	Chitosan nanocapsule	Curcumin	400±1	Chitosan/Tween 80/Span 80	Sodium dodecyl sulfate
Khalil et al. (131)	PLGA nanoparticle	Curcumin	161.9±6.7	PLGA	-
	PLGA-PEG nanoparticle	Curcumin	152.4±4.5	PLGA	PEG
Tsai et al. (132)	PLGA- low MW nanoparticle	Curcumin	166.0±7.4	PLGA (MW 5000-15000)	PVA
	PLGA- high MW nanoparticle	Curcumin	163.0±4.2	PLGA (MW 40000-75000)	PVA
Sun et al. (91)	Poloxamer nanoparticle	Curcumin	40–400	Poloxamer 407/Mannitol	-
Huang et al. (133)	Gal-BSA nanoparticles	Curcumin	n/a	Galactose, 4-O-β-d-galactopyranos	-
Duan et al. (134)	TPGS nanoparticle	Curcumin	~46	MPP, TPGS	-
Wang et al. (135)	TPGS2000 nanoparticle	Curcumin	17.8±0.3	Di-tocopherol PEG 2000 succinate	Pluronic F127
Khatik et al. (136)	Chitosan nanoparticle	Curcumin	173.0±4.5	Chitosan	-
	Eudragit coated chitosan nanoparticle	Curcumin	236.0±3.2	Chitosan/Eudragit	-
Xie et al. (137)	Polymeric nanoparticle	Curcumin	158	PLGA	PVA
Raja et al. (138)	Chitosan nanoparticle	Curcumin	199.4±6.3	Chitosan	-
Wang et al. (64)	Valine coated TPGS nanoparticle	Curcumin	15.36±0.67	TPGS	Valine
	Phenylalanine coated TPGS nanoparticle,	Curcumin	15.22±0.31	TPGS	Phenylalanine

Authors	NDS	Curcumin form	Particle size (nm)	Carrier/Co-carrier	Coating agent/ Cryo-protectant/ Adsorbent
	TPGS nanoparticle	Curcumin	15.50±0.13	TPGS	-

- PVP; Polyvinyl pyrrolidone
- PVA; Polyvinyl alcohol
- HPC SL; Hydroxypropyl cellulose SL
- HPMC-AS; Hydroxypropyl methylcellulose acetate succinate
- HPMC; Hydroxypropyl methylcellulose
- Cur/Na_2GA; Curcumin/Disodium salt of glycyrrhizic acid
- PLGA; polylactic glycolic acid
- MPP; Methoxy poly(ethylene glycol)-poly(lactide)(mPEG-PLA)
- TPGS; D-α-tocopherol polyethylene glycol 1000 succinate
- TPGS2000; D-α-tocopheryl polyethylene glycol 2000 succinate

3.3.1 γ-Cyclodextrin

Purpura et al., reported the effect of γ-cyclodextrin curcumin complex in 12 healthy volunteers using a randomized, double-blind, cross-over study over a 12-h time period. The study design was similarly with the study of Purpura et al., in the section 3.2.1.The γ-cyclodextrin curcumin complex provided a C_{max} of ~328 ng/ml within 1 h and AUC of ~70 ng/ml/h with the relative bioavailability of 16.-fold as compared to free curcumin (96). Conversely, Flory et al., evaluated the effect of curcumin-cyclodextrin complex in 12 healthy adult volunteers over a 24-h period. Its C_{max} and AUC were just 0.11±0.10 ng/ml and 0.57±0.47 ng/ml/h, respectively, with T_{max} lower than 1 h (98).

3.3.2 Solid dispersion

Only one clinical study was conducted in healthy volunteers. Jäger et al., reported the effect of curcumin solid dispersion with cellulose derivative in 12 healthy volunteers using a randomized, double-blind, cross-over study. The study design was similarly with the study of Flory et al., in the section 3.2.1.The relative bioavailability of curcumin solid dispersion provides a C_{max} within 2 h and AUC of ~27

ng/ml and ~308 ng/ml/h, respectively, with the relative bioavailability of 45.9-fold as compared to free curcumin (97).

Eleven studies reported the effect of curcumin solid dispersion in animal models. Munjal et al., (93), Gao et al. (122) and Liao et al., (139) investigated the potential of solid dispersion with hydrophilic polymer as carrier, PVP K30, and showed the 4.9, 15.4 and 58.6-fold increase in relative bioavailability of curcumin compared to free curcumin with T_{max} less than 1 h. Onoue et al., compared nanocrystal solid dispersion and amorphous solid dispersion using HPC and HPMC, respectively, as a carrier. Both solid dispersions showed a C_{max} of 194 and 147-fold, respectively, with similar T_{max} 1 h, and AUC of 16 and 12-fold, respectively, as compared to free curcumin (108). Similarly, Chuah et al., prepared the solid dispersion with HPMC, lecithin and isomalt. The C_{max} and AUC increased to 184 ng/ml and 345 ng/ml/h, respectively, after 80 min administration (123). Hu et al., reported that solid dispersion using Cremophor RH40, poloxamer 188, and polyethylene glycol 4000 as carriers increased the relative bioavailability of curcumin to 2.6-fold higher than free curcumin with T_{max} lower than 1 h (126). Zhang et al., developed curcumin solid dispersion with low to high concentration of disodium glycyrrhizin (Na_2GA). When the ratio of Na_2GA was increased to 3, 2 and 1, the relative bioavailability increased by ~20, ~13 and ~7-fold, respectively (127). Moreover, Zhang et al., also investigated the effect of curcumin solid dispersion using macromolecule polysaccharide arabinogalactan (AG) as a carrier. The results revealed a T_{max} < 1 h with an 8-fold increased in relative bioavailability as compared to free curcumin (128). Wan et al., prepared curcumin solid dispersion using cellulose acetate and mannitol as a carrier to investigate the prolonged release of curcumin. The C_{max} and AUC were ~187 ng/ml and ~1095 ng/ml/h, respectively, with T_{max} within 2 h (124). Likewise, Fan et al., prepared curcumin solid dispersion using Eudragit RS/RL as a hydrophobic carrier. Its relative bioavailability of curcumin was 3-fold greater than free curcumin and provided a sustained release effect with T_{max} ~2 h (125).

3.3.3 Polymeric nanoparticle

Thirteen studies reported the effect of curcumin polymeric nanoparticle in animal models. Harigae et al., (129), Xie et al., (137) and Khalil et al., (131) found that curcumin loaded PLGA nanoparticles (PLGA NPs) and showed

similar T_{max} ~2 h with an 2-26-fold increase in relative bioavailability compared to free curcumin. Additionally, coated PLGA NPs with PEG showed 56-fold increased relative bioavailability with a prolonged T_{max} ~3 h (131). Tsai et al., prepared curcumin loaded PLGA nanoparticles (PLGA NPs) with low and high molecular weight (MW) PLGA. The relative bioavailability of high MW PLGA was increased to 2-fold higher than that of low MW PLGA, the T_{max} was ~15-30 min (132). Sun et al., found that polybutylcyanoacrylate nanoparticles (PBCNs) showed similar T_{max} ~2 h with an ~9-fold increase in relative bioavailability compared to free curcumin, with the main absorption sites were ileum and colon (91). Huang et al., found that the curcumin-loaded galactosylated albumin nanoparticles (Gal-BSA NPs) showed the T_{max} ~30 min with an 1.4-fold increase in relative bioavailability compared to free curcumin (133).

Marin et al., (130), Raja et al., (138), and Khatik et al., (136) investigated the potential of curcumin-chitosan nanoparticles and showed the 9, 4.5 and 2.1-fold increase in relative bioavailability compared to free curcumin, respectively, with the T_{max} ~2-4 h. Additionally, coated chitosan NPs with Eudragit S 100 showed 3.6-fold increased relative bioavailability with a prolonged T_{max} ~8 h (136).

Duan et al., prepared curcumin polymeric micelle with methoxy poly (ethylene glycol)-poly (lactide) and di -tocopherol polyethylene glycol 1000 succinate (CUR-MPP-TPGS). The relative bioavailability was increased to 9.3-fold compared to free curcumin, and the T_{max} ~1 h (134). Similarly, Wang et al., found that curcumin polymeric micelles using Di-tocopherol polyethylene glycol 2000 succinate as a carrier revealed a T_{max} < 1 h with an 2.9-fold increase in relative bioavailability as compared to free curcumin (135). In another study, Wang et al., prepared curcumin polymeric micelle using D-α-tocopheryl polyethylene glycol 1000 succinate micelles (TP-PMs) without and with valine or phenylalanine (Val-PMs or Phe-PMs) grafted onto the particle surface. The relative bioavailability of Val-PMs was increased ~8 fold higher than that of Phe-PMs and TP-PMs, and all of them possessed the T_{max}~0.25 h (140).

4. Discussion

Many various techniques for increasing curcumin bioavailability have been studied in the recent past, including the design and manufacturing of NDS for effective curcumin administration (141). Only 3 studies on curcumin NDS in humans have been published, and the others were studied with animal models. Our research compiled the most relevant evidence on the efficacy and bioavailability of curcumin NDS. However, variation in pharmacokinetic parameters was observed in similar NDS due to differences in subjects, analytical methods, study design and administration dose. Overall, most studies found that all studied NDS could improve oral bioavailability of curcumin compared to free curcumin. Curcumin was rapidly absorbed and exhibited a long residence time after oral administration of curcumin NDS. Only one human study found that curcumin loaded liposomes had non-significant clinical parameters in 12 healthy volunteers compared to free curcumin (98). In controversy, animal studies showed significantly greater relative bioavailability from curcumin loaded liposomes as compared to free curcumin (100-102).

Curcumin loaded NLC could be detected in the heart, liver, spleen, lung, kidney, and brain tissue after intragastric administration. High curcumin concentrations in various tissues are essential for curcumin to have pharmacological activity. It is worth noting that curcumin loaded NLC could be detected in the brain tissue after intragastric administration. This indicates that curcumin loaded NLC can easily pass through the blood–brain barrier into brain tissue, suggesting potential application of NDS for delivering drugs to the brain (121).

The enhanced oral bioavailability of curcumin could be arisen from advantages of NDS including (i) increased curcumin water solubility (ii) improved curcumin stability (iii) enhanced adhesion to the GI tract, and (iv) provided more absorption routes of curcumin.

The nano-size of NDS is responsible for increasing water solubility of curcumin. In general, the intrinsic water solubility is related to the particle size; as a particle becomes smaller, the surface area to volume ratio increases. This would allow greater interaction with the solvent, consequently, increasing curcumin water solubility (91, 93, 94, 96-98, 102, 104, 106-108, 110-112, 114-118, 122, 126-129, 132-135, 137-140, 142, 143). Additionally, changing the drug crystalline structure into an

energetically unstable amorphous form, employing amorphous carriers or water soluble carrier, as well as surfactant often allows for a water solubility improvement (91, 93, 106, 108, 123, 125-128, 143). For instance, amorphous solid dispersion provided better wettability and dispersibility as the drug was in its supersaturated state due to forced solubilization in the hydrophilic carrier (127).

The stability of curcumin was improved when encapsulated in NDS. This reduces its exposure to bacteria and enzymatic degradation during the absorption process (94, 100, 102, 104, 107, 109, 110, 112, 120, 121, 124, 126, 129, 132, 135, 137, 143, 144). For instance, cyclodextrins can help maintaining curcumin concentration in the intestine by encapsulating curcumin in the particles. This could increase the duration of the apparent absorption phase by making stable curcumin available for absorption (93). Similarly, after oral administration of curcumin mixed micelles, the micelles maintained their integrity and avoided premature dissolution in the gastric (134). In controversy, liposomes are unstable at low pH, and in the presence of bile acids and pancreatin, which explains the observed low digestive stability, solubility, micellization efficiency and consequently smaller curcumin amounts that are available for the absorption by intestinal cells (98). However, coating liposome with TMC could protect liposomes from disruption in the hostile environment of the gut (100).

After oral administration, adhesion of nanoparticles to the GI tract is a common performance of most nanoparticles owing to their nano-size. The high adhesion makes particle closely contact with the GI tract for a long period, therefore, transmembrane transport of the drug in the GI tract could be promoted (94, 100, 101, 104, 107, 109, 116, 118, 120, 121, 123, 134-138, 140, 144). The mucus on GI tract contained many pores and channels, the size of mucus mesh ranged from 100 nm to 1000 nm, which was beneficial to the diffusion of small particles. Besides, the particle size within 100 nm greatly facilitated the penetration across the pre-epithelial medium mucus (134). Apart from nano-size, the bioadhesive polymer such as chitosan, PLGA, and surfactant also promote adhesion properties of NDS. Chitosan could prolong contact duration between NDS and the absorptive surface due to the interaction between positively charged chitosan and negatively charged mucin (138). TMC-coated liposomes demonstrated the greatest absorption and slowest elimination, compared to uncoated liposomes. Adhesion of TMC to the mucosal surface of the intestine tenue

prolonged drug-residence time (100). It has been revealed that curcumin loaded PLGA nanoparticles are principally associated with the prolonged absorption phase. PLGA may have bioadhesive properties and bind with the mucosa of the GI tract (137). Furthermore, use of surfactants such as tween 80, lecithin and poloxamer 188, in the preparation of SLNs and solid dispersion, could enhance the permeability of curcumin in the intestinal membrane, resulting in improved oral bioavailability (94, 123, 126). In addition, prolonged drug residence time *in vivo* could be achieved by the preparation of solid dispersion with a high molecular weight carrier, which showed slightly delayed absorption (125).

After the adhesion process, curcumin is released from the NDS and absorbed mostly via passive diffusion (133-135). Additionally, NDS could enhance the transport of curcumin in the intestinal membrane via (i) increased membrane fluidity, (ii) open tight junction, (iii) endocytosis, and (iv) bypass first pass metabolism via lymphatic uptake.

The use of surfactants could reduce the interfacial surface tension and increase cell membrane fluidity, leading to enhanced penetration of the drug through the epithelial cells. For instance, Cremophor RH40, Tween 80 and lecithin, in the preparation of SEDDS, SLNs and solid dispersion, respectively (94, 123, 126). NDS could facilitate the paracellular transport by using positively charged TMC to open the tight junctions via exploiting the negatively charged sites on the cell membrane through ionic interaction and, as a result, exhibited an excellent absorption-enhancing effect, even in neutral environments (100, 101).

Although endocytosis is involved in the uptake of both curcumin and curcumin loaded NDS, the concentration of curcumin NDS in different intestinal segments was higher than free curcumin (132, 135, 140). Endocytosis pathway; including clathrin–mediated, caveolae-mediated, macropinocytosis, and clathrin-, caveolin–independent endocytosis, is one of the main entry routes of nanoparticles into the cell (135, 140). The size and surface properties of nanoparticles influence the route of internalization. NDS with particle size < 100 nm are preferentially uptake by enterocytes via endocytosis (145, 146). The surface modification with amino grafted on micelles may cause different endocytic pathway in Caco-2 cells, because the micelles with different

surface modification may bind or adsorb different cell-surface membrane proteins (140).

Curcumin is metabolized extensively in the liver, mostly by conjugation reactions such as sulfation and glucuronidation, leading to rapid systemic elimination (93, 108). To this end, NDS, especially lipid-based NDS, can bypass the liver first pass metabolism by selectively shifting uptake via the lymphatic pathway (94, 102, 103, 107, 111, 116-118, 131, 134, 135, 140, 142). It was revealed that the long chain oils promote lipoprotein synthesis and subsequently promote lymphatic absorption (147). The particle size less than 500 nm was also a key factor in efficient uptake in the lymphoid sections (148). For example, the curcumin with polybutylcyanoacrylate was preferentially absorbed by the M cells of the Peyer's patches (91). The surfactant coating on the surface of the nanoparticles also reduces the interactions between the nanoparticles and the digestive enzymes, leading to increased drug uptake into the bloodstream and lymphatic tissue (131).

5. Conclusion

The curcumin-based NDS is being used with the principal objective of enhancing curcumin bioavailability. In the present study, a total of 48 studies were identified, 3 studies were randomized controlled clinical trials, while 45 studies were animal models. Excited data have emerged from the studies identified by our systematic review confirming the bioavailability improvement using NDS. By incorporating curcumin in these formulations, the solubility and stability in the GI system were improved, thus, increasing the absorption of curcumin. According to our systematic review, all NDS offer rapid absorption, as evidenced by the short time taken to reach peak plasma concentration, with a prolonged resident time. However, most curcumin NDS have been studied in animal models, with only 5 curcumin NDS have been studied in healthy volunteers: γ-cyclodextrin, phytosome, liposome, microemulsion and solid dispersion. Therefore, to elucidate the effect of different NDS on the enhancement of curcumin bioavailability, the number of clinical trials is expected to increase. In conclusion, this study showed evidence of the positive effect of the nanocarrier system for enhancement of curcumin oral bioavailability. It also has high potential to enhance the permeability of curcumin into the brain.

CHAPTER IV

IMPROVING ORAL DELIVERY OF CURCUMIN EMPLOYING SOLID SELF-EMULSIFYING DRUG DELIVERY SYSTEM

This chapter is the manuscript currently under revision for publication.

Abstract

Curcumin is a phenolic compound of turmeric with remarkable pharmacological properties. However, curcumin inherent poor water solubility, permeability, and instability in gastrointestinal tract hinder its therapeutic use. Herein, curcumin loaded solid self-micro- and nanoemulsifying drug delivery system (C-SSMEDDS and C-SSNEDDS) were developed using Neusilin®UFL2 as a solid carrier. All developed formulations significantly showed improvement in curcumin water solubility, > 100-folds as compared to the free curcumin. In both the simulated stomach (pH 1.2) and intestinal (pH 6.8) conditions, C-SSMEDDS and C-SSNEDDS enhanced the dissolution profiles of curcumin with ~100% release within 5 min and possessed an average droplet diameter of ~100 and ~150 nm, correspondingly. Moreover, permeation studies in Caco-2 cell monolayer revealed that both formulations provided significantly greater cellular accumulation and absorption compared with the free curcumin. Lastly, the C-SSMEDDS and C-SSNEDDS were physicochemically stable at room temperature for at least 1 year. In summary, the findings indicated that C-SSMEDDS and C-SNEDDS are an important strategy for improving curcumin oral bioavailability.

Keywords absorption, curcumin, dissolution, self-emulsifying drug delivery system, oral administration

1. Introduction

Curcumin, a highly lipophilic compound commonly obtained from the *Curcuma longa* L. (turmeric) rhizomes (149), has been widely explored as an interesting candidate to treat central nervous system (CNS) disorders possibly due to its anti-inflammation, antioxidant, and neurotransmitter modulating properties (150). It has been reported that curcumin protects neuronal cells in Alzheimer's disease from beta-amyloid-induced oxidative stress (151). In *in vivo* settings, curcumin decreases the invasion of inflammatory cells in the brain by inhibiting differentiation and development of cell expression (152). Moreover, at a dose of 100 mg/kg, curcumin possesses antidepressant-like action in mice by increasing the brain dopamine, norepinephrine, and serotonin levels, comparable to the oral administrations of fluoxetine and imipramine (4). Additionally, curcumin has been proven its safeness in human, since the long-term administrations (i.e., 18 months) of curcumin doses of as high as 8 g/day do not cause any potential toxicity in clinical trial (153). However, the clinical use of curcumin has been limited by its poor bioavailability, which was correlated to low aqueous solubility, extensive hepatic and intestinal metabolism, and fast systemic elimination (154, 155). In addition, a number of studies have reported various factors affecting the decomposition process of curcumin, such as exposure to ultraviolet and visible light, which could be a challenging task for long-term preservation (156). Therefore, it is important to develop novel oral delivery system for curcumin.

Due to the benefits of lipid-based nanodrug delivery systems over other systems, these systems have been increasingly developed for curcumin delivery (157, 158). The two most potential advantages of these systems are (1) the utilizations of biocompatible and biodegradable natural non-toxic lipids as carriers, and (2) the ability to selectively improve the absorption of lipophilic drugs in the gastrointestinal (GI) tract via lymphatic uptake pathway (159). Among various well-known systems, self-emulsifying drug delivery systems (SEDDS) are attractive approaches to enhance curcumin water solubility and oral bioavailability (160-162). SEDDS, commonly classified as self-microemulsifying/-nanoemulsifying drug delivery systems (SMEDDS/SNEDDS), are isotropic combinations of surfactants, oil, and active ingredient that could re-constitute to become an emulsion upon contacting with the GI

fluid after orally administration. Owing to their tiny particle sizes and high solubilization potential, SEDDS is a technology that is anticipated to improve the lipophilic drug water solubility. These properties allow for enhancing drug permeation through the GI membrane, leading to an increase in drug bioavailability (15, 163). However, as a liquid state, SEDDS may cause the drug to be physicochemical unstable (i.e., precipitation, leakage) at ambient temperature due to the incompatibilities between the gelatinous capsules and the volatile excipients. This disadvantage could be overcome without affecting self-emulsifying properties by preparing these systems in a solid form using an absorbent (164-166).

Therefore, the present research developed curcumin loaded solid-SEDDS (SSEDDS) with improved oral bioavailability. The system physicochemical properties of droplet size, morphology, zeta potential, drug loading capacity, and drug recovery were investigated. The particles *in vitro* release profiles in the simulated GI fluids were then examined. Additionally, the *in vitro* cytotoxicity and Caco-2 cell permeability of the systems were also investigated. Finally, the system long-term storage stability was determined at room temperature.

2. Materials and methods

2.1 Materials

Curcumin (purity of ≥ 80%) was bought from Thai-China Flavours and Fragrances Industry (Bangkok, Thailand). The standard curcumin was imported from Sigma-Aldrich (MO, USA). Transcutol® HP (diethylene glycol monoethyl ether) and Labrasol® (PEG-8 caprylic/capric glycerides, LS) were obtained from Gattefosse (Cedex, France). Oleic acid, castor oil, and Lexol® (medium chain triglyceride) were bought from Namsiang trading (Bangkok, Thailand). Neusilin®UFL2 was imported from Fuji Chemical Industry CO., Ltd. (Toyama, Japan). All other utilized chemicals were of reagent grade or higher.

Caco-2 cells (HTB-37™) were imported from the American Type Culture Collection (VA, USA). Dulbecco's modified Eagle's medium (DMEM F-12), fetal bovine serum, trypsin, antibiotic/antifungal, and other relevant chemicals for cell culture were bought from Sigma-Aldrich (MO, USA). The 12-mm-transwell-plates with 0.4-mm-pore-size polycarbonate membrane were obtained from Corning Costar

(NY, USA). The XTT assay kits were bought from Roche Diagnostics Corporation (ThermoFisher Scientific, Thailand).

2.2 Development of curcumin loaded solid SEDDS (C-SSEDDS)

2.2.1 Solubility studies

To evaluate the curcumin solubility, an excess curcumin amount was subjected to 1 mL of several vehicles as indicated in Table 1, magnetically stirred (900 rpm) for 1 h, and the samples were centrifuged at 14,000 rpm, 30 min after equilibrium (Mikro 120 Hettich, Burladingen, Germany). The supernatant was then diluted with an appropriate mobile phase and the curcumin content was quantified by high performance liquid chromatography (HPLC) (LD10A, Shimadzu, Kyoto, Japan), with a C18 column (Vertisep, 250 mm x 4.6 mm x 5 µm), a mobile phase consisted of acetonitrile and acetate buffer (50:50, v/v), a flow rate of 1.2 mL/min, and an UV detection wavelength of 425 nm. The curcumin concentrations were then calculated based on a calibrated standard curve with a linear range of 0.1-100 µg/mL.

2.2.2 Pseudo-ternary phase diagram

The pseudo-ternary phase diagrams were systematically observed in the absence of curcumin at ambient temperature by a water titration method and created utilizing the CHEMIX School software (version 3.51). The surfactant and co-surfactants (S_{mix}) were established in various ratios of 1:0.25, 1:0.5, 1:1, and 2:1 (v/v). The oil and S_{mix} were then thoroughly blended, with the oil and S_{mix} ratios varied from 9:1 to 1:9 (v/v). To establish equilibrium condition, the distilled water was subjected dropwise to every clear mixtures with mild agitation. Next, the mixtures transparency was visually observed and evaluated. Finally, the mixtures were being titrated with water until turbidity. The optimal ratios were chosen from samples with the isotropic and transparency properties, indicating that they were in the areas of a micro/nanoemulsion.

2.2.3 Preparation of curcumin loaded liquid SEDDS (C-SEDDS)

The SEDDS at the selected optimal ratios were fabricated for the curcumin incorporation. Curcumin was dissolved in SEDDS and mixed by stirring at 900 rpm to obtain a final curcumin content of 100 mg/mL.

2.2.4 Preparation of curcumin loaded solid SEDDS (C-SSEDDS)

C-SEDDS was prepared into a powder form, C-SSEDDS, by mortar-and-pestle technique using a solid inert carrier, Neusilin®UFL2. The optimized liquid C-SEDDS was mixed with Neusilin®UFL2 at a ratio of 1:1 (w/v) and kept in a desiccator for further experiments.

2.3 Characterizations of C-SSEDDS

2.3.1 Curcumin loading and recovery

The curcumin loading and recovery of C-SSEDDS formulations was analyzed immediately after preparation to confirm appropriate drug incorporation. An accurate weight of C-SSEDDS, 10 mg, was mixed with methanol and the curcumin amounts were measured using HPLC as described in the **section 2.2.1**. The percentage of curcumin loading and recovery percentages were determined using equation (1) and (2).

$$\text{Curcumin loading (\%)} = \frac{\text{Amount of the curcumin from C-SSEDDS}}{\text{Weight of the C-SSEDDS}} \text{ x } 100\% \quad \text{..... (1)}$$

$$\text{Curcumin recovery (\%)} = \frac{\text{Amount of the curcumin from C-SSEDDS}}{\text{Amount of curcumin added}} \text{ x } 100\% \quad \text{..... (2)}$$

2.3.2 Mean droplet size and polydispersity index

The mean droplet sizes and polydispersity indexes of C-SSEDDS were measured utilizing the photon correlation spectroscopy technique (ZetaPALS® zeta-analyzer, Brookhaven Instrument Corporation, Holtsville, USA). For this, 10 mg of samples were diluted with 15 mL of 3 different media, namely water, HCl (pH 1.2), and phosphate buffer (pH 6.8). The machine was run at a 90° angle for 6 measurement cycles.

2.3.3 Morphology

The morphology of the C-SSEDDS formulations were observed by transmission electron microscopy (TEM, Tecnai G TF20, Philips, USA). The samples were diluted with water at the ratio of C-SSEDDS: DI water at 1:1.5 w/v. For analysis, a drop of the C-SSEDDS solution was placed on a film-coated copper grid to form a thin liquid film, followed by negatively stained with 2% uranyl acetate, and air-dried. Finally, TEM micrographs of the samples were photographed.

2.4 *In vitro* dissolution studies

The dissolution tests were performed using USP apparatus II (Model UDT-804, Logan Instrument Corp., NJ, USA) at 100-rpm paddle speed. A fixed amount of C-SSEDDS, equivalent to 50 mg curcumin, was weighed and dispersed in the dissolution media composed of 300 mL of HCl (pH 1.2) or phosphate buffer solution (pH 6.8), and maintained at 37 ± 0.5 °C in the dark for the entire tests. Samples were withdrawn at 5, 15, 30, and 60 min and media refilled. The samples were then filtered and analyzed using HPLC as previously described. The emulsification time of micro/nano-emulsions was also visually assessed.

2.5 Determination of C-SSEDDS absorption in Caco-2 cells

2.5.1 *In vitro* cytotoxicity studies

Caco-2 cells (passage number 35-45) were cultured on a 96-well plate at a seeding amount of $1x10^4$ cells/well at 37 ºC, 5% CO_2 and 95% humidity. Then, the C-SSEDDS, equivalent to the curcumin concentrations of 5-25 µg/mL, were dispersed in serum-free medium and subjected to each separate well, followed by a 4-h incubation. After that, the medium was withdrawn and XTT solution (200 µL) was put into each well and incubated for another 4 h. Finally, the cell viability was quantified at a measuring wavelength of 490 nm employing microplate reader (DTX880, Beckmancoulter, CA). The control was the cell-free culture medium, representing 100% viability. The cell viability (%) was determined followed equation (3).

$$\text{Viability (\%)} = \frac{\text{Sample absorbance} - \text{Blank absorbance}}{\text{Control absorbance} - \text{Blank absorbance}} \text{ x } 100\% \ldots\ldots\ldots\ldots\ldots \text{ (3)}$$

2.5.2 Curcumin transport across Caco-2 monolayers

For the *in vitro* permeation studies of C-SSEDDS, Caco-2 cells at a density of $1x10^5$ cells/well were cultured on the apical side of the Transwell® plate (1.12 cm^2 surface area, 12 wells/plate), and incubated at 37 ± 0.5 ºC and 5% CO_2 for the entire experiments. Cells were maintained for 21 days with media changes every even days. Formation and integrity of Caco-2 monolayers and tight junctions were monitored by transepithelial electrical resistance (TEER) with a volt–ohm meter (Millicell® RERS-2, Millipore Corporation, MA). Monolayers with TEER below 400 $\Omega \cdot cm^2$ were

discarded. After cell differentiation, the apical compartment solution was replaced with 500 µL of the serum-free medium containing C-SSEDDS (equivalent to 7.5 µg curcumin), and the basolateral compartment solution was replaced with serum-free medium. A sample volume of 0.5 µL was taken from the basolateral side at 0.5, 1, 2, 3, and 4 h, and fresh medium refilled. The curcumin amount in the apical side and in the cell monolayer was determined after 4 h. The apical and basolateral samples were concentrated using a speed vacuum concentrator (Labconco Corporation, Missouri, USA) at 45 °C for 1 h, and the solid mass was dissolved in 200 µL methanol before injection into HPLC for quantification of curcumin content. The cell monolayers were washed thrice with 0.5 mL of PBS (pH 7.4), collected in 0.5 mL of acetonitrile, and diluted with methanol. The samples were then concentrated, re-dissolved, and subjected to HPLC as described above.

The curcumin transport from the apical side to the basolateral side was expressed as permeation amount in basolateral compartment versus time. The curcumin apparent permeability coefficient (P_{app}, cm/s) was determined based on equation (4).

$$P_{app} = (dQ/dt)/(C_0 x A) \quad \ldots\ldots\ldots\ldots\ldots\ldots \quad (4)$$

Where dQ/dt is the curve slope (mg/h), A is the diffusion area (1.12 cm^2), C_0 is the initial curcumin concentration in the apical side (15 µg/mL).

2.6 Stability of C-SSEDDS

The C-SSMEDDS and C-SSNEDDS were kept in the dark for 1 year at room temperature. After that time, the physical appearance, self-emulsifying time, and droplet size were evaluated. Using HPLC, as indicated above, the curcumin remaining percentages were determined.

2.7 Statistical analysis

The results were demonstrated as mean ± standard deviation (SD) from at least three separate measurements. For statistical comparisons, one-way analysis of variance (ANOVA) and Tukey's post hoc tests were utilized, with significant differences set at $p < 0.05$.

3. Results and discussions

SEDDS are isotropic combinations of surfactants/co-surfactants and oils that could emulsify spontaneously and form homogenous oil-in-water emulsions when being contacted with an aqueous phase with gentle agitation by gastric mobility (163). In terms of formulation factors, oil is the most crucial component because it could dissolve the lipophilic drugs or facilitate self-emulsification at a certain dose. It also enhances the transportations of these lipophilic drugs via the intestinal lymphatic route, thus improving the drug absorption from the GI system (15). Surfactants help solubilize lipophilic drugs and prevent their precipitation in the GI lumen. Furthermore, they help increasing the microemulsion thermodynamic stability by reducing the interfacial energy via absorption at the interface. After C-SSEDDS are diluted in aqueous solution, they immediately generate oil-in-water particles that rapidly spreads in the medium. The most commonly utilized surfactants are the nonionic molecules with a reasonably high hydrophilic-lipophilic balance (HLB), as they are less toxic and typically have a low critical-micelle concentration (163).

3.1 Development of curcumin loaded solid SEDDS (C-SSEDDS)

3.1.1 Solubility studies

SEDDS is a potential strategy to increase the water solubility of curcumin, a lipophilic drug with an aqueous solubility of ~ 0.02 mg/mL. Thus, the types of oils and surfactants were chosen based on the curcumin solubility in each vehicle. The castor oil and Lexol® showed higher curcumin solubility compared to that of the oleic acid, and thus, were selected as the oily vehicle. Regarding the surfactants, nonionic surfactants of Cremophor RH40® (HLB ~12-14), Labrasol® (HLB ~14), and Transcutol® (HLB ~4) yielded good curcumin solubility (~25-30 mg/mL) (Table 13).

Table 13 Solubility of curcumin in various vehicles

Vehicles	Curcumin solubility (mg/ml)
Water	0.02 ± 0.00
Oils	
Castor oil	1.00 ± 0.13
Lexol GT865®	0.82 ± 0.06
Oleic acid	0.04 ± 0.01
Surfactants	
Cremophor RH 40®	25.63 ± 2.20
Glycerin	0.79 ± 0.18
Labrasol®	29.75 ± 0.78
Propylene glycol	1.95 ± 0.37
Transcutol®	30.90 ± 1.82

3.1.2 Pseudo-ternary phase diagrams

To identify the micro/nanoemulsion area, pseudo-ternary phase diagrams were constructed in the absence of curcumin based on the results of solubility tests. Consequently, the optimal oil: surfactant: co-surfactant ratio was estimated.

Castor oil and Lexol® were used as oil in these systems. The phase diagrams were built for the 03 systems of (1) Labrasol® and Transcutol®, (2) Labrasol® and Cremophor RH40®, and (3) Transcutol® and Cremophor RH40®, which represented as S_{mix} (LT), S_{mix} (LC), and S_{mix} (TC). The maximum region of SEDDS was obtained with S_{mix} in the ratio of 1:1. Then, the effect of S_{mix} on phase diagrams was further investigated. Regardless of the oil types, the phase diagrams of the system with S_{mix} (LT) were turbid, indicating unstable system, and hence, were not employed. The phase diagrams of Lexol® and S_{mix} (TC) at the ratio of 1:9 showed the largest region of SNEDDS (Fig. 1a), similarly to the phase diagram of Lexol® and S_{mix} (LC) at the ratio of 2:8 (Fig. 1b). In addition, the phase diagram of castor oil and S_{mix} (TC) at the ratio of 1:9 showed large region of SMEDDS (Fig. 1c), similarly to the phase diagrams of Lexol® and S_{mix} (LC) at the ratio of 1:9 (Fig. 1b). Based on the results, 04 formulations of SEDDS were used for further experiments.

The phase diagrams also indicated that the micro/nanoemulsion area was achieved when using Transcutol® or Labrasol® with Cremophor RH40® due to the effect of the longer hydrocarbon chain length of Cremophor RH40® (C57) compared to Transcutol® (C6) and Labrasol® (C8-C10), which leads to increased oil dissolution and nano-size droplets (163, 167).

3.1.3 Preparation of curcumin loaded liquid SEDDS (C-SEDDS)

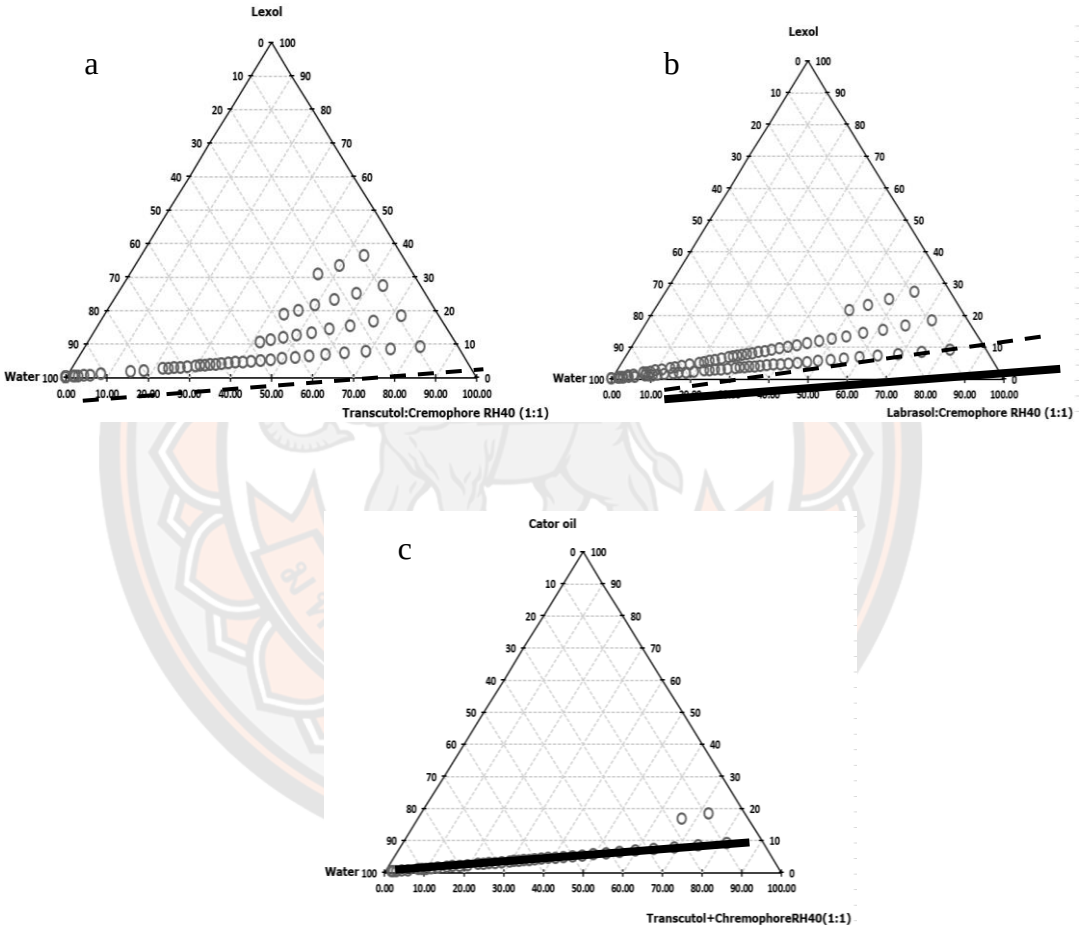

Figure 12 Pseudo-ternary phase diagrams of SEDDS formulations. (a) Lexol: S_{mix} (Transcutol® and Cremophor RH40®), (b) Lexol: S_{mix} (Labrasol® and Cremophor RH40®) and (c) castor oil: S_{mix} (Transcutol® and Cremophor RH40®). The black line (▬▬) represents SMEDDS and the black dash line (▬ ▬) represents SNEDDS

As discussed previously, 04 SEDDS formulations were chosen to fabricate C-SEDDS. The effect of S_{mix} on curcumin solubility was investigated by dissolving curcumin in 1 mL of oil:S_{mix} mixture at the ratio of 1:9. Regardless of the oil types, the SEDDS formulation with S_{mix} (TC) exhibited curcumin solubility of 100 mg/mL. On the contrary, SEDDS formulation of Lexol® and S_{mix} (LC) showed curcumin solubility of 70 mg/mL. Conclusively, 02 formulations composed of castor oil with S_{mix} (TC), and Lexol® with S_{mix} (TC) at the ratio of 1:9 were classified as C-SMEDDS and C-SNEDDS, respectively.

Transcutol®, Labrasol®, and Cremophor RH40® are nonionic surfactants with HLB value of 4, 14, and ~12-14, respectively (163). The fact that curcumin possesses higher solubility in S_{mix} (TC), a lipophilic-hydrophilic surfactant mixture, than in S_{mix} (LC), a hydrophilic-hydrophilic surfactant mixture, could be attributed to the lipophilic surfactants that dissolve curcumin more efficiently than hydrophilic ones (168).

Unfortunately, we found that after 1-month storage, the C-SEDDS showed only ~70% of the curcumin remaining. This discourage effect might be due to Cremophor RH40®, which possesses conjugated unsaturated bonding that is strongly vulnerable to oxidation, leading to the peroxyl radicals formation, and resulting in curcumin degradation (169, 170).

3.1.4 Preparation of curcumin loaded solid SEDDS (C-SSEDDS)

To increase the chemical stability of curcumin during storage, C-SMEDDS and C-SNEDDS was transformed into solid C-SMEDDS (C-SSMEDDS) and solid C-SNEDDS (C-SSNEDDS) using Neusilin®UFL2 as an adsorbent carrier. All C-SSEDDS, prepared at the C-SEDDS: Neusilin®UFL2 ratio of 1:1 (w/w), demonstrated fine powder with a free-flowing property. Curcumin loading was ~5% for each C-SSEDDS formulation, whereas curcumin recovery was > 80%, indicating that this technique was suitable for preparing C-SSEDDS (Table 14).

Table 14 Physicochemical characterization of C-SSMEDDS and C-SSNEDDS

Formulation	Curcumin loading (%)	Curcumin recovery (%)	Mean particle size (nm)		Emulsification time (Second)	
			Initial time	1 year	Initial time	1 year
C-SSMEDDS	5.08 ± 0.13	84.17 ± 1.51	104.7 ± 6.1	101.4±4.6	12.07±0.54	12.31±0.20
C-SSNEDDS	5.14 ± 0.13	86.92 ± 0.48	154.5 ± 4.0	152.1±7.6	11.69±0.30	12.08±0.50

3.2 Mean droplet size, morphology and emulsification time

To improve oral bioavailability, the nano-size of drug delivery carriers is one crucial property (157). In this study, deionized (DI) water, HCl (pH 1.2), and phosphate buffer saline (pH 6.8) were used as a dispersion medium. In all tested media, C-SMEDDS and C-SNEDDS showed similar droplet sizes, ~100 nm and ~ 150 nm, respectively. In addition, the C-SSMEDDS and C-SSNEDDS prepared with Neusilin®UFL2 gave a mean droplet sizes similar to those of C-SEDDS in the liquid form (Table 2). The polydispersity indexes were in the range of 0.175-0.280, indicating narrow size distribution. This result confirmed that the droplet size was remained stable, without aggregation, in the GI fluid. Furthermore, regardless of the formulation factors, TEM micrographs of C-SSMEDDS and C-SSNEDDS showed spherical micelles with an average size of ~100 and ~150 nm, respectively (Fig. 2), which was consistent with data obtained by photon correlation spectroscopy technique.

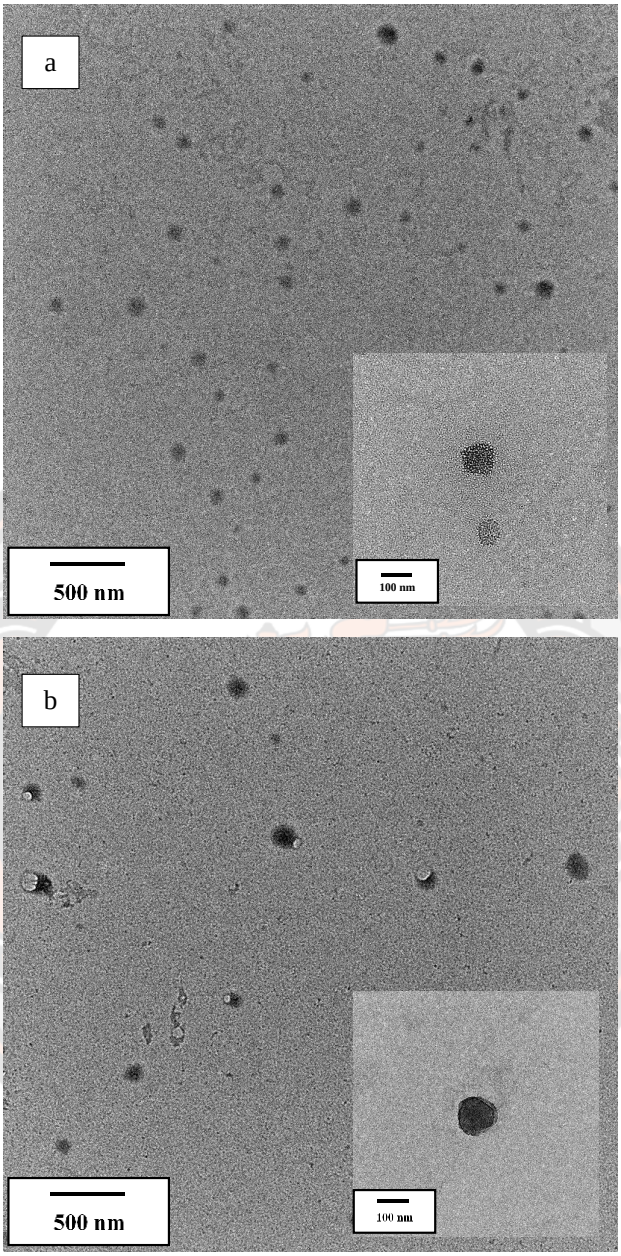

Figure 13 TEM micrographs of (a) C-SSMEDDS and (b) C-SSNEDDS after dilution with DI water.

3.3 *In vitro* dissolution studies

Emulsification time was assessed as an important factor for evaluating the self-emulsification efficiency. Upon mixing with all medium, C-SSMEDDS and C-SSNEDDS demonstrated instant self-emulsification with emulsification time of 10-15 s (Table 2) without phase separation or aggregation.

The *in vitro* release patterns of C-SSMEDDS and C-SSNEDDS in pH 1.2 and 6.8 are shown in Fig 3a and 3b, respectively. As expected, curcumin powder cannot be quantified by HPLC in both medium due to its extremely poor solubility and dissolution. On the contrary, SSEDDS could significantly improve the dissolution rates of curcumin. Specifically, curcumin was burstly released from C-SSMEDDS and C-SSNEDDS at pH 1.2, with % release of ~70% and ~60% within 5 min, respectively. Similarly, in pH 6.8, within 5 min, ~60% and ~70% of curcumin was released for C-SSMEDDS and C-SSNEDDS, respectively.

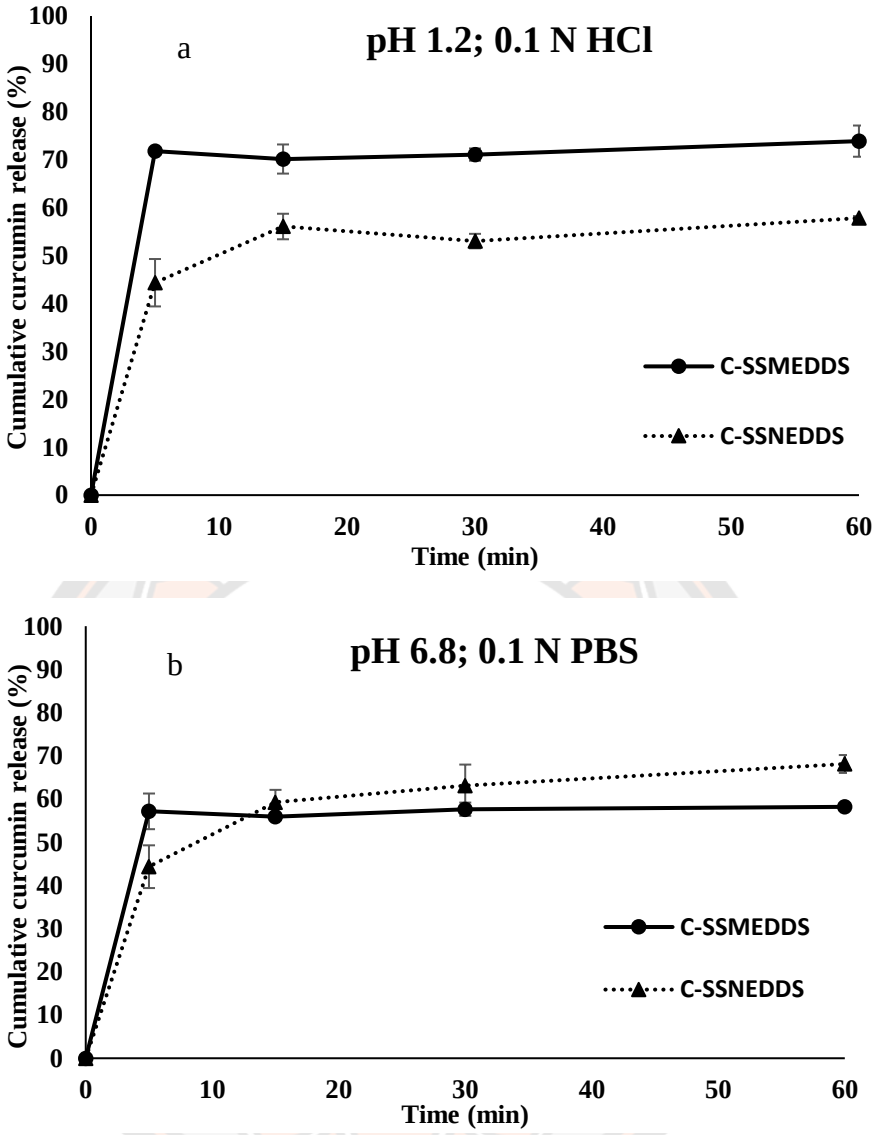

Figure 14 Cumulative percentage released of curcumin from C-SSMEDDS and C-SSNEDDS in (a) pH 1.2 0.1 N HCl and (b) pH 6.8 phosphate buffer solution. Each value represents the mean ± SD (n=3)

Rapid drug dissolution from the C-SSEDDS could be attributed to the nano-carriers obtained by means of rapid self-emulsification through establishing an interface between the dissolution medium and the oil (171). The self-emulsification efficiency of (co)-surfactants is closely associated to their respective HLB values. Cremophor RH40® (HLB 12-14) is generally considered as a surfactant with good self-emulsification efficiency (172). However, the released drug was < 100% due to the

drug-Neusilin®UFL2 complex formation, possibly via hydrogen bonding (173). Neusilin®UFL2, an amorphous powder of synthetic magnesium aluminosilicate, has a mean particle size of approximately 2.94 mm, an average pore-size of about 17 nm (high porosity), a pore volume of 1.37 cm^3/g, and a specific surface area of 300 m^2/g. Consequently, it offers great adsorption capacity (174).

3.4 Determination of C-SSMEDDS and C-SSNEDDS absorption in Caco-2 cells

The potential cytotoxicity of C-SSMEDDS and C-SSNEDDS on differentiated Caco-2 cells was investigated using the XTT assay prior to permeation studies. In accordance with the International Organization for Standardization (ISO 10993-5) (ISO 2009), a cell viability of more than 70% is seen as nontoxic. At dosages of 25 µg/mL curcumin, the viability of cells decreased to 50%, suggesting toxicity at this high concentration. On the other hand, all formulations with lower curcumin concentrations (5, 10, and 15 µg/mL) showed cell viabilities of > 70%, demonstrating no potential cytotoxicity. Thus, the amounts of C-SSMEDDS and C-SSNEDDS, equivalent to 15 µg/mL curcumin, were selected for permeation experiments.

Curcumin is not a substrate of the P-glycoprotein (P-gp) efflux transporter because it had the same P_{app} value in both directions, from the apical to the basolateral side and from the basolateral to the apical side. Therefore, only curcumin transported from the apical to the basolateral side was performed. After 4-h incubation, the free curcumin dispersion showed ~24% curcumin recovery (Table 3), which found only in the apical side, while curcumin could not be detected in the Caco-2 cell monolayer and basolateral compartment, indicating restricted curcumin absorption. This could be additionally explained by the curcumin rapid hydrolytic degradation at neutral conditions (9). On the contrary, curcumin distribution of C-SSMEDDS and C-SSNEDDS in the apical side, the basolateral side, and the cell monolayer showed no significant differences with ~100% curcumin recovery (Table 3). Moreover, Figure 4 shows that both formulations could help curcumin permeate through the cell monolayer as soon as 30 min after incubation, and showed linear kinetics up to 4 h.

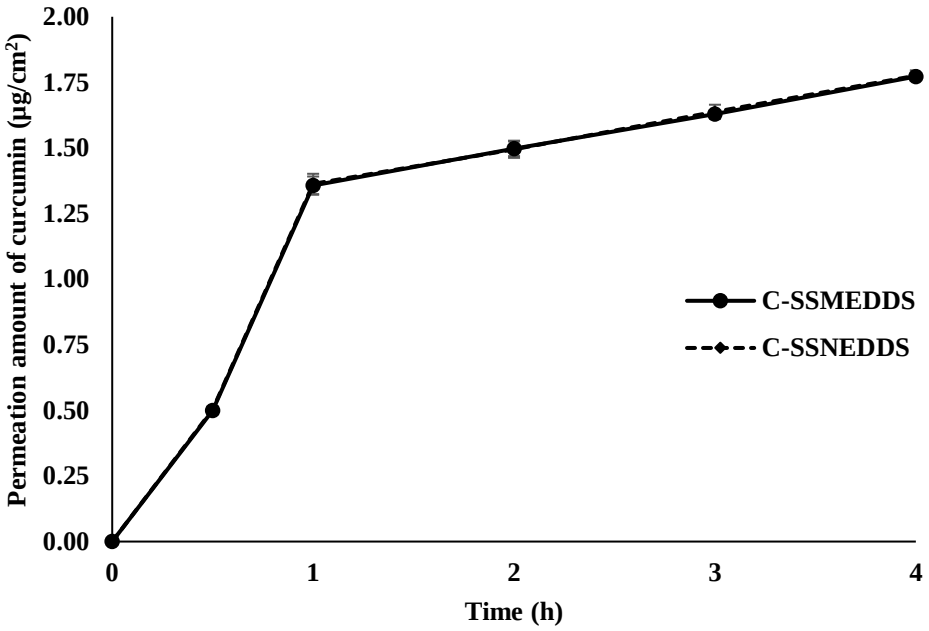

Figure 15 Permeation amount of curcumin across Caco-2 cells monolayer. Each value represents means ± SD (n=3)

Table 15 The Percentage of curcumin in apical side, basolateral side, cell monolayer and the apparent permeability coefficient across Caco-2 monolayer after 4 h incubation

Formulation	Curcumin ± SD (%)			P_{app} x 10^{-6} (cm/s)
	Apical side	Basolateral side	Caco-2 cells	
Curcumin dispersion	23.88 ± 1.14	Not detect	Not detect	Not detect
C-SSMEDDS	66.78 ± 2.61	26.46 ± 0.23	7.42 ± 1.15	5.11 ± 0.28
C-SSNEDDS	66.46 ± 1.74	26.51 ± 0.31	7.72 ± 0.98	5.11 ± 0.27

The corresponding P_{app} values were determined based on the curcumin ability to cross the cell monolayers. The C-SSMEDDS and C-SSNEDDS showed no significant difference for P_{app} value (Table 3). The associations between the permeability through the Caco-2 monolayer and absorbed fraction in human have been

evaluated in many studies (175, 176). A compound with P_{app} of < 1 x 10^{-6} cm/s, 1-10 x 10^{-6} cm/s, and > 10 x 10^{-6} cm/s is considered as *in vivo* low absorption (0-20%), moderate absorption (20-70%), and high absorption (70-100%), correspondingly (176). Thus, according to the P_{app} value, C-SSMEDDS and C-SSNEDDS were classified as moderate permeability systems, ~5.11 x 10^{-6} cm/s (Table 3).

It is worth to note that the cell monolayer TEER values after 4-h incubation was slightly decreased, ~340 Ω·cm^2, compared to those of pre-incubation, ~400 Ω·cm^2 (Table 4). This could be attributed to the surfactant that temporary disrupts the cell membrane (177). Nevertheless, the integrity of Caco-2 monolayer has been report with a TEER of 150-400 Ω·cm^2 (178). Therefore, the TEER value in this study indicated that the monolayer integrity was sustained throughout the *in vitro* permeability experiments.

Table 16 The TEER value of the Caco-2 cells monolayer before and after *in vitro* permeation studies

Formulations	TEER (Ω/cm^2)	
	Before tested	After tested at 4 h
C-SSMEDDS	404 ± 5	329 ± 10*
C-SSNEDDS	403 ± 11	344 ± 12*

* $p<0.01$ compared with before tested.

Overall, the results clearly showed that the degradation of curcumin in cell culture medium (pH 7.4) could be hindered by the C-SSMEDDS and C-SSNEDDS formulations. In addition, SSEDDS could significantly enhance the curcumin absorption efficiency because of several advantages of these systems. Firstly, SSEDDS increase the curcumin solubility. According to the Fick's first law, the permeation rate is generally influenced by the surface areas and the drug concentrations in the intestinal lumen. As the drug concentrations increase, more drug molecules exist at the epithelial cell surfaces, leading to a greater drug absorption via transcellular transport (179). Secondly, small nanoparticles (< 200 nm) would be directly taken up by cells via endocytosis (180). Thirdly, surfactant, in SSEDDS, could transiently disrupt cell

membrane integrity, which facilitates curcumin penetration through the cell membranes via transcellular transport (177). Lastly, the lipid core of the nanoparticles could stimulate the formation of chylomicrons and facilitate uptake into the lymph, bypassing hepatic first-pass metabolism (181).

3.5 Stability of C-SSEDDS

After 1-year storage at ambient temperature and without sunlight, the physicochemical properties of both C-SSEDDS were maintained. Both samples remained in the powder form with no physical changes. Upon dilution with water, a rapid self-emulsification time of 12 s was observed and the droplet sizes of C-SSMEDDS and C-SNEDDS was ~100 and ~150 nm, respectively, similar to their freshly-prepared counterparts (Table 2). Additionally, compared to the freshly-prepared formulations, no significant differences ($p > 0.05$) were noted in the percentages of remaining curcumin, which was ~100%. Thus, the finding indicated that C-SSEDDS demonstrated physically and chemically stability for at least 1 year at room temperature.

4. Conclusion

This study clearly demonstrated the possibility of C-SSMEDDS and C-SSNEDDS as promising delivery systems for curcumin. These nano-carrier systems could improve curcumin oral bioavailability by encapsulating and protecting curcumin degradation in the GI tract, and enhancing curcumin dissolution and absorption through intestinal monolayer. Upon dilution in water, the obtained C-SSMEDDS and C-SSNEDDS demonstrated fast and complete self-emulsification within 15 s, and possessed mean droplet sizes of ~100 and ~150 nm, respectively, with a narrow distribution. Furthermore, the droplet sizes of C-SSMEDDS and C-SSNEDDS were not affected by the pH variation in the GI tract. Curcumin dissolved and released completely in dissolution media within 15 min. In addition, the developed formulations showed a greater curcumin absorption in Caco-2 cell monolayer than the free curcumin, suggesting an improvement in the curcumin oral bioavailability. Nevertheless, these assumptions could be further investigated in animal studies to confirm safety and efficacy, followed by a full clinical evaluation, to facilitate the commercialization of these systems.

CHAPTER V

DEVELOPMENT, CHARACTERIZATION AND CACO-2 CELLS ABSORPTION OF CURCUMIN SOLID DISPERSION FOR ORAL ADMINISTRATION

This chapter is the manuscript currently under revision for publication.

Abstract

Curcumin is an active dietary compound. However, its low solubility and rapid metabolism limit its absorption in the gastrointestinal (GI) tract and reduces its systemic bioavailability. To overcome these drawbacks, curcumin solid dispersion (CSD) was developed employing polyvinylpyrrolidone (PVP) as a carrier without and with soybean phospholipids (SP) as a co-carrier and prepared using a melting solvent method. The influence PVP and SP on physicochemical properties and *in vitro* permeability of CSD was investigated. Curcumin in all developed CSD demonstrated amorphous state as confirmed by X-ray diffraction. Spherical particles of ~ 140 nm and ~ 190 nm were obtained when CSD without and with SP was diluted with water. Consequently, CSD without and with SP possessed significantly greater curcumin water solubility of ~ 4200-fold and ~ 6500-fold, respectively, as compared to free curcumin, which leading to enhanced curcumin absorption across Caco-2 cell. The dissolution studies, both in 0.1N HCl and phosphate buffer pH 6.8, of CSD showed that curcumin was quickly and completely dissolved within 5 min. Caco-2 cell permeation studies revealed that CSD with SP presented a lag time with slightly lower curcumin absorption than CSD without SP. Moreover, the physical and chemical stability of CSD was found to be stable for up to 6 months at 4ºC and room temperature. From these findings, CSD could be beneficial for enhancing the oral absorption profiles of curcumin.

keywords absorption, curcumin, Caco-2 cell, solid dispersion, oral administration

1. Introduction

Curcumin, chemically known as diferuloyl methane, is a lipophilic polyphenol extracted from the ground rhizomes of the plant Curcuma longa Linn. It has long been used as a dietary supplement and medicine. It has many potent pharmacological activities, for example, anti-inflammatory, antioxidant, wound healing and neuroprotective effects (3, 182). The fact that it proved nontoxic to humans at dosages up to 8 g/day for 18 months indicates that it is a very safe medication (153). However, the oral bioavailability of curcumin is very low (only 1% in rats) because it is poorly water soluble, extensively metabolized, readily degraded under alkaline conditions, and undergoes rapid excretion (154, 183, 184). Curcumin also chemically degrades when exposed to light or high temperatures, which promotes color fading (185).

Solid dispersions (SD) of poorly water-soluble drugs have been formulated with hydrophilic carriers to improve their solubility and dissolution rate (14, 85, 186, 187). Through manufacturing techniques such as hot melt, solvent, or melting solvent method, drug can be changed from a crystalline state into an amorphous state as well as reduced its particle size to a molecular level, which improved its water solubility. Additionally, the hydrophilic carrier promotes the SD porosity and wettability (12, 14, 186).

In addition to the conventional SD, several studies have attempted to further increase the drug water solubility by employing surfactant. Improved wettability, and dissolution enhancement as well as stabilization of amorphous state of drug, are some of the advantages that have been observed with SD containing surfactants (14, 186, 187). Phospholipids are one of the most interesting surfactants since they are typically naturally-occurring molecules that are both biocompatible and biodegradable, resulting in low acute and chronic toxicity in *in vivo* applications. (159).

In the present study, curcumin SD without and with phospholipid have been developed to enhanced curcumin oral bioavailability. The particle size, size distribution, percentage curcumin loading and recovery, X-ray diffraction (XRD) and storage stability were investigated. Drug release at physiological pH was evaluated. The ability to protect curcumin from degradation in GI fluid and permeability through the Caco-2 cell monolayers were also compared.

2. Materials and methods

2.1 Materials

Curcumin, ≥ 80% w/w, was purchased from Thai-China Flavours and Fragrances Industry (Bangkok, Thailand). Standard curcumin was purchased from Sigma (Lot No. SLBB7593V, MO, USA). Polyvinylpyrrolidone (PVP) was purchased from TTK Science Co. (Phitsanulok, Thailand). Soybean phospholipids (SP, Emulmetik® 900) was purchased from Lucas Meyer Cosmetic (Champlan, France). All other chemicals and reagents used were of analytical grade. Cellulose acetate filter membrane, diameter 76 mm, with a pore size of 0.2 µm (Milipore® YM100) was purchased from Millipore Corporation (MA, USA).

Caco-2 cells (HTB-37™, Passage no. 18) were purchased from the American Type Culture Collection (VA, USA). Dulbecco's modified Eagle's medium (DMEM F-12) and all the materials for cell culture were purchased from Sigma chemical (MO, USA). Cell culture plate and Transwell plate (12 mm diameter, 0.4 mm-pore-size polycarbonate membrane) were purchased from Corning Costar (NY, USA). Sodium30-(1-(phenyl-aminocarbonyl)-3,4-tetrazolium)-bis(4-methoxy-6-nitro) benzene sulfonic acid hydrate (XTT) was purchased from Roche Diagnostics Corporation (ThermoFisher Scientific, Thailand).

2.2 Preparation of curcumin solid dispersion (CSD)

CSD was prepared by a melt solution method using curcumin, PVP, and SP in ratios of 1:4:0, 1:6:0, 1:8:0, 1:8:0.25, and 1:8:0.5. PVP and SP were melted in absolute ethanol and then curcumin dissolved in absolute ethanol was added to the melted mixture with constant stirring until it was homogenized in an ice bath. Solidification was carried out in a hot air oven at 45ºC for 12 h. The dried mixture was pulverized using a glass mortar and pestle and stored in a desiccator until further studies. The curcumin physical mixture (CPM) was prepared by mixing curcumin, PVP without and with SP in a glass mortar and pestle.

2.3 Percentage of curcumin loading and recovery

For determination of %drug loading and recovery, accurately weighed CSD 10 mg was dissolved with methanol 10 mL. The sample was diluted with mobile phase. Concentration of sample was determined through a HPLC system (LD10A, Shimadzu, Kyoto, Japan) with UV detection at 425 nm and a Vertisep C18 column (5

μm, 4.6 x 250 mm). The mobile phase system consisted of the following: acetate buffer and acetonitrile 50:50 (v/v) with a flow rate of 1.2 mL/min. The percentage of curcumin loading and recovery was calculated using the equation 1 and 2, respectively.

$$\text{curcumin loading (\%)} = \frac{\text{Amount of the curcumin from CSD}}{\text{Weight of the CSD}} \text{x100} \ldots\ldots\ldots\ldots\ldots \text{(1)}$$

$$\text{curcumin recovery (\%)} = \frac{\text{Amount of the curcumin from CSD}}{\text{Amount of curcumin added}} \text{x100} \ldots\ldots\ldots\ldots \text{(2)}$$

2.4 Saturated solubility

Solubility studies were performed by adding an excess amount of the CSD to 1 mL of DI water. The mixture was stirred at 900 rpm for 6 h at room temperature. Samples were then centrifuged at 18000 rpm for 30 min to separate the undissolved CSD. The supernatant was diluted with the mobile phase and filtered through a 0.2 μm cellulose acetate filter membrane. Curcumin content was determined by HPLC as mentioned above. All tests were repeated three times.

2.5 Physico-chemical characterization of CSD

2.5.1 The mean droplet size (MS) and polydispersity index (PI)

MS and PI of CSD were measured using a Zetasizer (Brookhaven Instrument Corporation, Holtsville, USA) by dynamic light scattering (DLS) with a scattering angle of 90◦ at 25 ◦C. The mean diameter was determined using a hydrodynamic diameter. All tests were repeated three times.

2.5.2 Morphology

Morphological observation of CSD was performed using a transmission electron microscope (TEM, Tecnai G TF20, 200 kV, Philips, USA). One mL of DI water was used to disperse 10 mg of CSD. Ten μL of the diluent was placed on a carbon-coated copper grid coated with 10 μL of uranyl acetate (2% w/v), and the sample was air dried in a desiccator before observation.

2.5.3 X-ray diffraction

To observe the state of the CSD, the CSD was characterized using an X-ray diffractometer (D2 Phaser, Bruker, USA). A certain amount of CSD was mounted onto a quartz substrate and then analyzed by XRD. The scanning speed was 2°/min and the scanning range was 10 - 70° (2θ).

2.6 *In vitro* dissolution test

The USP II paddle apparatus (Model UDT-804, Logan Instrument Corp., Somerset, NJ, USA) was used to study the in vitro dissolution of curcumin from CSD. CSD containing 50 mg of curcumin were introduced in 300 mL of 0.1 N HCl solution and pH 6.8 phosphate buffer solution. The dissolution system was maintained at 37±0.5 °C and stirred at 100 rpm. After 5, 15, 30 and 60 min, 5 mL of sample was withdrawn and immediately replenished with a fresh medium. The sample was quantified by HPLC. All tests were repeated three times.

2.7 Cytotoxicity study

Cytotoxicity of CSD was evaluated on Caco-2 cells (passage number 35-45) using XTT assay. Caco-2 cells were maintained in DMEM with 10% FBS and 1%Penicillin/Streptomycin (PS) at 37 ºC, 5% CO2 and 95% humidity before seeded in a 96-well plate at a density of 1 x 10^4 cells/well. After overnight incubation, serum free medium containing CSD, with curcumin in a range of 5-25 µg/mL, was added. After 4 h incubation at 37 ºC in a 5% CO_2 incubator, the medium was removed, and the cell was washed with PBS. Then, 200 µL of XTT solution was added directly to each well and incubated for 4 h before determining the cell viability at 490 nm using microplate reader (DTX880, Multimode Detector, Beckmancoulter, CA). Cell-free medium was used as a blank, while the untreated cell was used as a control and represented 100% viability. The percentage of cell viability was calculated based on equation 3.

$$\text{Viability (\%)} = \frac{\text{Absorbance of sample} - \text{Absorbance of blank}}{\text{Absorbance of control} - \text{Absorbance of blank}} \text{x} 100 \quad \text{..... (3)}$$

2.8 *In vitro* permeation studies in Caco-2 cell monolayer

Caco-2 cells were collected at passages number 35-45 and seeds onto the 12-well Transwell® filter inserts at a density of 1x10^5 cells/well. Later, cells were cultured for 14-21 days within the medium as mention in the section 2.7. Thereafter, a transepithelial electrical resistance (TEER) using a volt–ohm meter equipped with a chopstick electrode (Millicell® RERS-2, Millipore Corporation, MA) was adopted to assess the quality of the monolayer grown on permeable membranes. In this study, the TEER value was 400 ± 100 Ω/cm^2. For permeation studies, CSD contained 7.5 µg

curcumin were mixed in 0.5 mL serum free medium and immediately added to the upper surface of Caco-2 cell monolayers, while, 1.5 mL of serum-free medium was added to the basolateral side. Samples were then taken from the basolateral chamber and immediately replaced with the same volume of medium at 37 ◦C at predetermined time intervals. The amount of curcumin from the basolateral side was concentrated using a speed vacuum concentrator (Labconco Corporation, Missouri, USA) at 45 °C for 1 h. The dried residue was re-dissolved in 200 µL of methanol and subjected to HPLC to quantify curcumin content. After 4 h incubation, the amount of curcumin in apical and cell monolayer was detected. The sample in the apical was taken out, concentrated by speed vacuum concentrator and re-dissolved in methanol before subjected to HPLC. The amount of curcumin in the cell monolayer was determined by washing the cell twice with 0.5 mL of pH 7.4 PBS and collected in 0.5 mL of acetonitrile and diluted with methanol. Similarly, the sample was concentrated and re-dissolved in methanol before exposed to HPLC.

2.9 Stability study of CSD

CSD formulations without and with SP were stored at 4 ºC and room temperature without sunlight. After 6-month storage, the curcumin remaining was evaluated by HPLC.

2.10 Statistical analysis

Data are presented as mean ± standard deviation (SD) for all data. Statistical analyses were performed using one-way ANOVA followed by Tukey's post hoc test. $p < 0.05$ indicated statistically significant differences.

3. Results

3.1 Preparation of curcumin solid dispersion (CSD)

In this study, we prepared CSD using the melting solvent method. Absolute ethanol was used to dissolve curcumin and then added to the molten mixed carrier under constant stirring in an ice bath. The solvent was evaporated until a solid was formed, which was then ground to obtain a fine, orange yellowish CSD powder.

3.2 Saturated solubility

The effects of carrier on the solubility of curcumin when PVP was used alone and in combination with SP were studied, Table 1. The results showed that free

curcumin had a very low solubility in water of 3.90±0.19 µg/mL. Due to the effect of carrier, the CPM without and with SP showed higher solubility than free curcumin, and the CSD showed greater solubility than CPM. The water solubility of CSD increased when the PVP content was increased. Hence, CSD 1:8 showed higher curcumin water solubility than CSD (1:4), ~17 and ~14 mg/mL, respectively. To further improve the solubility of curcumin, we attempted to develop CSD at the mass ratio of 1:8 by adding SP as a surfactant. The solubility enhancement of curcumin in the CSD with SP (1:8:0.25 and 1:8:0.5) was shown to be greater than that in the CSD 1:8, at ~ 20 mg/mL, suggesting a 6500-fold increase in comparison to the free curcumin. From the result, the CSD at the mass ratio of curcumin: PVP: SP at 1:8:0, 1:8:0.25 and 1:8:0.5 (CSD 1:8, CSD 1:8:0.25 and CSD 1:8:0.5) were chosen for further study. The CPM also exhibited higher curcumin water solubility than free curcumin, but lower than CSD.

Table 17 The effects of PVP and SP content on the physicochemical properties of CSD

Mass ratio of curcumin: PVP: SP	Curcumin water solubility ± SD (mg/ml)		Mean particle size ± SD (nm)	Polydispersity index ± SD
	CSD	CPM		
1:4	13.49 ± 0.15	0.66 ± 0.20	-	-
1:6	14.02 ± 0.11	1.24 ± 0.05	-	-
1:8	16.62 ± 0.87	1.18 ± 0.06	142.9 ± 5.2	0.126 ± 0.017
1:8:0.25	21.84 ± 1.41	1.34 ± 0.02	163.9 ± 4.1	0.243 ± 0.021
1:8:0.5	19.88 ± 1.53	1.28 ± 0.05	191.7 ± 7.2	0.249 ± 0.026

The results are presented as mean ± standard deviation; n=3.

In addition, all CSD showed high percentage of curcumin recovery, > 80%, suggesting a relatively low proportion of curcumin lost during the production process, Table 18.

Table 18 The effects of PVP and SP content on the percentage of curcumin recovery and curcumin loading from CSD

Mass ratio of curcumin: PVP: SP	Curcumin recovery ± SD (%)	Curcumin loading ± SD (%)
1:8	98.34 ± 3.79	11.22 ± 0.50
1:8:0.25	84.27 ± 4.97	8.45 ± 0.66
1:8:0.5	99.87 ± 1.71	9.67 ± 0.61

The results are presented as mean ± standard deviation; n=3.

3.3 Physico-chemical characterization of CSD

3.3.1 The mean droplet size (MS) and polydispersity index (PI)

Particle size analysis of the CSD was carried out using DLS technique. In case of CSD with SP, the MS was increased with an increase in SP concentration. Average particle size of CSD 1:8 prepared by only PVP after dilution in water was found to be ~140 nm, while the mean size of CSD with SP after dilution in water was ~ 160 and ~ 190 nm for CSD 1:8:0.25 and CSD 1:8:0.5, respectively. The PI value of CSD were less than 0.3 in all samples, which indicates that all samples had the uniform size distribution, Table 1. TEM micrographs of CSD 1:8, 1:8:0.15 and 1:8:0.5 showed spherical micelle, as shown in Figure 1. The particle size of CSD 1:8 was found to be smaller than CSD 1:8:0.5, which was in accordance with the DLS results.

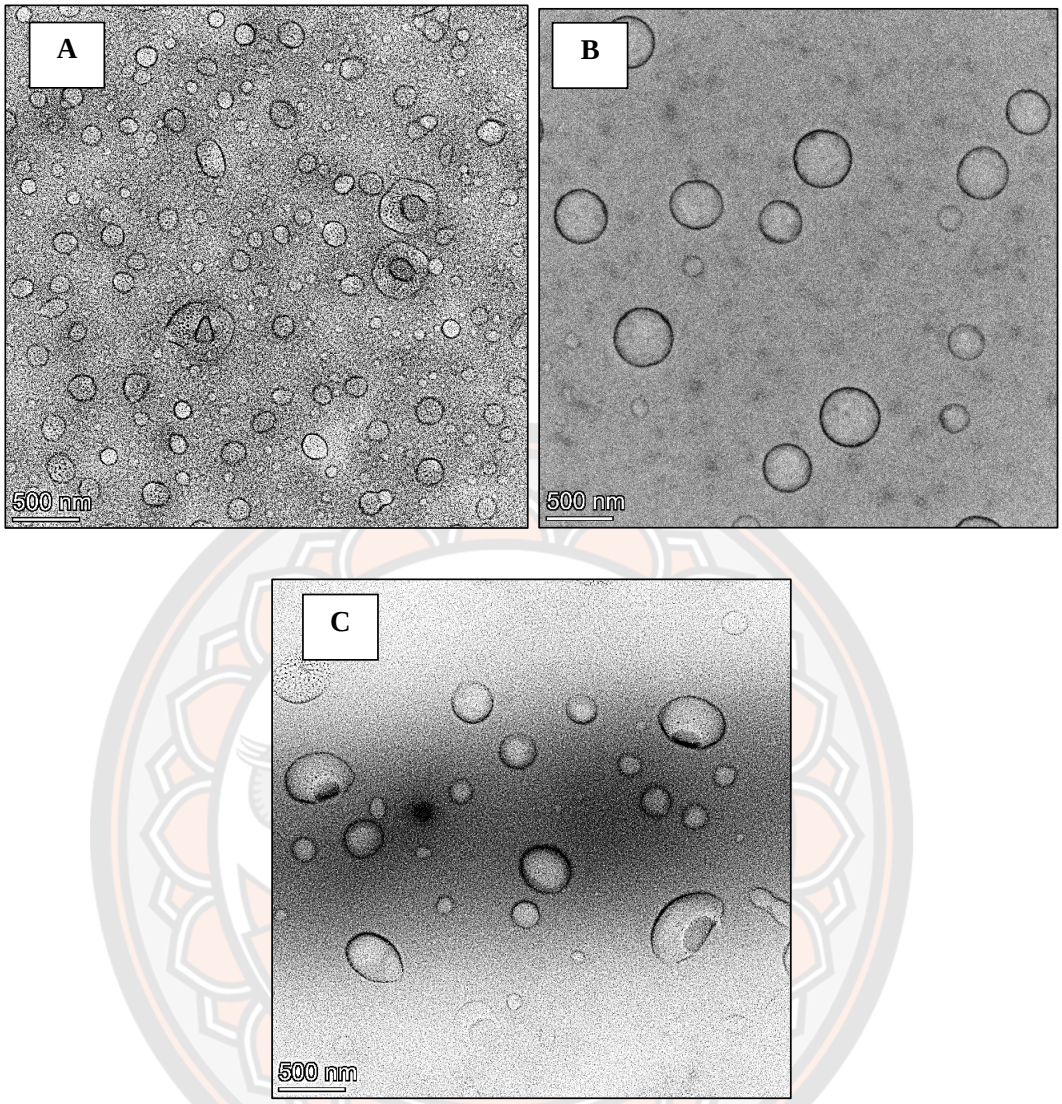

Figure 16 TEM micrographs of (A) CSD 1:8, (B) CSD 1:8:0.25 and (C) CSD 1:8:0.5

3.3.2 X-ray diffraction

The X-ray diffraction patterns of free curcumin, PVP, SP, CSD and CPM are shown in Figure 2. The X-ray spectrum of free curcumin exhibited numerous sharp diffraction peaks, indicating its highly crystalline nature, while PVP and SP illustrated a board diffraction peak, confirming their amorphous nature (188, 189). The diffraction patterns of CPM revealed overlapping peaks for the curcumin, SP and PVP, thus indicating that curcumin in the CPM was maintained in its crystalline state.

Conversely, XRD pattern of CSD showed distinct broad peak that correspond to the diffraction pattern of PVP and SP. Peaks that correspond to curcumin were completely absent, suggesting that curcumin in CSD existed in an amorphous state.

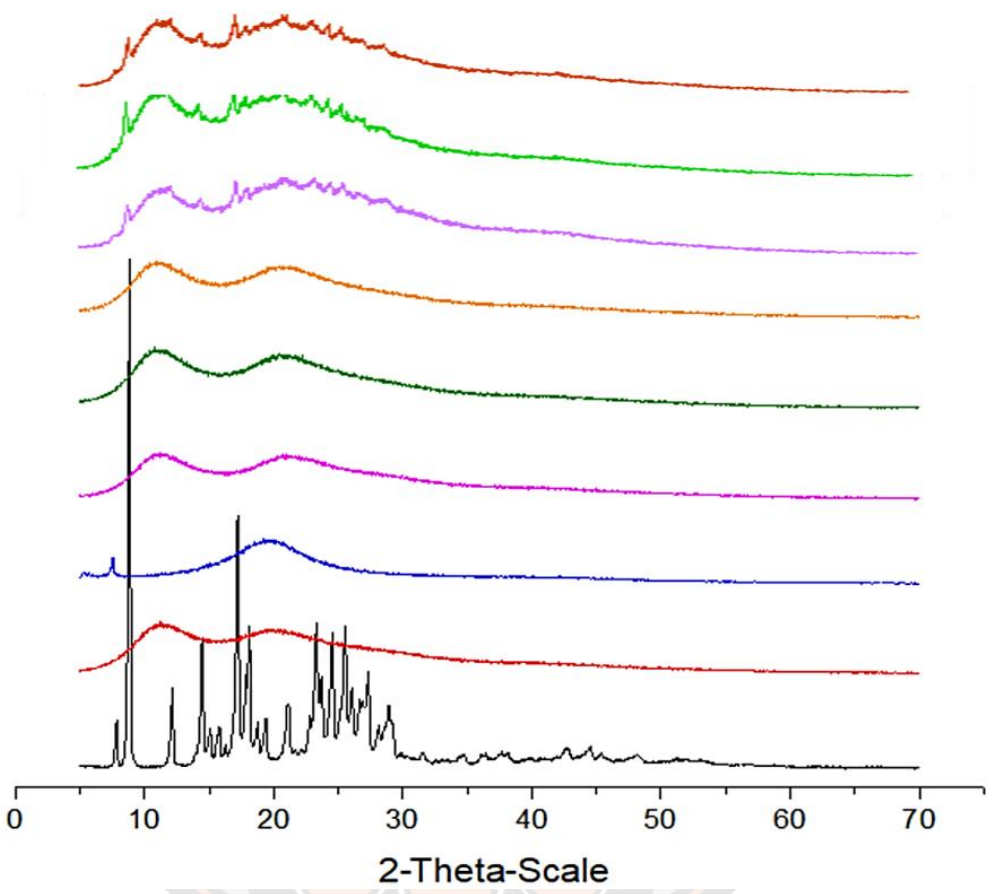

Figure 17 X-ray diffraction pattern of (1) free curcumin, (2) PVP, (3) SP, (4) CSD 1:8, (5) CSD 1:8:0.25, and (6) CSD 1:8:0.5 (7) CPM 1:8 (8) CPM 1:8:0.25 (9) CPM 1:8:0.5

3.4 *In vitro* dissolution test

The *in vitro* release profile of CSD 1:8, 1:8:0.25 and 1:8:0.5 in both medium, pH 1.2 and 6.8, were shown in Figure 3A and 3B, respectively. As expected, free curcumin cannot be quantified by HPLC in either medium due to its extremely poor water solubility. On the contrary, CSD formulations significantly enhanced the

dissolution rate of curcumin. In both medium, all CSD showed fast curcumin released, 100%, within 5 min.

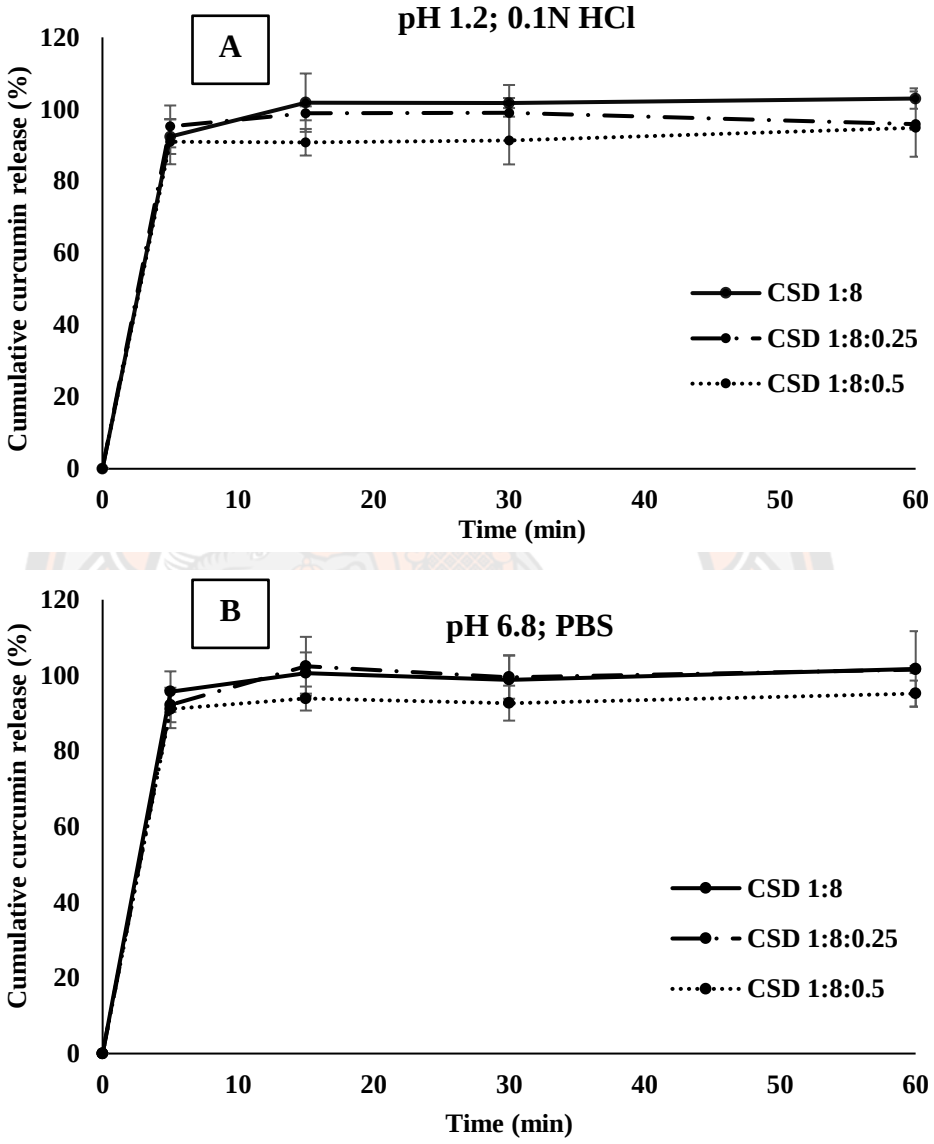

Figure 18 Cumulative percentage of released curcumin from CSD 1:8, CSD 1:8:0.25 and CSD 1:8:0.5 in different dissolution medium; (A) 0.1 N HCl, pH 1.2 and (B) phosphate buffer solution, pH 6.8. Each value represents the mean ± SD (n=3)

3.5 *In vitro* permeation studies in Caco-2 cell monolayer

The cytotoxicity of CSD toward Caco-2 cells were evaluated by XTT assay to assess a nontoxic concentration of curcumin. A cell viability value of > 70% ensured that curcumin concentrations were not toxic to cells according to the International Organization for Standardization (ISO 10993-5) (ISO 2009). At a high curcumin concentration (25 µg/mL), cell viability decreased to ~50%, whereas all CSDs at lower curcumin concentrations (5, 10, and 15 µg/mL), cell viability was > 70% indicating nontoxic. Therefore, the proposed curcumin working concentration was decided to be 15 µg/mL.

It has been reported that curcumin is not a substrate of the P-glycoprotein (P-gp) efflux transporter, leading to the study of curcumin transport from apical to basolateral only (190). The curcumin transport across Caco-2 cell monolayer of CSD 1:8, CSD 1:8:0.25 and CSD 1:8:0.5 were investigated comparing to free curcumin dispersion. The permeation amount of curcumin across Caco-2 cell monolayer from apical to basolateral compartment was presented in Figure 4. CSD 1:8 showed no lag time with curcumin absorption increased from < 0.5 µg/cm^2 during the first 30 min incubation to 1.25 µg/cm^2 at 1 h incubation, and slowly increased to 1.75 µg/cm^2 at 4 h. Conversely, CSD with SP; CSD 1:8:0.25 and CSD 1:8:0.5, demonstrated a lag time of 30 min and 2 h, respectively, with a lower permeation amount of curcumin than CSD 1:8.

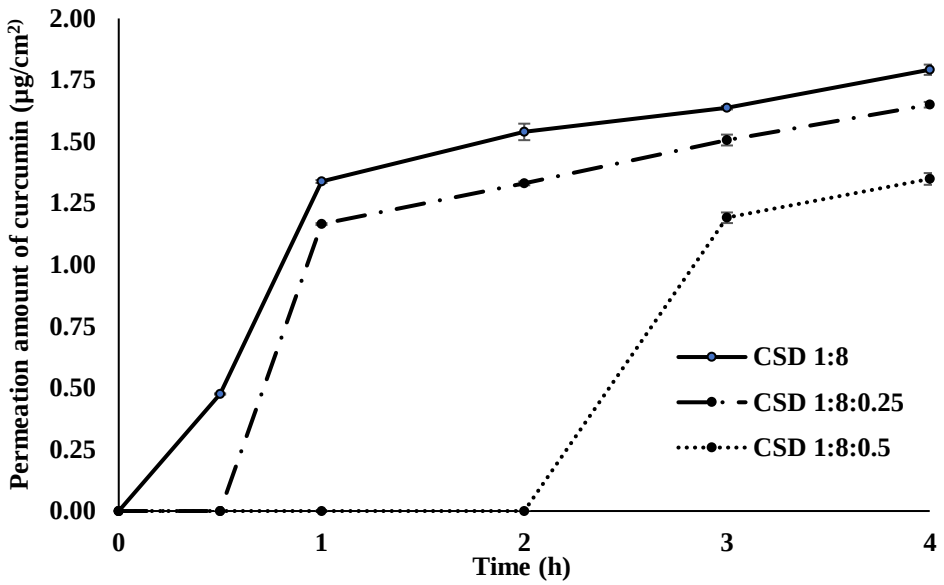

Figure 19 Permeation amount of curcumin across Caco-2 cells monolayer from CSD 1:8, CSD 1:8:0.25 and CSD 1:8:0.5. Each value represents means ± SD (n=3).

Table 19 shows the distribution of curcumin in the apical and basolateral sides and in the cell monolayer after 4 h of incubation. After 4 h treated with CSD, curcumin recovered from the apical, cellular, and basolateral compartments was ~ 85%, indicating that CSD could maintain the curcumin stability in culture medium. On the contrary, after 4 h incubation with free curcumin, no curcumin in the basolateral compartment and in the cell monolayer was detected, while only ~ 24% curcumin recovery was observed in the apical side. The restricted free curcumin absorption could be explained by curcumin rapidly degradation and poor solubility in culture medium (9, 191).

Table 19 The Percentage of curcumin in apical side, basolateral side, and cell monolayer after 4 h incubation

Mass ratio of curcumin: PVP: SP	Curcumin ± SD (%)		
	Apical side	Basolateral side	Caco-2 cells
Curcumin dispersion	23.88 ± 1.14	Not detect	Not detect
1:8	44.80 ± 1.29	26.76 ± 0.31	12.16 ± 0.55
1:8:0.25	45.91 ± 3.27	24.63 ± 0.17	14.24 ± 0.91
1:8:0.5	55.45 ± 1.61	20.14 ± 0.36	6.75 ± 0.70

The results are presented as mean ± standard deviation; n=3.

It is worth noting that the TEER value of cell monolayer after 4 h incubation was slightly decreased, ~340 Ω cm^2, compared to those of pre-incubation, ~400 Ω cm^2, Table 4. This could be attributed to the surfactant temporary disrupt the cell membrane (177). Nevertheless, the integrity of Caco-2 monolayer has been report with a TEER of 150-400 Ω.cm^2 (178). Thus, the TEER value in this study confirms that the integrity of the cell monolayer was maintained during the *in vitro* permeability experiment.

Table 20 The TEER value of the Caco-2 cells monolayer before and after in vitro permeation studies

Mass ratio of curcumin: PVP: SP	TEER (Ω/cm^2)	
	Before tested	After tested at 4 h
1:8	391 ± 13	351 ± 23*
1:8:0.25	391 ± 4	333 ± 14*
1:8:0.5	412 ± 2	361 ± 38*

The results are presented as mean ± standard deviation; n=3.

* $p<0.01$ compared with before tested.

3.6 Stability study of CSD

The physicochemical stability of CSD formulation were determined after storage at 4 ^{o}C and room temperature over a period of 6 months. After 6 months storage, the CSD 1:8 remained in a dry powder with curcumin remaining of ~ 90-100% at both storage temperatures, Figure 5. Whereas the curcumin remaining of CSD with SP; CSD 1:8:0.25 and 1:8:0.5 was slightly decreased to ~ 80% after 6-month storage.

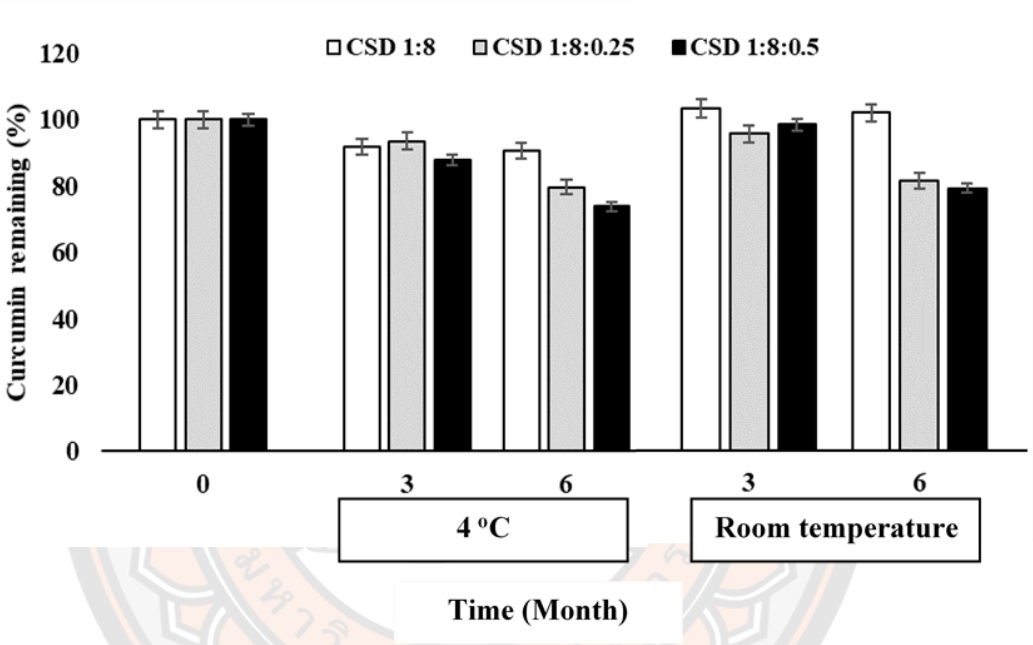

Figure 20 Percentage of curcumin remaining of CSD 1:8, CSD 1:8:0.25 and CSD 1:8:0.5 after 6-month storage at 4^{o}C and room temperature. Data were presented as mean ± SD (n = 3)

4. Discussions

Curcumin has a wide range of pharmacological effects, however because to its poor solubility in water, it has a low bioavailability (3, 182). Various formulation strategies have been employed to overcome the solubility challenges of curcumin. Among these strategies, SD technology has been well established for increasing hydrophobic drug solubility and dissolution rate. Additionally, its advantages include ease of optimization, simplicity, and easy to scale up. Therefore, in this study, CSD was

developed using PVP as a hydrophilic carrier without and with SP as a co-carrier, to further improve curcumin water solubility. CSD powder was successfully prepared using the melting solvent method. The preparation process is simple with a short duration of heat. The cooled mass of CSD were fragile enough to be ground easily. The final product showed a fine orange-yellowish powder. In addition, the results were reproducible with high percentage of curcumin recovery of > 80.

As expected, CSD illustrated a marked improvement in curcumin water solubility and dissolution behavior more than the CPM and the free curcumin, respectively. Upon dilution in water, CSD were dissolved quickly resulting in spherical particles, composed of curcumin enclosed with PVP and/or SP, with a mean size of ~140, ~160 and ~190 nm for CSD 1:8, 1:8:0.25 and 1:8:0.5, respectively (192, 193). Accordingly, CSD with SP showed slightly larger size than CSD without SP. The enhanced solubility behavior of CSD formulation could be attributed to the change from a crystalline to an amorphous state of curcumin as confirmed by XRD, Figure 2. The effects of PVP and SP ratio on the water solubility of curcumin were investigated. As the PVP content increased, the curcumin water solubility increased. The enhanced solubility behavior of CSD formulated without SP could be attributed to the hydrophilic carrier PVP, which provides good wettability, improves curcumin's dispersibility and, increases its surface area (188). Nevertheless, CSD with SP offered greater curcumin water solubility than CSD without SP. This could be explained by phospholipids act as solubility enhancer due to its amphiphilic nature and wetting properties, which resulting in further enhanced the curcumin water solubility (194). However, adding more SP did not improve the curcumin water solubility. This might be due to the hydrophilic/lipophilic balance (HLB) value of SP, which is ranging between 2-4 indicating a greater affinity for lipids than water (195).

Although, CPM showed less curcumin water solubility than CSD, but it exhibited higher curcumin water solubility than free curcumin. This can be attributed to the surface tension lowering effect of the hydrophilic polymer in the medium, resulting in improved wettability and dispersibility of the hydrophobic drug in the medium and therefore improved solubility of curcumin.(196).

Oral drugs must dissolve in GI fluids before they pass through the biological membranes of the GI tract and reach to the systemic circulation. Drugs with poorly aqueous solubility exhibit low dissolution, which leads to poor oral bioavailability. Our results proved that CSD could increase the dissolution of curcumin in GI fluid, completely released curcumin within 5 min. The next question was that whether CSD could enhance the permeation of curcumin. In this regards, Caco-2 cell monolayer was used as an intestinal absorption model. Caco-2 cells are human colon cancer cells that can differentiate to a monolayer of cells with typical properties of intestine enterocytes after cultured for 2-3 weeks (197). CSD significantly increased the permeability of curcumin through Caco-2 monolayer compared to the free curcumin. CSD enhanced curcumin absorption efficiency could be attribute to several advantages. First, the change of the crystallinity of the drug into an amorphous form is one of the mechanisms responsible for the improved solubility. According to the Fick's first law, the permeation rate of substance across surface of membrane is proportional to the concentration gradient in the intestinal lumen. More drug molecules are present at the epithelial cells' surface when drug concentrations increase leading to a greater drug absorption via transcellular transport (179). Secondly, small nanoparticles (<200 nm) would be directly up taken by cell via endocytosis (180). Third, amphiphilicity of phospholipids, which functioned as surfactants and assisted the curcumin to traverse across the membrane via transcellular transport (198). Furthermore, it has been reported that the formulation with a lipid ingredient can avoid the first-pass metabolism of drugs because the lipid ingredient could stimulate chylomicron formation, which then facilitates lymphatic uptake, resulting in increased therapeutic efficacy of drugs.(181). When adding SP to the ratios of CSD 1:8:0.25 and CSD 1:8:0.5, respectively, the curcumin water solubility of CSD increased but the curcumin permeability decreased. Moreover, CSD with SP at the mass ratio of 1:8:0.5 showed a lag time longer than CSD 1:8:0.25. Therefore, this study showed that the effect of lipid concentration could be used as parameters to determine the lag time of CSD transport across Caco-2 cells. The lag time could be explained by the accumulation of curcumin with SP, as a lipid, within the barrier until saturation of the lipid layer of the barrier was reached (199). As expected, the restricted free curcumin absorption was observed, which could be explained by curcumin rapidly degradation and poor solubility in

culture medium (9, 191). However, the findings show that curcumin permeation tends to increase as permeation time increases and might even continue to increase for a long period of time, suggesting that curcumin permeation might have been prolonged. The chemical stability of curcumin is also an important issue. CSD formulations demonstrated ~80-90% of curcumin remaining after 6-month storage at 4 ^{o}C and room temperature.

5. Conclusion

The developed CSD without and with SP were successfully prepared by melting solvent method with potential capability to enhance curcumin oral bioavailability. In comparison to free curcumin, they showed the ability to enhance water solubility, dissolution in GI fluid, and absorption through Caco-2 cell monolayers. After dissolved in water, the spherical particles of CSD without SP possessed a small size of ~ 140 nm, while CSD with SP possessed a mean size of ~ 160-190 nm. Although CSD with SP showed increased curcumin water solubility, but their Caco-2 cells absorption showed a lag time with lower drug permeation than CSD without SP. Nevertheless, all CSD can prevent curcumin degradation in basic pH as compared with free curcumin after 4 h incubation. Moreover, after 6 months storage at 4^{o}C and room temperature, the physical and chemical stabilities of CSD could be maintained. In conclusion, CSD present a promising oral drug delivery system for curcumin to improve its oral bioavailability. In addition, the findings herein should stimulate further *in vivo* evaluations and clinical trials.

CHAPTER V

COMPARISON OF CURCUMIN BASED NANO-FORMULATIONS ON INDUCED DEPRESSION RAT MODEL

This chapter is the manuscript currently under revision for publication.

Abstract

Purpose Curcumin, a major constituent of turmeric, has potential for treating neurodegenerative diseases. However, its low oral bioavailability hinders its application. The purpose of the study was to investigate the effects of curcumin nano-formulations including curcumin-loaded solid self-emulsification drug delivery systems (C-SSEDDS), and curcumin solid dispersions without (CSD) and with surfactant (CSD-S) on dexamethasone-induced depression in rats, inference with fluoxetine (Flu).

Methods Male Sprague-Dawley rats were randomly divided into 2 main groups including control and depressive group. Control rats received saline injections daily. Depressive rats received Dex 1.5 mg/kg.Bw injections daily. Then, all groups received daily oral administration of normal saline, curcumin nano-formulations or fluoxetine. Rats were subjected to the locomotor activity followed by forced swimming test after 28 days. On the 29th day, the rat was sacrificed, and the hippocampus and liver were collected to be stained with H&E to determine histopathological changes.

Results All curcumin nano-formulations given orally for 3 weeks showed an antidepressant-like effect on depressive rat model, as confirmed by the significantly higher rat body weight and sucrose consumption. Additionally, CSD and C-SSEDDS significantly reduced the immobility duration ($p<0.05$). Moreover, Dex also showed toxic effect to the hippocampus and liver cell. Interestingly, all curcumin nano-formulations exert protection and restoration effect on these cells.

Conclusions Overall results showed a great potential of curcumin nano-formulations for brain targeting in the effective treatment of depressive-like behavior.

Keyword; antidepressant, curcumin, forced swimming test, solid dispersion, solid self-emulsifying drug delivery system

1. Introduction

Depression is one of the most prevalent forms of mental illness. Current predictions indicate 76.2 million cases of anxiety disorders globally in 2020, with depressive disorders causing 49.4 million and anxiety disorders causing 44.5 million globally. After the COVID-19 pandemic, it has been predicted that there will be a significant increase in depressive disorders and anxiety disorders worldwide (200). In comparison to non-depressive individuals, it also contributes to the increased risk of morbimortality due to a variety of factors (201). Many theories proposed that depression is a multisystem involving neurotransmitter, and biochemical compounds. The hypothalamic-pituitary-adrenal (HPA) axis dysfunction that stimulate the adrenal secretion of stress hormone corticosterone (CORT) and the reduction of happiness monoamine neurotransmitters, serotonin, norepinephrine, and dopamine (202). Other theories postulate the involvement of neurodegeneration, neuroplasticity, inflammation, and the release of cytokines induced by stress (203-205).

Numerous synthetic chemical antidepressants that are currently available have poor response and remission rates as well as severe side effects (201). According to observational studies, the use of selective serotonin reuptake inhibitors has been linked to higher risks of fractures and falls (206). Meta-analyses, indicate that only some depressed individuals benefit from these medications (207). Besides, fluoxetine is also reported to have numerous undesirable side effects, including acute nausea and headaches, as well as chronic sexual dysfunction, weight gain, and diminished rapid eye movement sleep (208).

Curcumin, a major active component of turmeric (*Curcuma longa* L.) has been wildly attributed to a potential treatment to treat CNS disorders possibly by acting through its anti-inflammation and antioxidant properties, as well as modulating various neurotransmitter levels in the brain (4, 150, 182). Curcumin is a multi-target antidepressant that affects major depression models both *in vitro* and *in vivo*. Although curcumin has been deemed as the most effective drug with high efficacy for depression treatment, curcumin still poses major challenges in its use as an ideal antidepressant

due to its extremely low solubility in water and instability in GI fluids leading to poor bioavailability, which restricted curcumin delivery to the brain (1, 154, 155, 209).

To circumvent these drawbacks, nanotechnology-based drug delivery systems (NDS) are promising approaches to improve curcumin for more effective therapeutic potential of depression due to their advantages. Curcumin-loaded solid-self emulsification drug delivery systems (C-SSEDDS) and curcumin solid dispersion without and with surfactant (CSD and CSD-S, respectively) were developed in our previous study to increase curcumin oral bioavailability. Our results showed that curcumin nano-formulations can increase curcumin's water solubility >100 times in comparison to free curcumin with a particle size lower than 200 nm, leading to increased curcumin absorption through Caco-2 cells. Furthermore, curcumin is stable in a pH that mimics the GI tract.

To our knowledge, curcumin solid dispersion has been evaluated in a rat model but showed no effect on the brain (210). Additionally, C-SSEDDS have not yet been evaluated in animal model. Because of this, this is the first novel research to compare the efficacy of NDS. In the present study, the antidepressant effects of C-SSEDDS, CSD, and CSD-S were compared using the dexamethasone-induced depression in rats. This was performed by assessing the behavioral alterations, including the sucrose preference test and the forced swimming test. Additionally, investigations on liver cell damage and histopathological changes in the hippocampus were investigated.

2. Material and methods

2. 1 Animals

A total of 54 Sprague-Dawley male rats (weight of 180-220 g, aged 4-6 week) were obtained from Nomura Siam International Co., Ltd. The animals were acclimatized for 5 days prior to initiation of the experiments. Dependent on the size of the rat, 3 or 4 rats were housed per cage under standard laboratory environment (12 h light/dark cycle, room temperature of 25±1˚C ˚C, 60-70% relative humidity), with free access to standard food and water. The experimental protocols were approved by the Ethics Committee of the Centre for Animal Research of Naresuan University (Phitsanulok, Thailand) (approval no. AE630503) and conducted according to the

standards of animal care under the ethical guidelines and policies of Naresuan University.

2.2 Preparation of curcumin nano-formulations

2.2.1 C-SSEDDS

C-SSEDDS was prepared using SEDDS technique with oil (Lexol®), surfactant (Labrasol® and Cremophor RH40®) and solid carrier. C-SSEDDS appeared as a yellow powder with curcumin content of 5%. Upon dilution in water, the curcumin water solubility was higher than free curcumin (>100 times) and possessed a mean size of ~150 nm. In both pH 1.2 and pH 6.8 that mimic the GI system, the dissolution of curcumin reached ~100% release within 5 min. C-SSEDDS provided significantly greater cellular accumulation and absorption than free curcumin, according to permeation studies in a Caco-2 cell monolayer, and it also demonstrated physical and chemical stability for a year.

2.2.2 CSD and CSD-S

Using PVP as a carrier, CSD and CSD-S were developed, without and with soybean phospholipids as a surfactant, respectively. CSD and CSD-S appeared as a yellow powder, with a curcumin content of 10% and 12%, and both showed spherical micelles of ~140 nm and ~190 nm, respectively. These findings demonstrated that, in comparison to free curcumin, curcumin's water solubility increased to ~17 mg/ml and ~20 mg/ml (~4200-fold and ~6500-fold, respectively). This resulted in improved curcumin absorption throughout Caco-2 cells. They also demonstrated stability in a GI tract mimic medium, dissolving completely in 5 min and remaining stable for 4 h. According to permeation in a Caco-2 cell monolayer, CSD and CSD-S both offered significantly better cellular accumulation and absorption than free curcumin. They also showed physical and chemical stability for 6 months.

2.4 Experimental procedure and drug administration

In this study, the sample population was divided into 2 main groups including control and depressive group. Control group was randomly divided in to 4 groups (n=6/group) as follows: (a) vehicle, (b) CSD (c) CSD-S (d) C-SSEDDS group. Depressive group was randomly divided in to 5 groups (n=6/group) as follows: (e) dexamethasone (Dex) (Dex-induced depression), (f) Dex+ CSD (Dex-induced depression treated with CSD), (g) Dex+ CSD-S (Dex-induced depression treated with

CSD-S), (h) Dex+C-SSEDDS group (Dex-induced depression treated with C-SSEDDS), and (i) Dex+Flu group (Dex-induced depression treated with fluoxetine). CSD, CSD-S, C-SSEDDS or Flu was dissolved in distilled water. Dex was dissolved in 1% Tween 80 solution due to its partly soluble in water.

Rat from control group received a daily single injection of normal saline followed by daily oral administration of normal saline, CSD, CSD-S and C-SSEDDS for group (a), (b), (c) and (d), respectively. Whereas, rat from depressive group received a daily single injection of Dex 1.5 mg/kg.Bw to induce the depressive like behavior. After that, (e) has received daily oral administration of normal saline, while (f), (g) and (h) have received daily oral administration of CSD, CSD-S and C-SSEDDS with a dose of curcumin of 100 mg/kg.BW, whereas, (i) has received daily oral administration of fluoxetine (10 mg/kg.BW). The animals were treated daily for 28 days. At the end of the experiment, on the 28th day, rats were subjected to the locomotor activity followed by forced swimming test (FST). On the 29th day, rats were sacrificed.

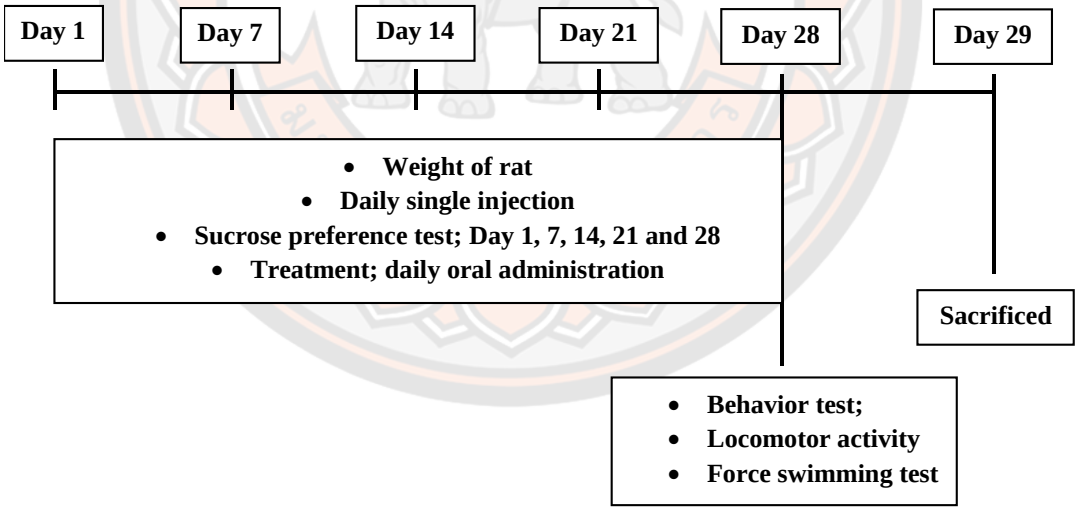

Figure 21 Schematic representation of in vivo study demonstrating experimental design and groups, sample size, behavioral analysis performed depressive like-behavior rat model.

2.5 Behavioral test

The antidepressant like activity of curcumin nano-formulations were evaluated by sucrose preference test (SPT), forced swimming test (FST) and locomotor activity was also tested. The body weight of each rat was measured every day.

2.5.1 Sucrose preference test (SPT)

The sucrose preference test was performed to assess anhedonia in rats as described by Sigwalt et al., with minor modifications (211). Before the first SPT, all rats forced to undergo to 30 h of forced exposure to 1% w/v sucrose solution and it was the only fluid available for consumption. The rats were then given a water for 16 h prior to performing the baseline SPT. In the test phase, rats placed individually in cages with two bottles, one filled with 100 ml of 1% w/v sucrose solution and the other 100 ml of tap water. The solution volume in the bottles were measured before and after 1 h test to be the rat intake from each bottle. Total intake was defined as the sum of the intake of water and sucrose, and the sucrose preference was expressed as the percentage of sucrose intake from the total intake following the formula: %sucrose preference = (sucrose intake*100)/total intake. The test performed once a week at day 1, 7, 14 and 21 between 12:00 and 1:00 PM. After the SPT, all rats received food and water ad libitum.

2.5.2 Locomotor activity by open-field test

The locomotor activity was performed as described by Zhao et al., with minor modifications (212). The locomotor activity was monitored in an open filed apparatus which consisted of a square area measuring 76 x 76 cm with walls 42 cm high and divided into 25 equal squares. Each rat was gently placed onto the middle square of the open-field apparatus and allowed to explore freely for 10 min. The animal's movements throughout the last 5 min of testing were determined by counting the number of crossings (at least three paws in a square). After each animal was tested, the testing apparatus was cleaned with a 70% alcohol solution to get rid of odors before the next test.

2.5.3 Forced swimming test (FST)

FST was applied to assess the effect of curcumin nano-formulations on rat with depressive like behavior. The animals were individually forced to swim in a measuring cylinder (50 cm high, 21 cm in diameter) filled with water (23–25°C) up

to a height of 30 cm (211). When an animal floated passively in the water with its nose above the surface, slightly hunched but upright, it was considered as immobile. The total immobility period during the 5 min test was recorded using a timer (212). The animal was removed from the cylinder after the conclusion of the swim test, dried using a towel, and returned in its cage. The water was changed after each rat swimming. All groups were compared with the control group and each other to determine whether there were changes in behavioral despair.

2.6 Histopathology

After the behavior test, the rat was sacrificed and blood was collecting. The hippocampus and liver were dissected and placed into a 10% neutral buffer formalin. The tissue was then taken out and processed onto standard tissue cassettes using a routine paraffin embedding protocol. The paraffin-embedded tissue cassettes were mounted onto a rotary microtome and sectioned to a thickness of ~5 μm and stained with Hematoxylin & Eosin (H&E) and mounted on glass slides. The slide was allowed to dry at room temperature and then visualized using bright field microscope (Olympus, BX51, Japan).

2.7 Statistical analysis

All the values are expressed as means ± SEM. The data were analyzed by one-way analysis of variance followed by Bonferroni post-hoc test. $p \leq 0.05$ was considered as statistically significant.

3. Results

3.1 The effect of Dex-induced depression on body weight of rat

Mean body weights were assessed to confirm the efficacy of curcumin nano-formulations, Figure 2. At week 0, average body weight of rat was similar. The mean body weight of the control group increased every week with no significant group differences indicating the safety of the curcumin nano-formulations, Figure 2A. However, after the first week of the Dex injection period to induce depressive like behavior, body weight was noticeably decreased in rats receiving Dex group. In Dex+CSD, Dex+CSD-S and Dex+C-SSEDDS group, the weight gain is more pronounced compared to Dex and Dex+Flu group. Post-hoc analysis indicated that animals exposed to Dex decreased mean body weight relative to non-depressive groups,

while Dex+CSD, Dex+CSD-S and Dex+C-SSEDDS group significantly ($p<0.05$) increased the body weight compared in both of Dex and Dex+Flu group after 3 weeks, Figure 22

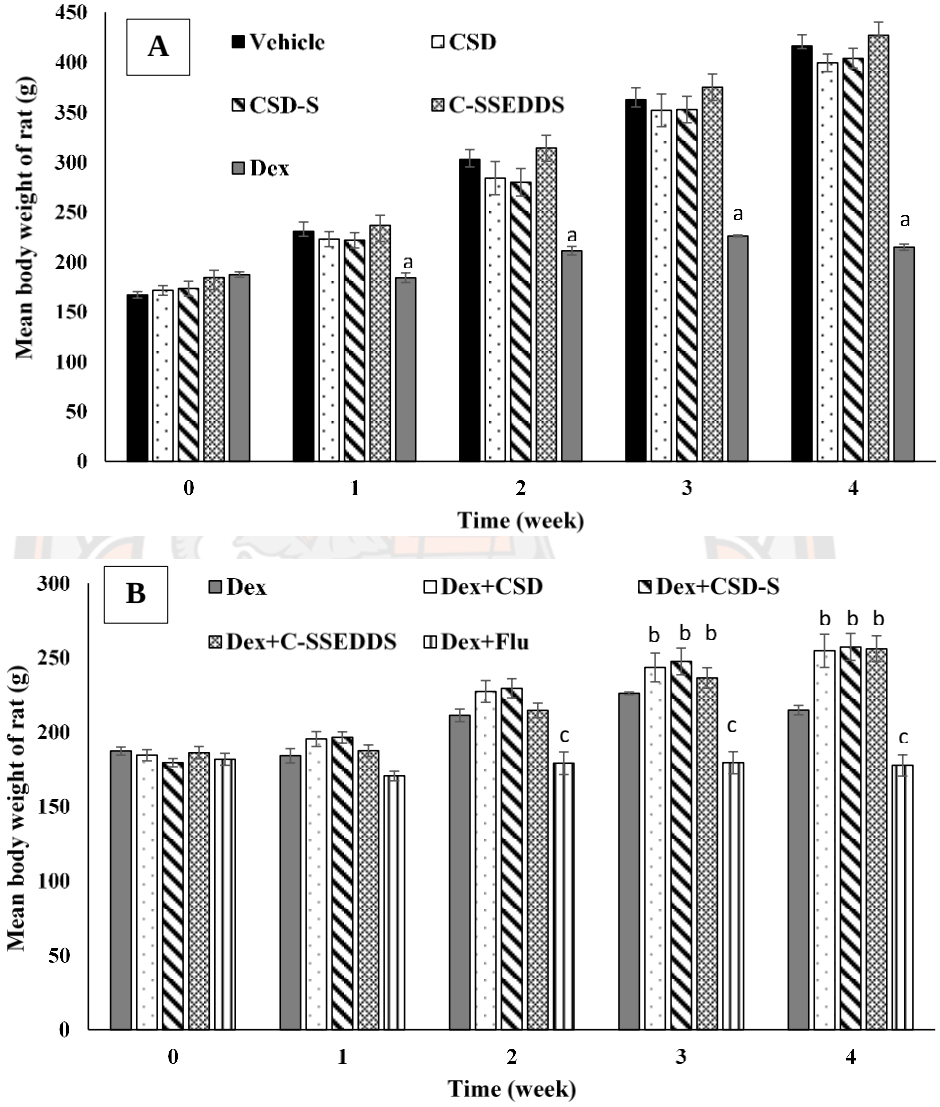

Figure 22 Effect of depressive like behavior on rat body weight (A) comparison between control group with Dex induced depression and (B) comparison between Dex induced depression with Dex induced depression treated with CSD, CSD-S and C-SSEDDS. Results are expressed as the mean ± SEM. (n = 6). a $p<0.05$ significantly lower than vehicle group. b $p<0.05$ significantly greater than Dex group. c $p<0.05$ significantly lower than Dex group.

3.2 Effects of different treatments on the SPT

Figure 23 shows the effect of curcumin nano-formulations treatment on sucrose preference in depressive rats. Reduced sucrose consumption is an indicator of anhedonia-like behavior. At 0 week, there was no significant difference among the 5 groups ($p<0.05$). The sucrose consumption of the control groups showed no significant differences indicating that the curcumin nano-formulations have no effect to the sucrose preference test. However, on the 3 weeks, Dex group showed significantly reduced the percentage of sucrose consumption as compared to the non-depressive group, Figure 3A. In contrast, Dex+CSD, Dex+CSD-S and Dex+C-SSEDDS treatment group significantly ($p<0.05$) increased the percentage of sucrose consumption compared to Dex group. In addition, in weeks 3 and 4, Dex+CSD-S group exhibited significantly lower sucrose consumption than the Dex+CSD group.

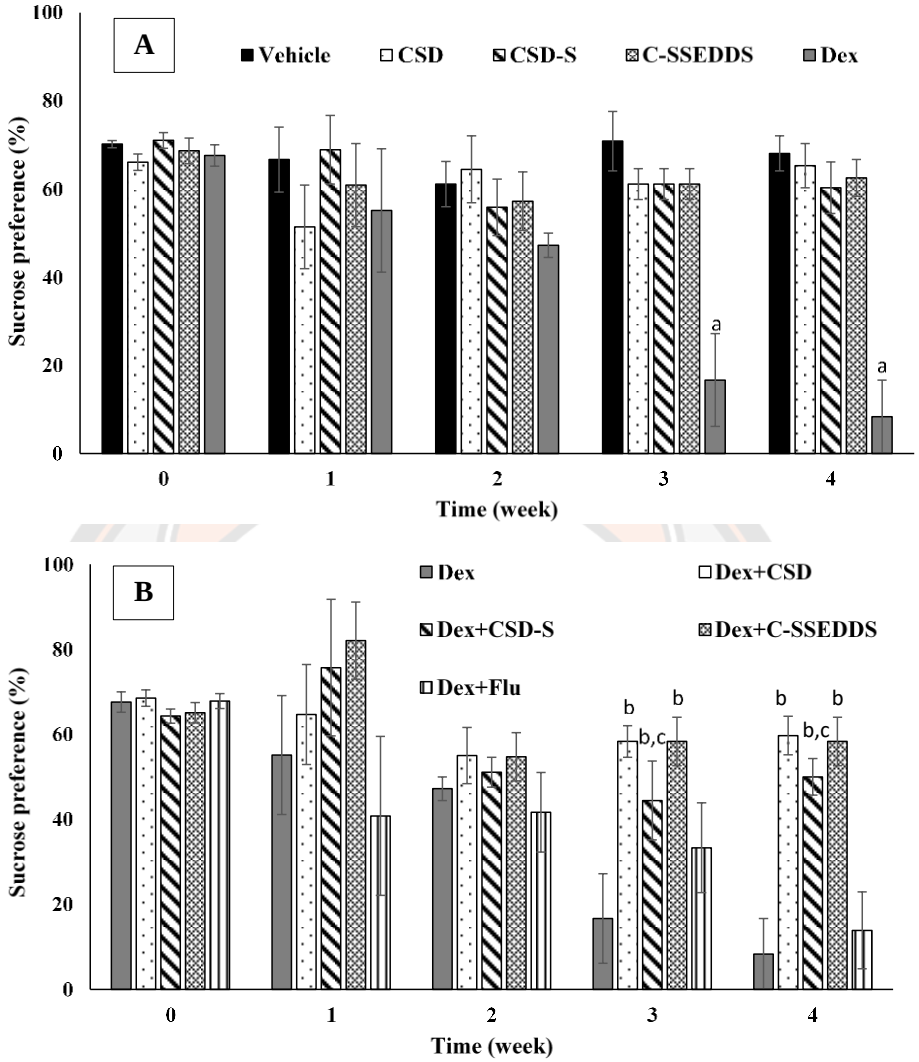

Figure 23 Effect of depressive like behavior on sucrose preference test (A) comparison between control group with Dex induced depression and (B) comparison between Dex induced depression with Dex induced depression treated with CSD, CSD-S and C-SSEDDS. Results are expressed as the mean ± SEM. (n = 6). a $p<0.05$ significantly lower than vehicle group. b $p<0.05$ significantly greater than Dex group. c $p<0.05$ significantly lower than Dex-CSD group

3.3 Effects of different treatments on the locomotor activity

Table 21 shows that there were no significant differences among the 5 groups ($p<0.05$) in distance traveled. Thus, this result indicated that locomotor activity was not impaired between control or Dex-induced depression group.

Table 21 Effect of Dex induced depression on number of crossing

Group	Locomotor activity (Number of crossing) ±SD
Control	
Vehicle	**51 ± 29**
CSD	**56 ± 6**
CSD-S	**67 ± 13**
C-SSEDDS	**59 ± 8**
Dex induced depression	
Dex	**70 ± 23**
Dex+CSD	**79 ± 9**
Dex+CSD-S	**58 ± 28**
Dex+C-SSEDDS	**82 ± 10**
Dex+Flu	**68 ± 34**

Results are expressed as the mean ± SD. (n = 6).

3.4 Effects of different treatments on the FST

At the end of the treatment, the depressive like behavior was evaluated using forced swimming test, Figure 4. The immobility time of the Dex group was significantly longer than that of control group ($p<0.05$), indicating that Dex induced a depression-like state in the rats, Figure 4A. Figure 4B shows a significant reduction in immobility time in the Dex+CSD, Dex+C-SSEDDS, and Dex+Flu groups as compared to the Dex group. However, there was no statistically significant difference in the mean immobility time between the Dex and Dex+CSD-S groups.

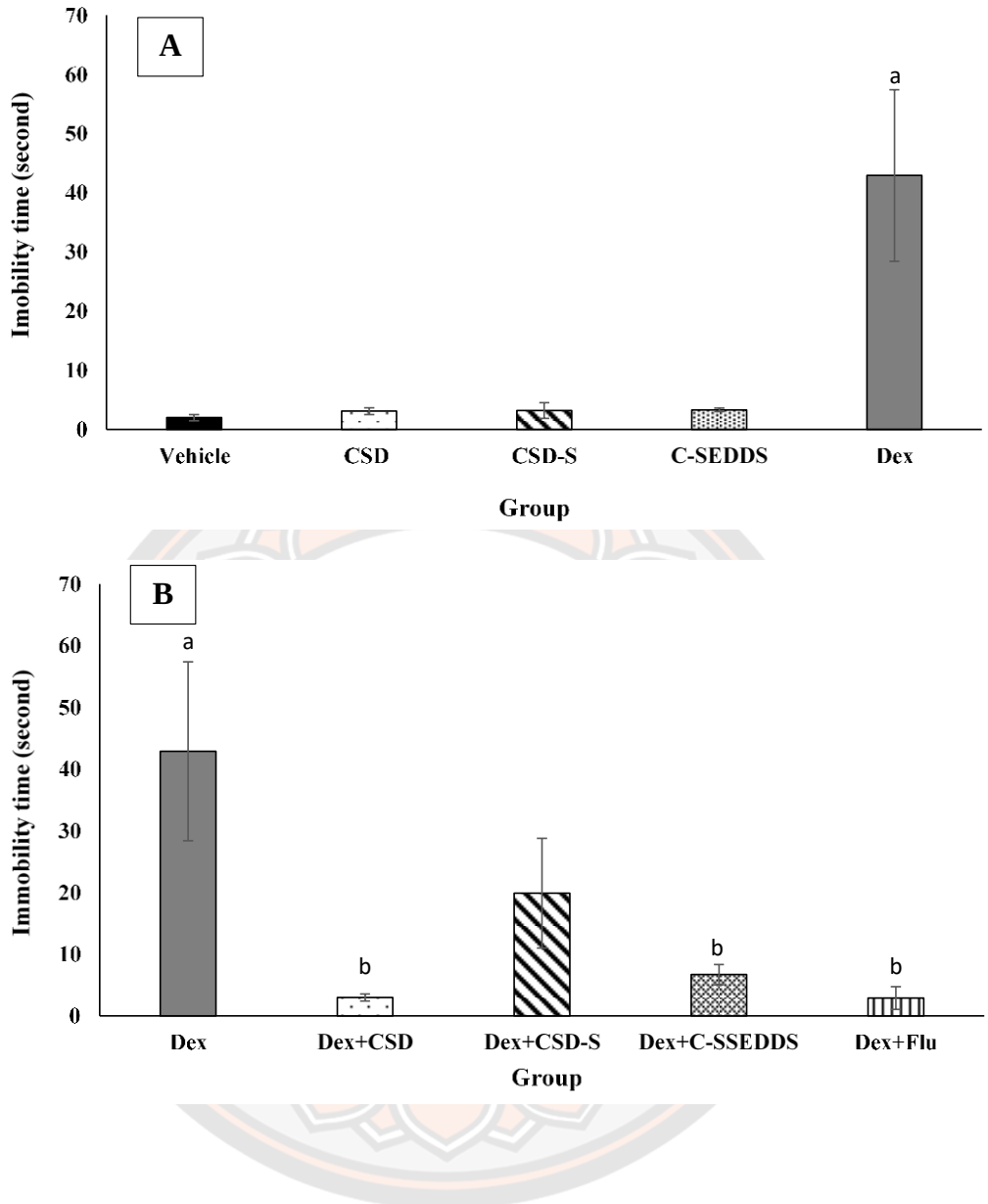

Figure 24 Effect of depressive like behavior on immobility time of rats in the force swimming test at day 28. (A) comparison between control group with Dex induced depression and (B) comparison between Dex induced depression with Dex induced depression treated with CSD, CSD-S and C-SSEDDS. Results are expressed as the mean ± SEM. (n = 6). a $p<0.05$ significantly greater than vehicle group. b $p<0.05$ significantly lower than Dex group

3.5 Effect of curcumin nano-formulations on Dex-induced neurodegeneration

Histopathological analysis of brain tissues was performed to evaluate the effects of CSD and CSD-S, and C-SSEDDS on the Dex-induced morphological changes and neurodegeneration. The notable morphological changes in the cornu ammonis (CA) and dentate gyrus (DG) from hippocampus was observed in Dex-induced depression group as compared to control group, Figure 5A. The CA and DG from the Dex group's hippocampus formation were thin; intercellular spaces were enlarged, the cells were irregularly arranged, indicating that the hippocampal tissue was damaged and cell apoptosis was occurred. In contrary, the DG and CA of Dex+CSD, Dex+CSD-S, and Dex+C-SSEDDS remained unaltered. Their hippocampal pyramidal cell layer was repaired and intercellular spaces were constricted in the CA and DG regions, demonstrating that these groups had a restored effect against damage to the hippocampus when compared to the Dex group, Figure 5A. However, the CA and DG regions of Dex+Flu group were repaired but some of intercellular space remained thin and irregularly arranged.

The effects of Dex induced depression revealed remarkable morphological changes in the liver, i.e., shrunken hepatocytes with chromatin condensation, Figure 5B. However, the hepatocytes of the control, Dex+CSD, Dex+CSD-S, and C-SSEDDS groups remained unaltered, demonstrating that curcumin nano-formulations does not damage the hepatocytes cell. The hepatocyte cell layer was repaired and intercellular spaces were constricted in Dex+CSD, Dex+CSD-S and Dex+C-SSEDDS demonstrating that curcumin nano-formulations had a restored effect against damage to the liver cell when compared to the Dex group. However, some shrunken hepatocytes with chromatin condensation was observed in Dex+C-SSEDDS group. Whereas, Dex+Flu showed hepatocyte damage similarly with Dex group.

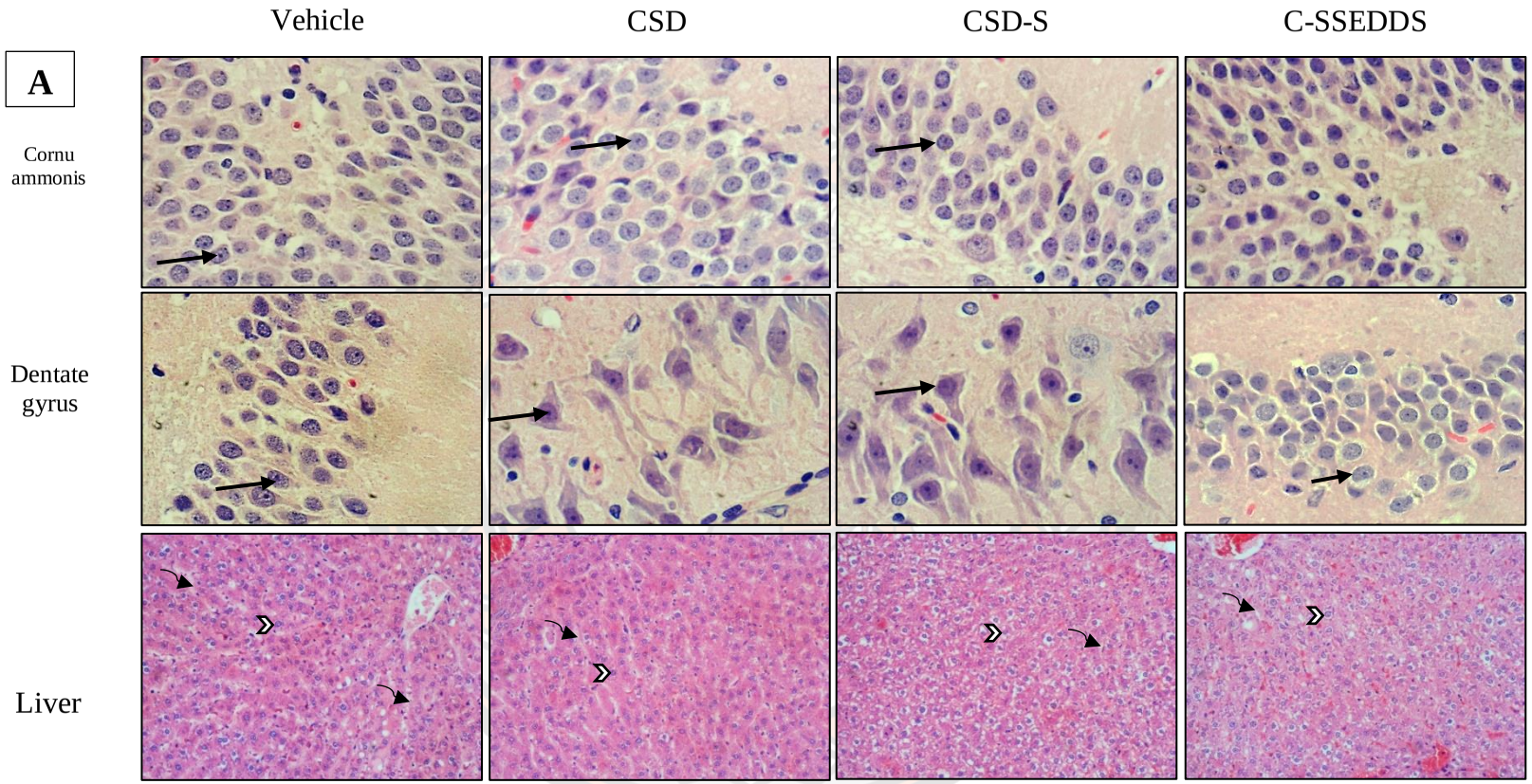
Vehicle
CSD
CSD-S
C-SSEDDS
A
Cornu ammonis
Dentate gyrus
Liver

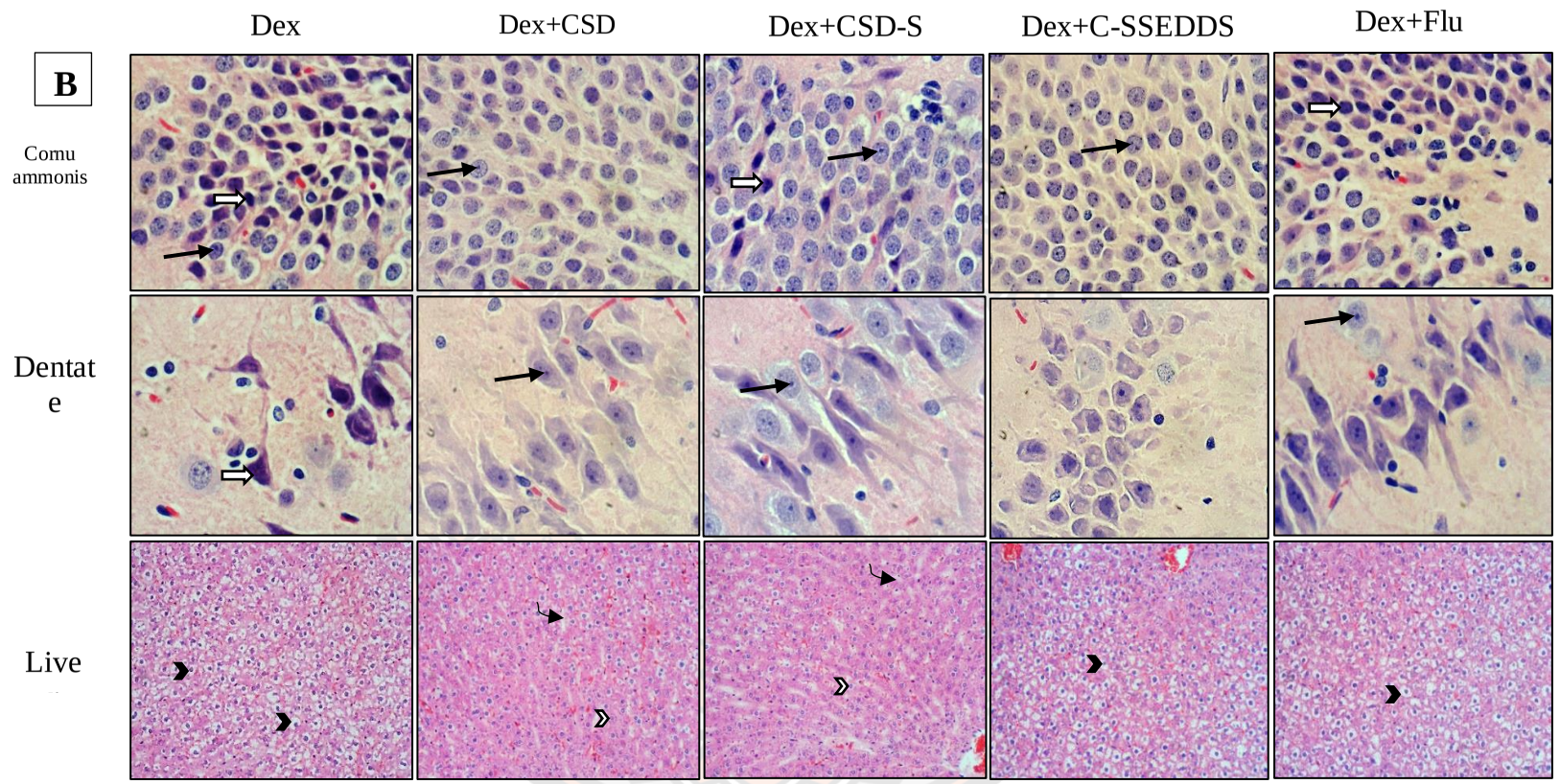

Figure 25 Histological after H&E staining of (A) cornu ammonus and dentate gyrus from hippocampus and (B) liver from control and Dex induced depression. (→ normal cell of neuron ⇨ morphological damage of neurons sinusoidal ⤷ hepatocyte ❯ shrunken hepatocyte)

4. Discussion

Depression is a major public health problem throughout the world. Low mood, loss of capacity to experience pleasure, increased sense of worthlessness, fatigue, and preoccupation with death and suicide are its characteristics (213). Curcumin is considered as an effective option for depression treatment, conceivably related to its antioxidant and anti-inflammatory properties (150, 154, 155, 209). In addition, curcumin could possess an antidepressant-like effect similar to that of fluoxetine by increasing serotonin and dopamine levels in the brain (182). According to some studies, curcumin can convert hepatic a-linoleic acid into the omega-3 fatty acid docosahexaenoic acid (DHA), which has anxiolytic-like drug properties (214). However, the major weakness of curcumin includes its low water solubility and poor oral bioavailability, which largely restrict its applicability (154, 155, 209). To increase the bioavailability of curcumin, we developed curcumin nano-formulations; polymer-based, CSD and CSD-S, and surfactant-based, C-SSEDDS. They showed high potential to deliver curcumin to the brain as evident from increased permeation across Caco-2 cells. Thus, in this study, we further explored and compared their antidepressant-like effects in animal model of depression.

As expected, the depression-like behaviors in rat model were successfully induced by Dex, a synthetic corticosterone (CORT). The main symptoms of depression, anhedonia (the loss of interest) and behavioral despair, were measured by SPT and FST, respectively. Dex group exhibited a significant decreased amount of sucrose consumption compared to control group, while the FST results demonstrated a significantly increased time of immobility confirming Dex induce depressive like behavior. Additionally, rat induced depressive behavior with Dex showed a clear decrease in body weight, which is a characteristic frequently observed in both of humans and animals' depression (211). Owing to the potential link between depression, oxidative stress, and inflammation, the stress hormone CORT can induce oxidative stress by increasing the reactive oxygen species (ROS) in the brain and trigger the release of inflammatory mediators. In addition, increased ROS activity also implies an increase in the activity of the enzyme monoamine oxidase (MAO), which is involved in the metabolism of the happiness monoamine neurotransmitter, serotonin (182). Thus, the oxidative stress induced by Dex could induce depression-like behavior in rat model.

Moreover, the oxidative stress also results in cell damage as observed in the morphological changes of CA and DG of hippocampus, and liver cell, Figure 5 A and B.

Interestingly, all curcumin nano-formulations given orally for 3 weeks demonstrated an antidepressant-like effect on depressive rat model, as confirmed by the significantly higher rat body weight and sucrose consumption. Additionally, CSD and C-SSEDDS significantly reduced the immobility duration ($p<0.05$). It is worth noting that due to fluoxetine side effects, weight loss and loss of appetite, fluoxetine group showed similar body weight and sucrose consumption as compared to Dex groups.

Based on these results, we suggest that all tested nano-formulations can accommodate curcumin across the brain, thus curcumin could effectively protect the neuron cells from oxidative stress and further evoking behavioral changes in rat. The positive effects of curcumin nano-formulations could be explained by the advantages of colloidal drug delivery systems.

By reducing the size of the particles to ~100–200 nm, the surface area to volume ratio rises, nano-formulations causing a higher curcumin saturation solubility (> 100 times greater than that of free curcumin). Importantly, encapsulated in nano-formulations, curcumin remains chemically intact during transportation in GI fluids. Subsequently, the curcumin is released from the nano-formulations and absorbed largely by passive diffusion (85). Therefore, the transport of the drug to the GI tract across the transmembrane could be promoted. In addition, a small size of < 200 nm could prolong the blood circulation time and thus increase the opportunity to transport across the brain. As a result, curcumin nano-formulations showed neuroprotective effect in hippocampus by protecting and repairing the neuron cell from CORT-induced damage. It should be noted, however, that the effectiveness of nano-formulation is dependent on the particle size. CSD-S, ~200 nm in size, showed slightly less effective than CSD and C-SSEDDS, ~100-150 nm. Comparing with Dex group, Dex+CSD and Dex+CSSEED groups showed significant increased sucrose consumption and reduced immobility time. However, Dex+CSD-S group demonstrated a trend of increased sucrose consumption and reduced immobility time, but without significantly different compared to Dex group. These results imply that curcumin nano-formulations can cross the brain and delivery curcumin into the brain and enhanced neuroprotective effects.

In addition, Dex caused oxidative stress also showed toxic effect on hepatocytes resulting in morphological changes, Fig 5 B. Interestingly, all curcumin nano-formulations were not only non-toxic to the hepatocytes, Fig5 A, but they also exerted protection and restoration effect on hepatocytes from Dex induced oxidative stress, Fig 5 B. As a result, the toxic of Dex on hepatocytes were restored by curcumin nano-formulations. Comparing among curcumin nano-formulations, the Dex+CSD and Dex+CSD-S groups showed healthy hepatocytes similar to the control group, while Dex+C-SSEDDS showed a partial damaged hepatocyte. However, the Dex+C-SSEDDS group showed greater hepatocyte restoration than the Dex+Flu group, which showed hepatocyte damage similar to the Dex group. A partial hepatocyte damage of Dex+C-SSEDDS could be a result from the high amount of surfactant, in the C-SSEDDS, can destroy the liver sinusoidal endothelium (215). Overall, the findings suggested that all tested curcumin nano-formulations were safe and could protect the cells from oxidative stress.

Conclusion

All of tested curcumin nano-formulations, including the polymer-based; CSD and CSD-S, and the lipid-based; C-SSEDDS, have demonstrated similarly a positive antidepressant-like effect on depressive rat models. Additionally, Dex-induced damage to the hippocampus and liver cells can be repaired with curcumin nano-formulations indicating successfully deliver curcumin to the brain. The high potential of nano-formulations to deliver curcumin to the brain is due to enhancement of curcumin transport across the GI barrier as a result from improved curcumin stability through encapsulation in the nanocarrier, as well as increased its water solubility. In addition, the development of curcumin nano-formulations with particles smaller than 200 nm could extend the blood circulation time resulting in an improvement in the amount of curcumin crossing the brain. Our study suggests that curcumin nano-formulations may have great potential for depression treatment.

CHAPTER V

CONCLUSION

Curcumin is the main biologically active principle of turmeric (*Curcuma longa*). Given its anti-inflammatory and antioxidant properties, it has been hypothesized that curcumin might be effective in treating symptoms of a variety of neuropsychiatric disorders, such as depression. However, several studies have found that curcumin's beneficial effects are limited by its low water-soluble, leading to low bioavailability. To circumvent these drawbacks, polymer- and lipid-based curcumin nano-formulations are promising approaches to improving curcumin water solubility and oral bioavailability.

In present work, polymer based; curcumin solid dispersion and lipid-based; solid self- emulsifying drug delivery systems have been successfully prepared. Two formulations of curcumin solid dispersion were prepared with polyvinylpyrrolidone (PVP) as a carrier without (CSD) and with surfactant as a co-carrier (CSD-S) have been successfully prepared using a solid dispersion (SD) techniques. While curcumin loaded solid self- emulsifying drug delivery systems (C-SSEDDS), as a lipid-based, were developed using Neusilin®UFL2 as a solid carrier. In comparison to free curcumin, they showed the ability to enhance water solubility, dissolution in GI fluid, and absorption through Caco-2 cell monolayers. After dissolved in water, the spherical micelle of CSD, CSD-S and C-SSEDDS possessed a mean droplet size lower than 200 nm, with a narrow distribution. Nevertheless, all curcumin nano-formulations can prevent curcumin degradation in basic pH as compared with free curcumin after 4 h incubation. In addition, the developed formulations showed a greater curcumin absorption in Caco-2 cell monolayer than free curcumin, suggesting an increase in the curcumin oral bioavailability. Although CSD-S showed increased curcumin oral bioavailability, but their Caco-2 cells absorption showed a lag time with lower drug permeation than CSD and C-SSEDDS. The physical and chemical stability of curcumin nano-formulations were stable for at least 6-month storage at 4 ºC and room temperature.

Then, we investigated the antidepressant activity of curcumin nano-formulations by using a Dex-induced depression model. The main symptoms of depression, anhedonia (the loss of interest) and behavioral despair, were measured by SPT and FST, respectively. Dex group exhibited a significant decreased amount of SPT compared to control group, while the FST results demonstrated a significantly increased time of immobility confirming Dex induce depressive like behavior. Additionally, rat induced depressive behavior with Dex showed a clear decrease in body weight. Interestingly, all curcumin nano-formulations given orally for 3 weeks demonstrated an antidepressant-like effect on depressive rat model, as confirmed by the significantly higher rat body weight and sucrose consumption with reduced the immobility duration. Additionally, Dex-induced damage to the hippocampus and liver cells can be repaired with curcumin nano-formulations indicating successfully deliver curcumin to the brain.

The high potential of nano-formulations to deliver curcumin to the brain is due to enhancement of curcumin transport across the GI barrier as a result from improved curcumin stability through encapsulation in the nanocarrier, as well as increased its water solubility. In addition, the development of curcumin nano-formulations with particles smaller than 200 nm could extend the blood circulation time resulting in an improvement in the amount of curcumin crossing the brain. Our study suggests that curcumin nano-formulations may have great potential for depression treatment.

REFERENCES

REFERENCES

1. Pawan Pandey, A.S., Umesh Gupta, Blood brain barrier: an overview on strategies in drug delivery, realistic in vitro modeling and in vivo live tracking. Tissue Barriers, 2016. 4: p. 1-14.
2. Joseph Dimasi, L.H.F., Abraham Seckler, Ann Wilson, Trends in risks associated with new drug development: success rates for investigational drugs. Clinical Pharmacology & Therapeutics, 2010. 87: p. 272-277.
3. Guddadarangavvanahally Jayaprakasha, J.R., Kunnumpurath Sakariah, Chemistry and biological activities of C. longa. Trends in Food Science & Technology, 2005. 16: p. 533-548.
4. Jayesh Sanmukhani, A.A., Chandrabhanu Tripathi, Evaluation of antidepressant like activity of curcumin and its combination with fluoxetine and imipramine: An acute and chronic study. Acta Poloniae Pharmaceutica Drug Research, 2011. 68: p. 769-775.
5. Darrick Kim, S.-Y.P., Jin-Yung Kim, Curcuminoids from Curcuma longa L. (Zingiberaceae) that protect PC12 rat pheochromocytoma and normal human umbilical vein endothelial cells from bA(1±42) insult. Neuroscience Letters, 2001. 303: p. 57-61.
6. Mythri, R.B., et al., Mitochondrial Complex I Inhibition in Parkinson's Disease: How Can Curcumin Protect Mitochondria? Antioxidants & Redox Signaling, 2007. 9: p. 399-408.
7. Hanne Hjorth Tønnesen, M.r.M.s., Thorsteinn Loftsson, Studies of curcumin and curcuminoids. XXVII. Cyclodextrin complexation: solubility, chemical and photochemical stability. International Journal of Pharmaceutics, 2002. 244: p. 127-135.
8. Rummy Sharma, A.J.G., William Stewart, Curcumin: the story so far. European Journal of Cancer, 2005. 41: p. 1955-1968.
9. Wang Ying-Jan, P.M.-H., Cheng Ann-Lii, Lin Liang-In, Ho Yuan-Soon, Hsieh Chang-Yao, Lin Jen-Kun Stability of curcumin in buffer solutions and characterization of its degradation products. Journal of Pharmaceutical and Biomedical Analysis, 1997. 15: p. 1867-1876.

10. Rodrigo Martins, S.P., Silvia Siqueira, Wellington and L.F. Salomão, Curcuminoid content and antioxidant activity in spray dried microparticles containing turmeric extract. Food Research International, 2013. 50: p. 657-663.
11. John Ringman, S.F., Edmond Teng, Aynun N Begum, Jenny Bardens, Maryam Beigi, Karen Gylys, Vladimir Badmaev, Dennis Heath, Liana Apostolova, Verna Porter, Zeba Vanen, Gad Marshall, Gerhard Hellemann, Catherine Sugar, Donna L Masterman, Thomas Montine, Jeffrey Cummings, Greg Cole, Oral curcumin for Alzheimer's disease: tolerability and efficacy in a 24-week randomized, double blind, placebo-controlled study. Alzheimer's Research & Therapy, 2012. 4: p. 1-8.
12. Fan Meng, U.G., and Harsh Chauhan, Classification of solid dispersions: correlation to (i) stability and solubility (ii) preparation and characterization techniques. Drug Development and Industrial Pharmacy, 2015. 41: p. 1401-1415.
13. Xueting Mei, D.X., Sika Xu, Yanping Zheng, Shibo Xu, Gastroprotective and antidepressant effects of a new zinc(II)-curcumin complex in rodent models of gastric ulcer and depression induced by stresses. Pharmacology Biochemistry and Behavior, 2011. 99: p. 66-74.
14. Suchiwa Pan-On, S.R., Anan Ounaroon, Waree Tiyaboonchai, Development and characterization of clay facial mask containing turmeric extract solid dispersion. Drug Development and Industrial Pharmacy, 2018. 44: p. 590-597.
15. Bappaditya Chatterjee, S.H.A., Ather Ahmed Mahdi Dukhan, Uttam Kumar Mandal, Pinaki Sengupta, Controversies with self-emulsifying drug delivery system from pharmacokinetic point of view. Drug Delivery, 2016. 23(9): p. 3639-3652.
16. Tao Yi, D.T., Fan Wang, Jiqiong Zhang, Jiao Zhang, Jirui Wang, Xiaoyu Xu, Jifen Zhang, Enhancing both oral bioavailability and brain penetration of puerarin using borneol in combination with preparation technologies. Drug Delivery, 2017. 24: p. 422-429.
17. Kaushik Thanki, R.G., Abhay Sangamwar, Sanyog Jain, Oral delivery of anticancer drugs: challenges and opportunities. Journal of Controlled Release, 2013. 170: p. 15-40.

18. Jayaprakasha, G.K., et al., Chemistry and biological activities of C. longa. Trends in Food Science & Technology, 2005. 16(12): p. 533-548.
19. Ishita Chattopadhyay, K.B., Uday Bandyopadhyay and Ranajit K. Banerjee, Turmeric and curcumin: Biological actions and medicinal applications. Current Science, 2004. 87: p. 44 -53.
20. Martins, R.M., et al., Curcuminoid content and antioxidant activity in spray dried microparticles containing turmeric extract. Food Research International, 2013. 50(2): p. 657-663.
21. Priyadarsini, K.I., The chemistry of curcumin: from extraction to therapeutic agent. Molecules, 2014. 19(12): p. 20091-112.
22. Jayaprakasha, G.K., L.J.M. Rao, and K.K. Sakariah, Antioxidant activities of curcumin, demethoxycurcumin and bisdemethoxycurcumin. Food Chemistry, 2006. 98(4): p. 720-724.
23. Wang, Y.-J., et al., Stability of curcumin in buffer solutions and characterization of its degradation products. Journal of Pharmaceutical and Biomedical Analysis, 1997. 15: p. 1867-1876.
24. Leung, M.H.M. and T.W. Kee, Effective Stabilization of Curcumin by Association to Plasma Proteins: Human Serum Albumin and Fibrinogen. Langmuir, 2009. 25(10): p. 5773-5777.
25. Pan, M.H., T.M. Huang, and J.K. Lin, Biotransformation of curcumin through reduction and glucuronidation in mice. Drug Metab Dispos, 1999. 27(4): p. 486-94.
26. Priyadarsini, K.I., Photophysics, photochemistry and photobiology of curcumin: Studies from organic solutions, bio-mimetics and living cells. Journal of Photochemistry and Photobiology C: Photochemistry Reviews, 2009. 10(2): p. 81-95.
27. Thankamma Ajithkumar, R.L., Saudamini Das, Detection and estimation of curcuma longa in ayurvedic preparations. Ancient Science of Life, 1995. 15: p. 43-52.
28. Tze-Pin Ng, P.-C.C., Theresa Lee, Hong-Choon Chua, Leslie Lim, and Ee-Heok Kua, Curry Consumption and Cognitive Function in the Elderly. American Journal of Epidemiology, 2006. 164: p. 898-906.

29. Phalguni Alladi, A.M., Yasha Chickabasaviah, Trichur Raju, Shankar kothapuram, Uday Muthane, Absence of age-related changes in nigral dopaminergic neurons of Asian Indians: relevance to lower incidence of Parkinson's disease. Neuroscience, 2009. 159: p. 236-245.
30. Shoba, G., et al., Influence of piperine on the pharmacokinetics of curcumin in animals and human volunteers. Planta Med, 1998. 64(4): p. 353-6.
31. Anand, P., et al., Bioavailability of curcumin: problems and promises. Mol Pharm, 2007. 4(6): p. 807-18.
32. Dulbecco, P. and V. Savarino, Therapeutic potential of curcumin in digestive diseases. World Journal of Gastroenterology : WJG, 2013. 19(48): p. 9256-9270.
33. Bansal, S.S., et al., Advanced drug delivery systems of curcumin for cancer chemoprevention. Cancer Prev Res (Phila), 2011. 4(8): p. 1158-71.
34. Shen, L.-R., et al., Curcumin and aging. BioFactors, 2013. 39(1): p. 133-140.
35. Sharma, R.A., et al., Phase I clinical trial of oral curcumin: biomarkers of systemic activity and compliance. Clin Cancer Res, 2004. 10(20): p. 6847-54.
36. Ping-Yang Yeh, M.B., Wade Samowitz, Pavia Kopekova, Jindfich Kopecek, Site-specific drug delivery and penetration enhancement in the gastrointestinal tract. Journal of Controlled Release, 1995. 36: p. 109-124.
37. Bahman Homayun, X.L., Hyo-Jick Choi, Challenges and recent progress in oral drug delivery systems for biopharmaceuticals. Pharmaceutics, 2019. 11: p. 1-29.
38. Yi Lu, N.T., Ruyue Lian, Jianping Qi,Wei Wu, Understanding the relationship between wettability and dissolution of solid dispersion. International Journal of Pharmaceutics, 2014. 465: p. 25-31.
39. Miha Homar, M.C., Miha Kotnik, Luka Peternel, Toward effective long-term prevention of thromboembolism: novel oral anticoagulant delivery systems. Seminars in Thrombosis and Hemostasis, 2010. 36: p. 113-122.
40. Johan Karlsson, A.-L.U., Johan Grasjo, Per Artursson, Paracellular drug transport across intestinal epithelia: influence of charge and induced water flux. European Journal of Pharmaceutical Sciences, 1999. 9: p. 47–56.
41. Lipinski, C., Drug-like properties and the causes of poor solubility and poor permeability. Journal of Pharmacological and Toxicological Methods, 2000. 44: p. 235-249.

42. Roos Oostendorp, J.B., Jan Schellens, The biological and clinical role of drug transporters at the intestinal barrier. Cancer Treatment Reviews, 2009. 35: p. 137-147.
43. Charles Awortwe, P.F., Bernd Rosenkranz, Application of Caco-2 Cell Line in Herb-Drug Interaction Studies: Current Approaches and Challenges. Journal of Pharmacy & Pharmaceutical Sciences, 2014. 17: p. 1–19.
44. Mohammad Alavijeh, M.C., Zeeshan Qaiser, Alan Palmer, Drug metabolism and pharmacokinetics, the blood-brain barrier, and central nervous system srug siscovery. The Journal of the American Society for Experimental NeuroTherapeutics, 2005. 2: p. 554–571.
45. Yan, Z. and G. Caldwell, Optimization in Drug Discovery: In Vitro Methods. 2004: Humana Press. 19-37.
46. Awortwe, C., P.S. Fasinu, and B. Rosenkranz, Application of Caco-2 cell line in herb-drug interaction studies: current approaches and challenges. J Pharm Pharm Sci, 2014. 17(1): p. 1-19.
47. Shah, P., et al., Role of Caco-2 cell monolayers in prediction of intestinal drug absorption. Biotechnol Prog, 2006. 22(1): p. 186-98.
48. Stefan Lundquist, M.R., Julien Brillault, Laurence Fenart, Roméo Cecchelli, Marie-Pierre Dehouck, Prediction of Drug Transport through the Blood-Brain Barrier in Vivo: A Comparison between Two in Vitro Cell Models. Pharmaceutical Research, 2002. 19: p. 976-981.
49. Per Garberg, J.B., David Borg, Romeo Cecchelli, Laurence Fenart, Audra Hurst, Tony Linmark, Aloïse Mabondzo, Olof Nilsson, Thomas Raub, Danica Stanimirovic, Osamu Terasaki, Jo Berg, Tor Osterberg, In vitro models for the blood–brain barrier. Toxicology in Vitro, 2005. 19: p. 299-334.
50. Jenni Hakkarainena, A.J., Tiina Kääriäinena, Pekka Rahkonena, Tetta Venäläinena, Juho Hokkanenb Jukka Mönkkönen, Marjukka Suhonena, Markus Forsberg, Comparison of in vitro cell models in predicting in vivo brain entry of drugs. International Journal of Pharmaceutics, 2010. 402: p. 27-36.
51. Reichel, A., The Role of Blood-Brain Barrier Studies in the Pharmaceutical Industry. Current Drug Metabolism, 2006. 7: p. 183-203.

52. Kawabata, Y., et al., Formulation design for poorly water-soluble drugs based on biopharmaceutics classification system: basic approaches and practical applications. International Journal of Pharmaceutics, 2011. 420(1): p. 1-10.
53. Vo, C.L.-N., C. Park, and B.-J. Lee, Current trends and future perspectives of solid dispersions containing poorly water-soluble drugs. European Journal of Pharmaceutics and Biopharmaceutics, 2013. 85(3): p. 799-813.
54. Chiou, W.L. and S. Riegelman, Pharmaceutical Applications of Solid Dispersion Systems. Journal of Pharmaceutical Sciences, 1971. 60: p. 1281-1302.
55. Nadia Saffoon, R.U., Naz Hasan Huda and Kumar Bishwajit Sutradhar, Enhancement of Oral Bioavailability and Solid Dispersion: A Review. Journal of Applied Pharmaceutical Science, 2011. 1: p. 13-20.
56. Sameer Singh, R.S.B.a.L.Y., A review on solid dispersion. International Journal of Pharmacy & Life Sciences, 2011: p. 1078-1095.
57. Aisha, A.F.A., et al., Solid dispersions of α-mangostin improve its aqueous solubility through self-assembly of nanomicelles. Journal of Pharmaceutical Sciences, 2012. 101(2): p. 815-825.
58. Vedamurthy Joshi, M.G.A., Sarasua Suresh, Rajesh Kowti, A Comparative Study: Solution Stability and Dissolution Behavior of Solid Dispersions Curcumin. Indian Journal of Novel Drug delivery, 2010. 2: p. 88-95.
59. Piero De Filippis , G.Z., Mario Gibellini, Fulvio Rubessa, Paolo Rupena, Dissolution rates of different drugs from solid dispersions with Eudragit RS. European Journal of Pharmaceutical Sciences, 1995. 3: p. 265-271.
60. Karel Six, G.V., Jef Peeters, Marcus Brewster, and Guy Van Den Mooter, Increased Physical Stability and Improved Dissolution Properties of Itraconazole, a Class II Drug, by Solid Dispersions that Combine Fast- and Slow-Dissolving Polymers. Journal of Pharmaceuticals Sciences, 2003. 93: p. 124-131.
61. Giri, T.K., et al., A novel and alternative approach to controlled release drug delivery system based on solid dispersion technique. Bulletin of Faculty of Pharmacy, Cairo University, 2012. 50(2): p. 147-159.
62. Alonzo, D.E., et al., Dissolution and precipitation behavior of amorphous solid dispersions. Journal of Pharmaceutical Sciences, 2011. 100(8): p. 3316-3331.

63. Erika Broman , C.K., Lynne S. Taylor, A comparison of alternative polymer excipients and processing methods for making solid dispersions of a poorly water soluble drug. International Journal of Pharmaceutics, 2001. 222: p. 139–151.
64. Shamma, R.N. and M. Basha, Soluplus®: A novel polymeric solubilizer for optimization of Carvedilol solid dispersions: Formulation design and effect of method of preparation. Powder Technology, 2013. 237: p. 406-414.
65. Ghebremeskel, A.N., C. Vemavarapu, and M. Lodaya, Use of surfactants as plasticizers in preparing solid dispersions of poorly soluble API: selection of polymer-surfactant combinations using solubility parameters and testing the processability. International Journal of Pharmaceutics, 2007. 328(2): p. 119-29.
66. Frank, K.J., et al., What is the mechanism behind increased permeation rate of a poorly soluble drug from aqueous dispersions of an amorphous solid dispersion? Journal Of Pharmaceutical Sciences, 2014. 103(6): p. 1779-86.
67. Vikas A Saharan, V.K., Mahesh Kataria, Manoj Gera, Pratim K Choudhury, Dissolution Enhancement of Drugs. Part I: Technologies and Effect of Carriers. International Journal of Health Research, 2009. 2: p. 3-20.
68. Ingle U.S., G.P.D., Bankar V.H., Pawar S.P., A review on solid dispersions: A discussion enhancment technique. International Journal of Research in Ayurveda & Pharmacy, 2011. 2: p. 751-757.
69. Kanaujia, P., et al., Amorphous formulations for dissolution and bioavailability enhancement of poorly soluble APIs. Powder Technology, 2015. 285: p. 2-15.
70. Vasconcelos, T., et al., Amorphous solid dispersions: Rational selection of a manufacturing process. Advanced Drug Delivery Reviews, 2016. 100: p. 85-101.
71. Zheng Cai, X.L., Zhufen Lin, Jie Zhao, Feizhen Wu, Zhaoxiang Yang, and Z.L. Junxue Pu, Preparation and evaluation of sustained-release solid dispersions co-loading gastrodin with borneol as an oral brain-targeting enhancer. Acta Pharmaceutica Sinica B, 2014. 4: p. 86-93.
72. Eman Abd-Elrasheed, S.E.-H., Manal EL-Ashmoony, Salwa Salah, Brain-targeted intranasal zaleplon solid dispersion in hydrophilic carrier system; 2(3) full-factorial design and in vivo determination of GABA neurotransmitter. Drug Development and Industrial Pharmacy, 2018. 44: p. 741-749.

73. Anna Stasiłowicz-Krzemie, M.G., Anita Płazinska, Wojciech Płazinski, Andrzej Miklaszewski, Marcin Zarowski, Zofia Adamska-Jerna´s, Judyta Cielecka-Piontek, The systems of naringenin with solubilizers expand its capability to prevent neurodegenerative diseases. International Journal of Molecular Sciences, 2022. 23: p. 1-24.
74. Anupama Kalia, M.P., Solid Dispersions: An Approch Towards Enhancing Dissolution Rate. International Journal of Pharmacy and Pharmaceutical Sciences, 2011. 3: p. 9-19.
75. Suresh D.Kumavat, Y.S.C., Manisha Badhe, Priyanka Borole and Khusbu Shenghani, Physical Stability of Solid Dispersion: A Review. International Journal of Pharmaceutical Archive, 2013. 2: p. 129-136.
76. Teja, S.B., et al., Drug-excipient behavior in polymeric amorphous solid dispersions. Excipients and Food Chem Journal, 2013. 4(3): p. 70-94.
77. Guo, Y., E. Shalaev, and S. Smith, Physical stability of pharmaceutical formulations: solid-state characterization of amorphous dispersions. TrAC Trends in Analytical Chemistry, 2013. 49: p. 137-144.
78. Neslihan Gursoy, S.B., Self-emulsifying drug delivery systems (SEDDS) for improved oral delivery of lipophilic drugs. Biomed Pharmacother, 2004. 58: p. 173-182.
79. McClements, D., Nanoemulsions versus microemulsions: terminology, differences, and similarities. Soft Matter, 2012. 8: p. 1719-1729.
80. Shweta Gupta, R.K., Abdelwahab Omri, Formulation strategies to improve the bioavailability of poorly absorbed drugs with special emphasis on self-emulsifying systems. ISRN Pharm, 2013. 2013: p. 1-17.
81. Bo Tang, G.C., Jian-Chun Gu, Cai-Hong Xu, Development of solid self-emulsifying drug delivery systems: preparation techniques and dosage forms. Drug Discovery Today, 2008. 13: p. 606-612.
82. Patcharawalai Jaisamut, K.W., Ruedeekorn Wiwattanapatapee, A novel self-microemulsifying system for the simultaneous delivery and enhanced oral absorption of curcumin and resveratrol. Planta Medica, 2017. 83: p. 461-467.

83. Sirigul Thongrangsalit, T.P., Vimolmas Lipipun, Garnpimol Ritthidej, Bromocriptine tablet of self-microemulsifying system adsorbed onto porous carrier to stimulate lipoproteins secretion for brain cellular uptake. Colloids and Surfaces B: Biointerfaces, 2015. 131: p. 162-169.
84. Tatyana Gershanik, S.B., Self-dispersing lipid formulations for improving oral absorption of lipophilic drugs. European Journal of Pharmaceutics and Biopharmaceutics, 2000. 50: p. 179-188.
85. Suchiwa Pan-On, P.D., Waree Tiyaboonchai, Trends in advanced oral drug delivery system for curcumin: A systematic review. Journal of Controlled Release, 2022. 348: p. 335-345.
86. Sneha Kulkarni, S.-S.F., Effects of particle size and surface modification on cellular uptake and biodistribution of polymeric nanoparticles for drug delivery. Pharmaceutical Research, 2013. 30: p. 2512-2522.
87. Rohan Ghadi , N.D., BCS class IV drugs: Highly notorious candidates for formulation development. Journal of controlled release, 2017. 248: p. 71-95.
88. Ishita Chattopadhyay, K.B., Uday Bandyopadhyay, Ranajit Banerjee, Turmeric and curcumin: Biological actions and medicinal applications. Current Sciences, 2004. 87: p. 44-53.
89. Seid Jafari, D.M., Nanotechnology approaches for increasing nutrient bioavailability. Advances in Food and Nutrition Research, 2017. 81: p. 1-30.
90. Jianbing Wu, J.W., Jue Zhang, Zhaozhu Zheng, David Kaplan, Gang Li, Xiaoqin Wang, Oral Delivery of Curcumin Using Silk Nano- and Microparticles. ACS Biomaterials Science and Engineering, 2018. 4: p. 3885-3894.
91. Min Sun, L.Z., Chenyu Guo, Fengliang Cao, Huanlei Chen, Liyan Zhao, Qi Tan, Xiuqing Zhu, Fanping Zhu, Tingting Ding, Yingjie Zhai, Guangxi Zhai, Evaluation of an oral carrier system in rats: bioavailability and gastrointestinal absorption properties of curcumin encapsulated PBCA nanoparticles. Journal of Nanoparticle Research, 2012. 14: p. 1-13.
92. Richard Urso, P.B., Giuseppe Giorgi, A short introduction to pharmacokinetics. European review for medical and pharmacological sciences, 2002. 6: p. 33-44.

93. Bhushan Munjal, Y.P., Sarsvatkumar Patel, Arvind Bansal, Comparative oral bioavailability advantage from curcumin formulations. Drug Delivery and Translational Research, 2011. 1: p. 322-331.
94. Vandita Kakkar, S.S., Dinesh Singla, Indu Kaur, Exploring solid lipid nanoparticles to enhance the oral bioavailability of curcumin. Molecular Nutrition & Food Research, 2011. 55: p. 495-503.
95. Mona Abdel-Mottaleb, D.N., Alf Lamprecht, Lipid nanocapsules for dermal application: a comparative study of lipid-based versus polymer-based nanocarriers. European Journal of Pharmaceutics and Biopharmaceutics, 2011. 79: p. 36-42.
96. Martin Purpura, R.L., Jacob Wilson, Haider Mannan, Gerald Münch, Valentina Razmovski-Naumovski, Analysis of different innovative formulations of curcumin for improved relative oral bioavailability in human subjects. European Journal of Nutrition, 2017. 57: p. 929-938.
97. Ralf Jäger, R.L., Allison Calvanese, Jordan Joy, Martin Purpura, Jacob Wilson, Comparative absorption of curcumin formulations. Nutrition Journal, 2014. 13: p. 1-8.
98. Sandra Flory, N.S., Kathrin Haas, Sina Jehle, Eva Kienhöfer, Reinhard Waehler, Günther Adler, Sascha Venturelli, and Jan Frank, Increasing post-digestive solubility of curcumin is the most successful strategy to improve its oral bioavailability: a randomized cross-over trial in healthy adults and in vitro bioaccessibility experiments. Molecular Nutrition & Food Research, 2021. 65: p. 1-10.
99. Timothy Marczylo, R.V., Darren Cooke, Paolo Morazzoni, William Steward, Andreas Gescher Comparison of systemic availability of curcumin with that of curcumin formulated with phosphatidylcholine. Cancer Chemother Pharmacol, 2007. 60(2): p. 171-177.
100. Huanlei Chen, J.W., Min Sun, Chenyu Guo, Aihua Yu, Fengliang Cao, Liyan Zhao, Qi Tan, Guangxi Zhai, N-trimethyl chitosan chloride-coated liposomes for the oral delivery of curcumin. Journal of Liposome Research, 2012. 22: p. 100-109.

101. Mei-Ping Tian, R.-X.S., TingWang, Meng-Jie Sun, Ya Liu, Xi-Guang Chen, Inducing sustained release and improving oral bioavailability of curcumin via chitosan derivatives-coated liposomes. International Journal of Biological Macromolecules, 2018. 120: p. 702-710.
102. Makoto Takahashi, S.U., Kensaku Takara, Yonathan Asikin, Koji Wada, Evaluation of an oral carrier system in rats: bioavailability and antioxidant properties of liposome-encapsulated curcumin. Journal of Agricultural and Food Chemistry, 2009. 57: p. 9141-9146.
103. Shengfeng Peng, Z.L., Liqiang Zou, Wei Liu, Chengmei Liu, David McClements, Enhancement of Curcumin Bioavailability by Encapsulation in Sophorolipid-Coated Nanoparticles: An in Vitro and in Vivo Study. Journal of Agricultural and Food Chemistry, 2018. 66: p. 1488-1497.
104. Liandong Hu, Y.J., Feng Niu, Zheng Jia, Xun Yang, Kuiliang Jiao, Preparation and Enhancement of Oral Bioavailability of Curcumin Using Microemulsions Vehicle. Journal of Agricultural and Food Chemistry, 2012. 60: p. 7137-7141.
105. Alaina Esperon-Rojas, R.B.-J., Dalia Santos-Luna, Luz Velasco, Laura Ochoa-Rodríguez, Hugo García, Bioavailability of curcumin in nanoemulsions stabilized with mono- and diacylglycerols structured with conjugated linoleic acid and n-3 fatty acids. Biocatalysis and agricultural biotechnology, 2020. 26: p. 1-6.
106. Pei Lu, B.I., Bing Chen, Determination of oral bioavailability of curcuminoid dispersions and nanoemulsions prepared from Curcuma longa Linnaeus. 2018. 98: p. 51-63.
107. Angélica Ochoa-Flores, J.H.-B., Adriana Cavazos-Garduño, Ida Soto-Rodríguez, María Sanchez-Otero, Eduardo JVernon-Carter, Hugo García, Enhanced Bioavailability of Curcumin Nanoemulsions Stabilized with Phosphatidylcholine Modified with Medium Chain Fatty Acids. Current Drug Delivery, 2017. 14: p. 377-385.
108. Satomi Onoue, H.T., Yohei Kawabata, Yoshiki Seto, Junya Hatanaka, Barbara Timmermann, Shizou Yamada, Formulation design and photochemical studies on nanocrystal solid dispersion of curcumin with improved oral bioavailability. Journal of Pharmaceutical Sciences, 2010. 99: p. 1871-1881.

109. Rubi Chávez-Zamudio, A.O.-F., Ida Soto Rodríguez, Rebeca Garcia-Varelad, Hugo García, Preparation, characterization and bioavailability by oral administration of O/W curcumin nanoemulsions stabilized with lysophosphatidylcholine. Food & Function, 2017. 8: p. 3346-3354.
110. Yi-Dong YAN, J.K., Mi Kwak, Bong Yoo, Chul Yong, Han-Gon Choi, Enhanced oral bioavailability of curcumin via a solid lipid-based self-emulsifying drug delivery system using a spray-drying technique. Biol Pharm Bull, 2011. 34: p. 1179-1186.
111. Xuemei Wu, J.X., Xiuwang Huang, Caixia Wen, Self-microemulsifying drug delivery system improves curcumin dissolution and bioavailability. Drug Development and Industrial Pharmacy, 2011. 37: p. 15-23.
112. Saipin Setthacheewakul, S.M., Narubodee Phadoongsombut, Wiwat Pichayakorn, Ruedeekorn Wiwattanapatapee, Development and evaluation of self-microemulsifying liquid and pellet formulations of curcumin, and absorption studies in rats. European Journal of Pharmaceutics and Biopharmaceutics, 2010. 76: p. 475-485.
113. Dinesh Dhumal, P.K., Rahul Kalhapure, Krishnacharya Akamanchi, Self-microemulsifying drug delivery system of curcumin with enhanced solubility and bioavailability using a new semi-synthetic bicephalous heterolipid: in vitro and in vivo evaluation. RSC Advances, 2015. 5: p. 90295-90306.
114. Arpa Petchsomrit, N.S., Ruedeekorn Wiwattanapatapee, Hydroxypropylmethyl cellulose-based sponges loaded self-microemulsifying curcumin: Preparation, characterization, and in vivo oral absorption studies. Journal of Applied Polymer Science, 2016. 133: p. 429661-429670.
115. Patcharawalai Jaisamut, K.W., Potchanapond Graidist, Yaowaporn Sangsen, Ruedeekorn Wiwattanapatapee, Enhanced Oral Bioavailability of Curcumin Using a Supersaturatable Self-Microemulsifying System Incorporating a Hydrophilic Polymer; In Vitro and In Vivo Investigations. American Association of Pharmaceutical Scientists, 2017. 2: p. 730-740.

116. Liu Zhongfa, M.C., Jiang Wang, Wei Chen, Winston Yen, Patty Fan-Havard, Lisa Yee, Kenneth Chan, Enhancement of curcumin oral absorption and pharmacokinetics of curcuminoids and curcumin metabolites in mice. Cancer Chemotherapy and Pharmacology, 2012. 69: p. 679-689.
117. Razieh Nazari-Vanani, L.M., Hossein Heli, In vivo evaluation of a self-nanoemulsifying drug delivery system for curcumin. Biomed Pharmacother, 2017. 88: p. 715-720.
118. Hongyu Ji, J.T., Mengting Li, Jinmei Ren, Nannan Zheng, Linhua Wu, Curcumin-loaded solid lipid nanoparticles with Brij78 and TPGS improved in vivo oral bioavailability and in situ intestinal absorption of curcumin. Drug Delivery, 2016. 23: p. 459-470.
119. Tanvi Gupta, J.S., Sandeep Kaur, Simarjot Sandhu, Gurpal Singh, Indu Kaur, Enhancing bioavailability and stability of curcumin using solid lipid nanoparticles (CLEN): a covenant for its effectiveness. Frontiers in Bioengineering and Biotechnology, 2020. 8: p. 1-14.
120. Prakash Ramalingam, S.Y., Young Ko, Nanodelivery systems based on mucoadhesive polymer coated solid lipid nanoparticles to improve the oral intake of food curcumin. Food Research International, 2016. 84: p. 113-119.
121. Min Fang, Y.J., Wei Bao, Hui Gao, Mengjin Xu, Di Wang, Xia Wang, Ping Yao, Liegang Liu, In vitro characterization and in vivo evaluation of nanostructured lipid curcumin carriers for intragastric administration. International Journal of Nanomedicine, 2012. 7: p. 5395-5404.
122. Ying Gao, G.C., Xiaojiao Luan, Meijuan Zou, Hongyu Piao, Gang Cheng, Improved oral absorption of poorly soluble curcumin via the concomitant use of borneol. AAPS PharmSciTech, 2019. 20: p. 1-10.
123. Ai Chuah, B.J., Zhang Jie, Subbarayan Ramesh, Shibajee Mandal, Jithesh Puthan, Parag Deshpande, Vadakkanchery Vaidyanathan, Richard Gelling, Gaurav Patel, Tapas Das, Sathyavageeswaran Shreeram, Enhanced bioavailability and bioefficacy of an amorphous solid dispersion of curcumin. Food Chemistry, 2014. 156: p. 227-233.

124. Shuxin Wan, Y.S., Xiuxiang Qi, Fengping Tan, Improved bioavailability of poorly water-soluble drug curcumin in cellulose acetate solid dispersion. AAPS PharmSciTech, 2012. 13: p. 159-166.
125. Wenling Fan, X.Z., Wenjing Zhu, Liuqing Di, The Preparation of Curcumin Sustained-Release Solid Dispersion by Hot-Melt Extrusion-. Optimization of Preparation Process and Evaluation In Vitro and In Vivo. Journal of Pharmaceutical Sciences, 2020. 109: p. 1253-1260.
126. Liandong Hu, Y.S., Jian Li, Na Gao, Jing Ji, Feng Niu, Queting Chen, Xiaoning Yang, Shaocheng Wang, Enhancement of Oral Bioavailability of Curcumin by a Novel Solid Dispersion System. AAPS PharmSciTech, 2015. 16: p. 1327-1334.
127. Qihong Zhang, N.P., Yulia Chistyachenko, Mikhail Khvostovd, Tatjana Frolovad, Tatjana Tolstikovad, Alexandr Dushkinc, Weike Su, Preparation of curcumin self-micelle solid dispersion with enhanced bioavailability and cytotoxic activity by mechanochemistry. Drug Delivery, 2018. 25: p. 198-209.
128. Qihong Zhang, L.S., Yulia Chistyachenko, Veronika Evseenko, Mikhail Khvostov, Nikolay Polyakov, Alexandr Dushkin, Weike Su, Preparation, physicochemical and pharmacological study of curcumin solid dispersion with an arabinogalactan complexation agent. International Journal of Biological Macromolecules, 2019. 128: p. 158-166.
129. Takahiro Harigae, K.N., Taiki Miyazawa, Nao Inoue, Fumiko Kimura, Ikuo Ikeda, Teruo Miyazawa, Metabolic fate of poly-(lactic-co-glycolic acid)-based curcumin nanoparticles following oral administration. International Journal of Nanomedicine, 2016. 11: p. 3009-3022.
130. Edgar Marin, M.I.B., Alicia Torres, Catherina Caballero-George, New Curcumin-Loaded Chitosan Nanocapsules: In Vivo Evaluation. Planta Med, 2017. 83: p. 877-883.
131. Najeh Khalil, T.N., Diani Casa, Luciana Dalmolin, and I.H. Ana Mattos, Marco Romano, Rubiana Mainardes, Pharmacokinetics of curcumin-loaded PLGA and PLGA-PEG blend nanoparticles after oral administration in rats. Colloids and Surfaces B-Biointerfaces, 2013. 101: p. 353-360.

132. Yin-Meng Tsai, W.-L.C.-L., , Chao-Feng Chien, Lie-Chwen Lin, Tung-Hu Tsai, Effects of polymer molecular weight on relative oral bioavailability of curcumin. International Journal of Nanomedicine, 2012. 7: p. 2957-2966.
133. Yike Huang, S.D., Xinxin Luo, Yi Liu, Wanjun Xu, Jingmiao Pan, Min Wang, Zhining Xia, Evaluation of intestinal absorption mechanism and pharmacokinetics of curcumin-loaded galactosylated albumin nanoparticles. International Journal of Nanomedicine, 2019. 14: p. 9721-9730.
134. Yuwei Duan, B.Z., Lianjun Chu, Henry Tong, Weidong Liu,Guangxi Zhai, Evaluation in vitro and in vivo of curcumin-loaded mPEG-PLA/TPGS mixed micelles for oral administration. Colloids and Surfaces B: Biointerfaces, 2016. 141: p. 345–354.
135. Jinling Wang, W.M., Pengfei Tua, The mechanism of self-assembled mixed micelles in improving curcumin oral absorption: In vitro and in vivo. Colloids and Surfaces B-Biointerfaces, 2015. 133: p. 108-119.
136. Renuka Khatik, R.M., Ashwni Verma, Pankaj Dwivedi, Vivek Kumar, Varsha Gupta, Sarvesh Paliwal, Prabhat Mishra, Anil Dwivedi, Colon-specific delivery of curcumin by exploiting Eudragit-decorated chitosan nanoparticles in vitro and in vivo. Journal of Nanoparticle Research, 2013. 15: p. 1-15.
137. Xiaoxia Xie, Q.T., Yina Zou, Fengyi Zhang, Miao Guo, Ying Wang, Hui Wang, Qian Zhou, Shuqin Yu, PLGA nanoparticles improve the oral bioavailability of curcumin in rats: characterizations and mechanisms. Journal of Agricultural and Food Chemistry, 2011. 59: p. 9280-9289.
138. Mazhar Raja, S.Z., Muhammad Arif, Chenguang Liu, Self-assembled nanoparticles based on amphiphilic chitosan derivative and arginine for oral curcumin delivery. International Journal of Nanomedicine, 2016. 11: p. 4397-4412.
139. Se-Chun Liao, W.-H.H., Zi-Yi Huang, Kun-Lin Chuang, Kuan-Ting Lin, Chia-Ling Tseng, Tung-Hu Tsai, Anh-Hoang Dao, Chun-Li Su, Chi-Ying Huang, Bioactivity Evaluation of a Novel Formulated Curcumin. Nutrients, 2019. 11: p. 1-22.

140. Jinling Wang, L.W., Ying Li, Xiaohui Wang, Pengfei Tu, Apically targeted oral micelles exhibit highly efficient intestinal uptake and oral absorption. International Journal of Nanomedicine, 2018. 13: p. 7997-8012.
141. Murali Yallapu, P.N., Meena Jaggi, Subhash Chauhan, Therapeutic Applications of Curcumin Nanoformulations. The AAPS Journal, 2015. 17: p. 1341-1356.
142. Yutong Wang, C.W., Jing Zhao, Yanfang Ding, Lei Li, A cost-effective method to prepare curcumin nanosuspensions with enhanced oral bioavailability. Journal of Colloid and Interface Science, 2017. 485: p. 91-98.
143. Ahmed Allam, I.K., Mohamed Fouda, Ossama Abdallah, Preparation, characterization and in vivo evaluation of curcumin self-nano phospholipid dispersion as an approach to enhance oral bioavailability. International Journal of Pharmaceutics, 2015. 489: p. 117-123.
144. Donatella Paolino, A.V., Donato Cosco, Tiziana Pecora, Simona Cianciolo, Massimo Fresta, Rosario Pignatello, Improvement of oral bioavailability of curcumin upon microencapsulation with methacrylic copolymers. Frontiers in Pharmacology, 2016. 7: p. 1-9.
145. Nuri Oh, J.-H.P., Endocytosis and exocytosis of nanoparticles in mammalian cells. International Journal of Nanomedicine, 2014. 20: p. 51-63.
146. Longfa Kou, J.S., Yinglei Zhai, Zhonggui He, The endocytosis and intracellular fate of nanomedicines: Implication for rational design. Asian Journal of Pharmaceutical Sciences, 2013. 8: p. 1-10.
147. Natalie Trevaskis, W.C., Christopher Porter, Lipid-based delivery systems and intestinal lymphatic drug transport: a mechanistic update. Advanced Drug Delivery Reviews 2008. 60: p. 702-716.
148. Shuxin Wan, Y.S., Li Sun, Fengping Tan, Chitosan microparticles for oral bioavailability improvement of the hydrophobic drug curcumin. Pharmazie, 2012. 67: p. 525-528.
149. Raghavendhar Kotha, D.L., Curcumin: biological, pharmaceutical, nutraceutical, and analytical aspects. Molecules, 2019. 24: p. 1-27.
150. John Ringman, S.F., Gregory Cole, Donna Masterman, Jeffrey Cummings, A potential role of the curry spice curcumin in alzheimer's diseas. Current Alzheimer Research, 2005. 2: p. 131-136.

151. Siddharth Kulkarni, A.D., Kiran Akula, Potentials of curcumin as an antidepressant. ScientificWorldJournal, 2009. 9: p. 1233-1241.
152. Lin Xie, X.-K.L., Naoko Funeshima-Fuji, Hiromitsu Kimura, Yoh Matsumoto, Yoshitaka Isaka, Shiro Takahara, Amelioration of experimental autoimmune encephalomyelitis by curcumin treatment through inhibition of IL-17 production. International Immunopharmacology, 2009. 9: p. 575-581.
153. Biji Kurien, A.D.S., Robert Scofield, Heat-solubilized curry spice curcumin inhibits antibody-antigen interaction in in vitro studies: a possible therapy to alleviate autoimmune disorders. Molecular Nutrition & Food Research, 2010. 54: p. 1202-1209.
154. Preetha Anand, A.K., Robert Newman, Bharat Aggarwal, Bioavailability of Curcumin: Problems and Promises. Molecular Pharmaceutics, 2007. 4: p. 807–818.
155. Hanne Tonnesen, J.K., Studies on curcumin and curcuminoids: VI. kinetics of curcumin degradation in aqueous solution Z Leb-ensm Unters Forsch, 1985. 180: p. 402-404.
156. Hanne Tønnesen, M.M., Thorsteinn Loftsson, Studies of curcumin and curcuminoids. XXVII. Cyclodextrin complexation: solubility, chemical and photochemical stability. International journal of pharmaceutics 2002. 244: p. 127-135.
157. Soroor Malvajerd, A.A., Zhila Izadi, Masoumeh Kurd, Tahereh Dara, Maryam Dibaei, Mohammad Zadeh, Hamid Javar, Mehrdad Hamidi, Brain delivery of curcumin using solid lipid nanoparticles and nanostructured lipid carriers: preparation, optimization, and pharmacokinetic evaluation. ACS Chemical Neuroscience, 2018. 10: p. 728-739.
158. Nayyer Karimia, B.G., Hamed Hamishehkar, Bahareh Mehramuz, Hossein Kafild, Antioxidant, antimicrobial and physicochemical properties of turmeric extract-loaded nanostructured lipid carrier (NLC). Colloid and Interface Science Communications, 2018. 22: p. 18-24.

159. Poovi Ganesan, D.N., Lipid nanoparticles: different preparation techniques, characterization, hurdles, and strategies for the production of solid lipid nanoparticles and nanostructured lipid carriers for oral drug delivery. Sustainable Chemistry and Pharmacy, 2017. 6: p. 37-56.
160. Namfa Sermkaew, W.K., Prapaporn Boonme, Narubodee Padoongsombat, Ruedeekorn Wiwattanapatapee, Liquid and solid self-microemulsifying drug delivery systems for improving the oral bioavailability of andrographolide from a crude extract of Andrographis paniculata. European journal of pharmaceutical sciences, 2013. 50: p. 459-466.
161. Bok Kang, J.L., Se Chon, Sang Jeong, Soon Yuk, Gilson Khang, Hai Lee, Sun Cho Development of self-microemulsifying drug delivery systems (SMEDDS) for oral bioavailability enhancement of simvastatin in beagle dogs. International Journal of Pharmaceutics, 2004. 274: p. 65-73.
162. Ping Zhang, Y.L., Nianping Feng, Jie Xu, Preparation and evaluation of self-microemulsifying drug delivery system of oridonin. International Journal of Pharmaceutics, 2008. 355: p. 269-276.
163. Reyhan Gursoy, S.B., Self-emulsifying drug delivery systems (SEDDS) for improved oral delivery of lipophilic drugs. Biomed Pharmacother, 2004. 58(3): p. 173-82.
164. Catherine Tuleu, M.N., Jayna Rose, Danielle Euler, Robert Saklatvala, Ashley Clarke, Steven Booth, Comparative bioavailability study in dogs of a self-emulsifying formulation of progesterone presented in a pellet and lquid form compared with an aqueous suspension of progesterone. Journal of Pharmaceutical Sciences 2004. 93: p. 1495–1502.
165. Erica Franceschinis, D.V., Mario Grassi, Beatrice Perissutti, Jelena Filipovic-Grcic, Anita Martinac, Francesco Meriani-Merlo, Self-emulsifying pellets prepared by wet granulation in high-shear mixer: influence of formulation variables and preliminary study on the in vitro absorption. International Journal of Pharmaceutics, 2005. 291: p. 87-97.

166. Sarwar Beg, S.J., Ch Niranjan Patra, Mohammad Rizwan, Suryakanta Swain, J. Sruti, M.E. Rao, Bhupinder Singh, Development of solid self-nanoemulsifying granules (SSNEGs) of ondansetron hydrochloride with enhanced bioavailability potential. Colloids and Surfaces B: Biointerfaces, 2013. 101: p. 414-423.
167. Biswajit Acharya, P.S.G., Sukalyan Dash, Tween-80–n-butanol–diesel–aater microemulsion system—a class of alternative diesel fuel. Journal of Dispersion Science and Technology, 2014. 35: p. 1492-1501.
168. Sameer Bhandari, V.R., Ashok Tiwary, Antimalarial solid self-emulsifying system for oral use: in vitro investigation. Therapeutic Delivery, 2017. 8: p. 201–213.
169. Mahesh Kharat, G.Z., David McClements, Stability of curcumin in oil-in-water emulsions: Impact of emulsifier type and concentration on chemical degradation. Food Research International, 2018. 111: p. 178-186.
170. Santi Babu, D.S., Naba Ghosh, Arpita Saha, and S.B. Nirmal Sukul, Enhancement of membrane damage by saponins isolated from acacia auriculiformis. Japanese Journal of Pharmacology 1997. 75: p. 451-454.
171. Duncan Craig, S.B., Devid Banning, Steven Booth, An investigation into the mechanisms of self-emulsification using particle size analysis and low frequency dielectric spectroscopy. International Journal of Pharmaceutics, 1995. 114: p. 103-110.
172. Panayiotis Constantinides, C.L., Joseph Marcello, David Chiossone, Donald Orner, Ismael Hidalgo, Philip Smith, Ani Sarkahian, Seang Yiv, Albert Owen Enhanced intestinal absorption of an RGD peptide from water-inoil microemulsions of different composition and particle size Journal of Controlled Release, 1995. 34: p. 109-116.
173. Manish Gupta, A.V., Robin Bogner, Formation of physically stable amorphous drugs by milling with Neusilin. Journal of Pharmaceutical Sciences, 2003. 92: p. 536-551.
174. Fuji Chemical Industries Co. L. Neusilin®. Available at: http://www.neusilin.com/product/pharmacopoeia.php. : p. Accessed Aprio 28, 2020.

175. Per Artursson, J.K., Correlation between oral drug absorption in humans and apparent drug permeability coefficients in human intestinal epithelial (caco-2) cells. Biochemical and Biophysical Research Communications, 1991. 175: p. 880-885.
176. Shiyin, Y., In vitro permeability across caco-2 cells (colonic) can predict in vivo (small intestinal) absorption in man—fact or myth. Pharmaceutical Research, 1997. 14: p. 763–766.
177. Sam Maher, J.H., Fiona McCartney, Seona Waters, Sinéad Bleiel, David Brayden, Effects of surfactant-based permeation enhancers on mannitol permeability, histology, and electrogenic ion transport responses in excised rat colonic mucosae. Indian Journal of Pharmacology, 2018. 539: p. 11-22.
178. Balaji Srinivasan, A.K., Mandy Esch, Hasan Erbil Abaci, Michael Shuler, James Hickman, TEER measurement techniques for in vitro barrier model systems. Journal of Laboratory Automation, 2015. 20: p. 107-126.
179. Arik Dahan, H.L., Gordon Amidon, The fraction dose absorbed, in humans, and high jejunal human permeability relationship. Molecular Pharmaceutics, 2012. 9: p. 1847-1851.
180. Mehnert Wolfgang, M.K., Solid lipid nanoparticles Production, characterization and applications. Advanced Drug Delivery Reviews, 2001. 47: p. 165–196.
181. Aji Alex, A.C., Surabhin Jose, Eliana Souto, Lopinavir loaded solid lipid nanoparticles (SLN) for intestinal lymphatic targeting. European Journal of Pharmaceutical Sciences, 2011. 42: p. 11-18.
182. Shrinivas Kulkarni, M.B., Mahendra Bishnoi, Antidepressant activity of curcumin: involvement of serotonin and dopamine system. Psychopharmacology, 2008. 201: p. 435-442.
183. Kuo-Yi Yang, L.-C.L., Ting-Yu Tseng, Shau-Chun Wang, Tung-Hu Tsai, Oral bioavailability of curcumin in rat and the herbal analysis from Curcuma longa by LC-MS/MS. Journal of Chromatography B, 2007. 853: p. 183-189.
184. Hanne Tonnesen, J.K., Studies on curcumin and curcuminoids. VI. kinetics of curcumin degradation in aqueous solution. Zeitschrift für Lebensmittel Untersuchung und Forschung, 1985. 180: p. 402–404.

185. Hanne Tennesen, J.K., Gerard Henegouwen, Studies on curcumin and curcuminoids photochemical stability. VIII. photochemical stability of curcumin. Z Lebensm Unters Forsc, 1986. 183: p. 116–122.
186. Suchiwa Pan-On, S.R., Anan Ounaroon, Chuenjid Krongkaew, Waree Tiyaboonchai, Development, characterization and skin irritation of mangosteen peel extract solid dispersion containing clay facial mask. International journal of applied pharmaceutics, 2018. 10: p. 202-207.
187. Bin Li, S.K., Lindsay Wegiel, Lynne Taylor, Kevin Edgar, Both solubility and chemical stability of curcumin are enhanced by solid dispersion in cellulose derivative matrices. Carbohydrate Polymers, 2013. 98: p. 1108-1116.
188. Gabriel Loh, Y.T., Kok Peh, Hydrophilic polymer solubilization on norfloxacin solubility in preparation of solid dispersion. Powder Technology, 2014. 256: p. 462-469.
189. Li Pan, H.W., Keren Gu, Nanoliposomes as vehicles for astaxanthin:characterization, in vitro release evaluation and structure. Molecules, 2018. 23: p. 1-12.
190. Banrida Wahlang, Y.P., Arvind Bansal, Identification of permeability-related hurdles in oral delivery of curcumin using the Caco-2 cell model. European Journal of Pharmaceutics and Biopharmaceutics, 2011. 77: p. 275-282.
191. Sanipon Chanburee, W.T., Enhanced intestinal absorption of curcumin in Caco-2 cell monolayer using mucoadhesive nanostructured lipid carriers. Journal of Biomedical Materials Research, 2018. 106: p. 734-741.
192. Kim Min-soo, K.J.-s., Park Jun Hee, Cho Kyung Won, Cha Kwang-Ho, Hwang Sung-Joo Enhanced bioavailability of sirolimus via preparation of solid dispersion nanoparticles using a supercritical antisolvent process. International Journal of Nanomedicine, 2011. 6: p. 2997-3009.
193. Sophia Fong, S.M., Martin Brandl, Annette Bauer-Brandl, Solid phospholipid dispersions for oral delivery of poorly soluble drugs: investigation into celecoxib incorporation and solubility-in vitro permeability enhancement. Journal of Pharmaceutical Sciences 2016. 105: p. 1113-1123.

194. Sooho Yeo, J.A., Changhee Park, Dohyun Kim, Jaehwi Lee, Design and characterization of phosphatidylcholine-based solid dispersions of aprepitant for enhanced solubility and dissolution. Pharmaceutics, 2020. 12: p. 1-20.
195. Felix Otto, P.H., Frank Syrowatka, State Heinl, Reinhard Neubert Assessment of the applicability of HLB values for natural phospholipid emulsifiers for preparation of stable emulsions. Pharmazie, 2020. 75: p. 365-370.
196. Vyas, V., et al., Physicochemical characterization of solid dispersion systems of tadalafil with poloxamer 407. Acta Pharm, 2009. 59: p. 453–461.
197. Wen Ting, N.B., Zhou Yixian, Pan Xin, Quan Guilan, Wu Chuanbin Fenofibrate solid dispersion processed by hot-melt extrusion: elevated bioavailability and its cell transport mechanism. Current Drug Delivery, 2019. 16: p. 538-547.
198. Suprit Saoji, V.D., Pradip Dhore, Yamini Bobde, Connor Mack, Deepak Gupta, Nishikant Raut, The role of phospholipid as a solubility- and permeability-enhancing excipient for the improved delivery of the bioactive phytoconstituents of Bacopa monnieri. European Journal of Pharmaceutical Sciences, 2017. 108: p. 23-35.
199. Ann-Christin Jacobsen, P.E., Annette Bauer-Brandl, Martin Brandl, A dynamic in vitro permeation study on solid mono- and diacyl-phospholipid dispersions of celecoxib. European Journal of Pharmaceutical Sciences, 2019. 127: p. 199-207.
200. Damian Santomauro, A.H., John Shadid, Peng Zheng, Charlie Ashbaugh, David Pigott, et al., Global prevalence and burden of depressive and anxiety disorders in 204 countries and territories in 2020 due to the COVID-19 pandemic. Lancet, 2021. 398: p. 1700-1712.
201. Alize Ferrari, A.S., Amanda Baxter, Rosana Norman, Scott Patten, Theo Vos, Harvey Whiteford, Global variation in the prevalence and incidence of major depressive disorder: a systematic review of the epidemiological literature. Psychological Medicine, 2013. 43: p. 471-481.
202. Wang Yan-Shuo, S.C.-Y., Jiang Jian-Guo, Antidepressant active ingredients from herbs and nutraceuticals used in TCM: pharmacological mechanisms and prospects for drug discovery. Pharmacological Research, 2019. 150: p. 1-49.

203. Susanne Brummelte, L.G., Chronic high corticosterone reduces neurogenesis in the dentate gyrus of adult male and female rats. Neuroscience, 2010. 168: p. 680-690.
204. Anca Motataianu, G.S., Laura Barcutean, Rodica Balasa, Oxidative Stress in Amyotrophic Lateral Sclerosis: Synergy of Genetic and Environmental Factors. International Journal of Molecular Sciences, 2022. 23: p. 1-18.
205. Roger Pamphlett, M.S., Sian Thomas, Oxidative damage to nucleic acids in motor neurons containing mercury. Journal of the Neurological Sciences, 1998 159: p. 121–126.
206. Zachary Marcum, P.S., Thorpe Joshua, Switzer Galen, Nicholas Castle, Elsa Strotmeyer, Eleanor Simonsick, Hilsa Ayonayon, Caroline Phillips, Susan Rubin, Audrey Zucker-Levin, Douglas Bauer, Ronald Shorr, Yihuang Kang, Shelly Gray, Joseph Hanlon, Health ABC Study, Antidepressant use and recurrent falls in community-dwelling older adults: findings from the health ABC study. Annals of Pharmacotherapy, 2016. 50: p. 525-533.
207. Sidney Kennedy, H.A., Michael Thase, Escitalopram in the treatment of major depressive disorder: a meta-analysis. Current Medical Research and Opinion, 2009. 25: p. 161-175.
208. Danielle Gerhard, E.W., Ronald Duman, Emerging treatment mechanisms for depression: focus on glutamate and synaptic plasticity. Drug Discovery Today, 2016. 21: p. 454-464.
209. Zhang Zong-yong, J.M., Fang Jie, Yang Ming-feng, Zhang Shuai, Yin Yan-xin, Li Da-wei, Mao Lei-lei, Fu Xiao-yan, Hou Ya-jun, Fu Xiao-ting, Fan Cun-dong, Sun Bao-liang Enhanced therapeutic potential of nano-curcumin against subarachnoid hemorrhage-induced blood-brain barrier disruption through inhibition of inflammatory response and oxidative stress. Molecular Neurobiology, 2017. 54: p. 1-14.
210. Thanyaphon Phothi, S.T., Waree Tiyaboonchai, Onrawee Khongsombat, Effects of curcumin and gamma-oryzanol solid dispersion on the brain of middle-aged rats. Biomedical Repports, 2022. 17: p. 1-9.

211. André Sigwalt, H.B., Ingo Helmich, Vojko Glaser, Karina Ghisoni, Santo Lanza, Eduardo Cadore, Francisco Lhullier, Daryl Bem, Angela Hohl, Francisco José, Rui Oliveira, Susanne Prediger, Luiz Guglielmo, Alexandra Latini, Molecular aspects involved in swimming exercise training reducing anhedonia in a rat model of depression. Neuroscience, 2011. 192: p. 661-674.
212. Zhiyu Zhao, W.W., Hongzhu Guo, Dongfeng Zhou, Antidepressant-like effect of liquiritin from Glycyrrhiza uralensis in chronic variable stress induced depression model rats. Behavioural Brain Research, 2008. 194: p. 108-113.
213. Leonard, B.E., The concept of depression as a dysfunction of the immune system. Current Immunology Reviews, 2010. 6: p. 205-212.
214. Yanqing Wu, F.W., Edward Reece, Peixin Yang, Curcumin ameliorates high glucose-induced neural tube defects by suppressing cellular stress and apoptosis. American Journal of Obstetrics and Gynecology, 2015. 212: p. 1-16.
215. Victoria Cogger, S.H., David Sullivan, Michael Muller, Robin Fraser, David Couteur Hyperlipidemia and surfactants: the liver sieve is a link. Atherosclerosis, 2006. 189: p. 273-281.